UNIVERSITY OF OKLAHOMA

GRADUATE COLLEGE

LABORATORY STUDY OF DURABILITY OF RECYCLED CONCRETE AGGREGATE INCLUDING DRAINAGE FOR USE IN PAVEMENT BASE COURSE

A THESIS

SUBMITTED TO THE GRADUATE FACULTY

in partial fulfillment of the requirements for the degree of

MASTER OF SCIENCE

By

PAUL CANCINO

Norman, Oklahoma

2023

LABORATORY STUDY OF DURABILITY OF RECYCLED CONCRETE AGGREGATE INCLUDING DRAINAGE FOR USE IN PAVEMENT BASE COURSE

A THESIS APPROVED FOR THE SCHOOL OF CIVIL ENGINEERING AND ENVIRONMENTAL SCIENCE

BY THE COMMITTEE CONSISTING OF

Dr. Musharraf Zaman, Chair

Dr. Syed Ashik Ali

Dr. Royce Floyd

Dedicated

to

My Family

ACKNOWLEDGEMENTS

I would like to begin by expressing my heartfelt gratitude for the blessings I have received from God. I am deeply grateful for the support and guidance of my family, friends, and mentors. My family's image has always brought me the strength to push beyond my limits. My younger brothers and sister have always been in my thoughts, and their image has brought me strength. I will always strive to make them proud.

I would like to express my deepest gratitude to Dr. Musharraf Zaman, my supervisor and the Chair of my thesis committee, for providing invaluable guidance and support throughout my studies at the University of Oklahoma. His comments, insights, and advice have contributed significantly to my formation as an Engineer. I feel honored to have had the opportunity to learn from such an experienced and respected professional. I also want to extend my sincere thanks to Dr. Syed Ashik Ali for his unwavering support and guidance during my research. He has been an excellent mentor, guiding me through laboratory testing and providing me with important feedback that helped improve my research and writing skills. I am also grateful to Mr. Kenneth R. Hobson for his guidance and for sharing his ample experience in laboratory testing. I would like to acknowledge the rest of Dr. Zaman's research group for their support and collaboration. They are excellent professionals with vision and an incredible work ethic.

I am deeply grateful to the Oklahoma Department of Transportation (ODOT) and the Southern Plains Transportation Center (SPTC) for providing the financial support and materials needed for my research. Without their help, this project would not have been possible.

TABLE OF CONTENTS

LIST OF TABLES

LIST OF FIGURES

ABSTRACT

Recycled concrete aggregates (RCAs) have been used as a cost-effective and environmentally friendly material in pavement base construction for quite some time. However, there is a lack of information on the durability, strength, and hydraulic properties of RCA in Oklahoma. The purpose of this study was to generate data on these properties of commonly used RCAs in Oklahoma through laboratory testing and to determine the changes in properties caused by field placement and compaction. Additionally, the performance and costs were evaluated using AASHTOWare Pavement ME simulations. The service life (performance-based) and life cycle cost analyses (LCAs) of aggregate bases of two selected pavements, a flexible pavement (SH-48) and a rigid pavement (SH-33), were studied using the AASHTOWare Pavement ME software.

To address the lack of data on RCAs in Oklahoma, laboratory testing and AASHTOWare Pavement ME simulations were conducted. In this study, three different RCAs (RCA-1, RCA-2, and RCA-3) and one virgin limestone aggregate (VLA-1) were collected from local sources. Also, to determine the relation between laboratory and field compaction, a field compacted sample of RCA-3 (CRCA-3) was collected. All aggregates were conditioned using different abrasion cycles (0, 100, 300 and 500) in a Los Angeles (LA) abrasion machine to simulate changes in gradation and the change of associated properties (durability and strength) a pavement would experience during placement and construction.

Laboratory testing in this study included particle size distribution, shape indices (angularity and texture), wash loss, optimum moisture content (OMC) and maximum dry density (MDD), Los Angeles (LA) abrasion, durability indices (D_c and D_f), hydraulic conductivity (k), and resilient modulus (M_r) for the selected gradation. Type A gradation was used as specified by

the Oklahoma Department of Transportation (ODOT) for pavement bases. The upper and lower limits of the selected gradation were used for laboratory testing to reduce variability in results.

It was found that the source material used to produce the RCAs had a significant impact on the quality and properties in terms of stiffness, durability, and performance, with RCAs produced on-site from highway pavements having improved properties compared to those produced in recycling plants. Also, it was found that RCA-1 and RCA-2 exhibited unsatisfactory values for the durability of fines (D_f), according to ODOT specifications. The durability of fines (D_f) was found helpful as a screening tool for RCAs since most of the RCAs did not meet the ODOT's requirements. Also, based on laboratory test results, the permeability of the aggregate bases is expected to exhibit a significant reduction in permeability (k) with field placement and compaction. From performance simulation results using the AASHTOWare Pavement ME software, it was evident that, for flexible pavements, good performance can be expected from RCA aggregates produced on-site from existing highway pavements. For rigid pavements, performance simulations showed that RCA may be a valuable alternative due to the dominance of the concrete layer. This study also showed that recycled aggregate bases could be built at a lower cost compared to virgin aggregates. These findings suggest that recycled aggregates can be a sustainable and cost-effective alternative for pavement bases, provided that proper selection and quality control measures are implemented.

1. CHAPTER ONE: INTRODUCTION

1.1. Background

The construction industry is a significant contributor to the waste stream in the United States (U.S.), making up more than twice the amount of municipal solid waste. Construction and demolition (C&D) waste is primarily generated by constructing and demolishing buildings, pavements, bridges, and other structures. According to the United States Environmental Protection Agency (EPA), an estimated 600 million tons of C&D waste was generated in the U.S. in 2018 (EPA Fact Sheet, 2020). A sizable portion of the C&D waste is currently being discarded in landfills causing significant environmental hazards. Using C&D waste in construction is increasingly becoming more attractive to stakeholders because of the need to minimize environmental impact and conserve natural resources. In 2018, the total amount of C&D waste placed in landfills was approximately 144 million tons. However, using C&D waste in different engineering applications has also increased. Increased environmental awareness, scarcity of raw materials, and the growing cost of waste disposal are primarily responsible for the increased use of C&D waste (Apotheker, 1990; Gavilan and Bernold, 1994; Hoyos et al., 2011; Arulrajah et al., 2014; Zhang et al., 2021).

Concrete constituted the most significant portion of the total C&D waste among different components. According to EPA, in 2018, approximately 67% of the total C&D waste was concrete (EPA Fact Sheet, 2020). Concrete from C&D waste is generally crushed, and the steel is extracted to produce recycled concrete aggregate (RCA). Generally, RCAs have been used as a partial or complete replacement for virgin aggregates in many engineering applications. The most common uses of RCA in the U.S. include new concrete, erosion control, bulk fills, and base and subbase of roadway pavements (FHWA, 2004; Cackler, 2018; Mukhopadhyay et al., 2018).

Among different applications, the use of RCA as a base and subbase material for new pavements has been found suitable by several researchers (Poon et al., 2006; Edil et al., 2012; Arshad & Ahmed, 2017). In some cases, RCAs have been used in combination with virgin aggregates or other recycled materials, such as reclaimed asphalt pavement (RAP), recycled bricks, glass, and fly-ash for use as a pavement base and subbase (Hoyos et al., 2011; Gabr and Cameron, 2012; Arulrajah et al., 2012; Arisha et al., 2018).

Several studies have evaluated the use of RCAs for use as a pavement base and subbase. Several researchers have reported similar or better behavior in terms of strength of the RCA compared to virgin aggregates (Kim et al., 2012; Arulrajah et al., 2012; Bozyurt et al., 2012; Gabr et al., 2013; Arulrajah et al., 2014; Arshad & Ahmed, 2017). Whether RCAs exhibit better performance in terms of pavement distresses during the service life of the pavement than virgin aggregates depend on various factors, including the quality of the original aggregate, age, environmental conditions, crushing operation, and other factors (Mukhopadhyay et al., 2018; Cavalline et al., 2022). Also, the performance of rigid and flexible pavements, in terms of pavement distresses, has been studied by several researchers (Kim et al., 2011; Arisha et al., 2018; Zhang et al., 2021). Some of these studies have reported RCA's performance similar to or better than the bases constructed with virgin aggregates (Ram et al., 2011; Kim et al., 2013; Arisha et al., 2018; Reza et al., 2020; Coban et al., 2020; Zhang et al., 2021). In spite of the results reported in previous studies, there are concerns among the state DOTs and private companies about the durability, permeability, and service life of pavement bases and subbases constructed with RCA. Also, very limited data are available on the strength, durability, and drainage properties of RCAs produced in Oklahoma. The quality of RCAs depends on several factors, including aggregate source, quality of original aggregates, recycling methods, and

specifications (Cavalline et al., 2022). Therefore, this study was focused on generating new data on the durability, strength, permeability, and service life of RCAs locally available in Oklahoma for potential use in pavement bases. Several previous studies have reported that the strength of aggregate bases can be significantly influenced by the type of gradation (Zaman et al., 1994; Tian et al., 1998; Khoury et al., 2010;). The gradation of the base materials can change due to the placement and compaction in the field and durability loss during the service life of the pavement. Therefore, the effect of the changes in gradation due to construction and service life on the strength and durability of RCA bases needs to be studied. In addition to contributing to strength or stiffness, aggregate bases are intended to serve as a drainage layer. Although essential, very few previous studies have addressed the drainage aspects of aggregate bases (Cedergren, 1994; Randolph et al., 2000; Khoury et al., 2010). The present study seeks to address this need based on laboratory testing. The results from such a study will help improve the understanding of the behavior of RCA materials and the design of pavements in Oklahoma.

1.2. Research Objectives

As noted in the preceding section, very limited data are available on the properties of RCAs commonly available in Oklahoma related to strength, stiffness, durability and drainage performance. The primary purpose of this study was to generate such data on commonly available RCAs in Oklahoma through laboratory testing and AASHTOWare Pavement ME simulations, focused on assessing the performance of RCA as an unbound base layer for both flexible and rigid pavements. Specifically, the laboratory study herein involved the following: particle size distribution or gradation, aggregate shape indices, optimum moisture content (OMC) and maximum dry density (MDD) or maximum unit weight, durability (both coarse and fine), resilient modulus (M_r), and hydraulic conductivity (k). The resilient modulus (M_r) serves

as an important parameter to assess the stiffness and stability of the aggregate base and is also used to estimate the service life and performance of the pavement. To this end, laboratory tests were conducted to determine the M_r of RCAs obtained from three different sources and compared with the results of virgin aggregates from one source. The drainage capability of the RCAs was assessed using the hydraulic conductivity or coefficient of permeability. Also, the durability of the selected RCAs was evaluated using Los Angeles (LA) abrasion and durability index (DI) tests. The performance and service life of pavements with RCA bases were assessed using the AASHTOWare Pavement ME simulations, in which the properties determined through laboratory testing were used. Finally, the effect of the changes in gradation due to construction on the aforementioned properties of RCAs was examined. The specific objectives of this study are listed below:

1) Assess the stiffness, durability (for both coarse and fine), and drainage-related properties of RCAs commonly available in Oklahoma, as measured by gradation, optimum moisture content and maximum dry density, aggregate shape indices, resilient modulus, permeability, and presence of contaminants through laboratory tests.
2) Generate resilient modulus, permeability, and durability data for these RCAs and compare them with the corresponding results from a virgin aggregate commonly used in Oklahoma as an aggregate base.
3) Evaluate the changes in gradation, aggregate shape indices, resilient modulus, and permeability of selected RCAs due to field placement and compaction, and the resulting changes in durability.
4) Evaluate and compare the performance and service life of pavement bases constructed with recycled and virgin aggregates using the AASHTOWare Pavement ME simulations.

1.3. Significance of This Study

In recent years, the use of recycled materials in highway construction has increased significantly due to emphasis on the conservation of natural resources and increased environmental stewardship and sustainability. Based on the experience of the transportation agencies (FHWA, 2004; Zhang et al., 2021), the use of RCA has shown a potential to produce durable pavements with improved performance and service life. Reconstruction of streets and roadways produces a huge amount of waste that can be recycled, alleviating disposal costs and reducing the consumption of energy from the hauling and production of virgin aggregates. Some waste management strategies are based on placing the C&D waste in landfills, causing considerable negative environmental impacts. Concrete constitutes the most significant portion of waste generated by the construction industry in the United States. By using recycled concrete aggregate in new construction or reconstruction, the amount of concrete waste can be reduced significantly, reducing the amount of materials placed in landfills. The quality of RCA can vary widely depending upon the source and quality of the original aggregates, age, environmental conditions, recycling process, specifications, and contaminants present in RCAs. The specifications for concrete mixes vary among state DOTs. Also, the specifications for acceptance or rejection of RCAs are currently lacking, particularly relative to drainage. As noted previously, very limited data are available on RCAs, making it difficult for state DOTs to develop objective specifications for acceptance of such materials in new construction and reconstruction of roadway pavements. The present study sought to fill this gap through laboratory testing, addressing both the stiffness and permeability of selected RCAs that are commonly used in constructing aggregate bases of roadway pavements in Oklahoma. The results from a commonly used virgin aggregate are used for comparison.

1.4. Thesis Organization

This thesis is composed of six chapters. An overview of each chapter is given below:

Chapter 1: This chapter provides an overall background of this study. This chapter briefly describes the production of RCA in the U.S. and mentions the benefits of recycling concrete waste. Also, the objectives of this study are included in this chapter.

Chapter 2: This chapter reviews the available literature on stiffness, durability, and drainage-related properties of aggregate bases. Additionally, the properties of RCAs, performances and cost analyses found in the literature are reported in this chapter.

Chapter 3: This chapter discusses the materials used in this study and outlines the methodology used for laboratory testing. The specific standards used for testing are also mentioned in this chapter.

Chapter 4: This chapter contains the results from the laboratory testing congruent with the properties found in the literature. Discussion of these results is also presented in this chapter for all three RCAs and one virgin aggregate.

Chapter 5: This chapter contains simulations of the expected performance of a flexible pavement and a rigid pavement relative to selected distresses, using the commonly used AASHTOWare Pavement ME software. The pavement sections were simulated using three RCAs and one virgin aggregate as aggregate bases. The results obtained from the life cycle cost analysis (LCCA) of the flexible pavement are also presented in this chapter and the LCCA values are compared (i.e., RCA vs virgin aggregate).

Chapter 6: This chapter presents the overall conclusions from this study, along with pertinent recommendations. The recommendations are focused on the properties of the RCAs and virgin aggregates and the selection of aggregate base thicknesses (i.e., RCA vs. virgin aggregate) for similar performance.

2. CHAPTER TWO: LITERATURE REVIEW

In recent years, using recycled materials in the construction of bases and subbases of new and reconstructed roadway pavements has received increased attention due to increased awareness for the conservation of natural resources and increased environmental stewardship and sustainability. Based on the experience of the transportation agencies (FHWA, 2004), recycled concrete aggregate (RCA) can be used as bases and subbases in the construction of new pavements and reconstruction of existing pavements without compromising durability and serviceability. Reconstruction of roadways and demolition of bridges, buildings, and other structures create an enormous amount of waste that can be recycled, alleviating disposal costs and reducing energy consumption from the hauling and production of virgin aggregates. The use of RCA can help conserve natural resources by reducing the need for virgin aggregates for engineering applications, including the construction of pavement bases and subbases. For example, in urban settings, RCA plants are usually located much closer than the virgin aggregate quarry, reducing the hauling distance significantly. For the production of RCA aggregates, the concrete waste is typically crushed and used in projects nearby, thus considerably reducing the travel distance. Also, the impact of heavy loads imposed by the vehicles used in transporting aggregates can be reduced significantly because of reduced travel distance.

The literature review in this chapter focuses on RCA as a base and subbase layer in the construction of new pavements and reconstruction of existing pavements. The following topics are covered in the literature review: generation of concrete waste and quality of RCA, use of RCA in different engineering applications and pavement bases, the DOT specifications for pavement base construction, properties of RCA (stiffness, durability, and hydraulic conductivity), performance, and costs of RCA bases.

2.1. Generation of Concrete Waste and Quality of RCA

The generation of C&D waste in the United States is significant by any measure. According to the United States Environmental Protection Agency (EPA), approximately 600 million tons of C&D waste were generated in the U.S. in 2018, of which 67% were concrete waste (Figure 2-1). Figure 2-1 shows that the most dominant materials in C&D waste were asphalt concrete (18%) and concrete (67%). The total amount of C&D waste relocated in landfills in the same year was about 144 million tons. Currently, placing in landfills is one of the ways of managing C&D waste (EPA, 2020). However, as the landfill tipping fees increase and landfill capacity decreases, the construction cost increases proportionately and sometimes disproportionately. Concrete waste being the most dominant component of C&D waste, increased use of RCA in construction can better preserve natural resources and the environment (EPA, 2020).

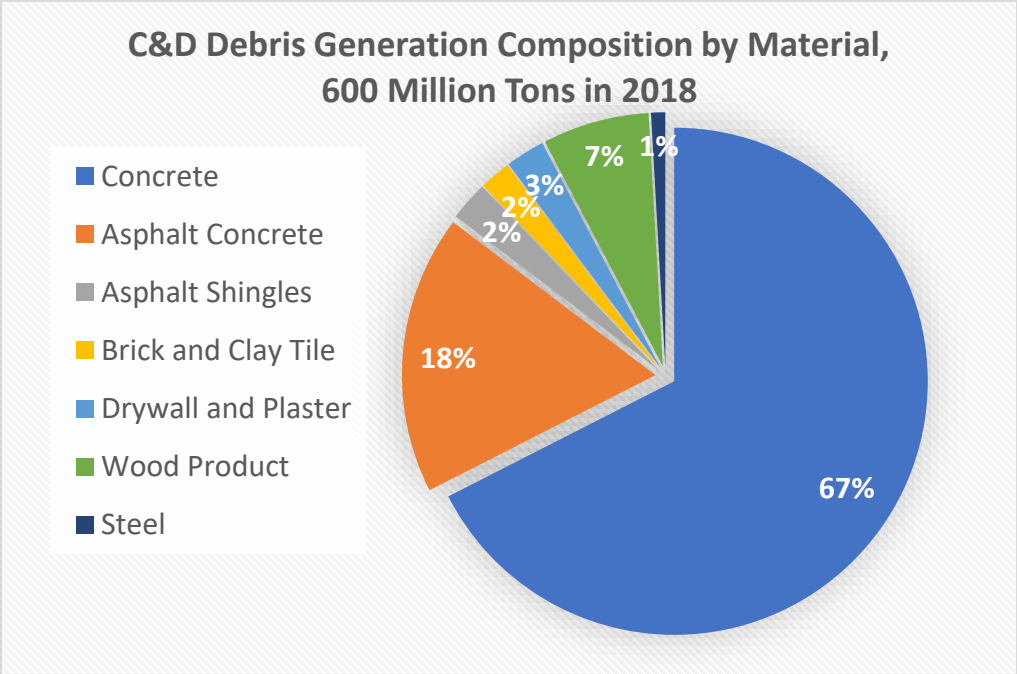

Figure 2-1: C&D waste generation (after EPA, 2020)

Regardless of the many possible uses of RCAs, processing concrete waste and producing RCA of uniform quality is difficult because of the variability in materials, processing methods, and other factors. Variabilities are caused by differences in concrete strengths and types, local standards and construction practices, aggregate sources and quality, and the use of additives. A study of RCAs focused on locally available and commonly used materials can be of significant value to transportation agencies and construction companies. Particularly, the characterization of RCAs is of paramount importance.

2.2. Use of RCA in Different Engineering Applications and Pavement Bases

According to a survey conducted by the Federal Highway Administration (FHWA, 2004), RCA was found to be a valuable resource that can be used in making new concrete for Portland cement concrete (PCC) pavements and aggregate bases through careful selection and evaluation. It was noted that 38 out of 50 states in the U.S. have successfully used RCA as an aggregate base. Also, It was noted that RCAs had been used in blends with other materials for base layer applications. Some of the most common materials found by the FHWA for these blends are other C&D wastes (for example, bricks) and reclaimed asphalt pavement (RAP).

As noted before, one of the ways of managing C&D waste has been disposal in landfills. However, it has been recognized that the volume of C&D waste and disposal costs are expected to increase significantly as available landfill volume for such disposal shrinks nationally. RCAs could be used in pavements, ground improvement, pipe bedding, and other applications. Researchers have studied incorporating recycled materials in the construction of new pavements and reconstruction of existing pavements. The feasibility and sustainability of using recycled materials, such as glass, RAP, RCA, fly ash, crushed clay bricks (CB), steel slag, and different types of polymers (polyethylene terephthalate (PET); high-density polyethylene (HDPE); and

low-density polyethylene (LDPE)) have been studied previously by researchers (Arulrajah, 2014; Zhang et al., 2021). According to Edil et al. (2012), RAP and RCA are the most commonly used materials for base layer applications. The amount of materials that can be used for constructing pavement bases and subbases are huge, which creates a considerable opportunity to use recycled materials. Therefore, this study focuses on the use of RCA as the base and subbase of pavements.

Recycled aggregates can be classified as RCAs and construction and demolition recycled aggregates (CDRA). The RCAs predominantly contain mostly crushed concrete, whereas CDRA is a mixture of different C&D wastes, such as ceramics, concrete blocks, mortar, steel, plastic, and wood. Etipola et al. (2021) studied the properties of different blends of CDRA and RCA for pavement base applications in terms of particle size distribution, flakiness index (FI), elongation index (EI), modified Proctor compaction test, and California bearing ratio (CBR). The results showed that the FI & EI values of RCA and CDRA were well within the range, which indicates satisfactory performance under heavy loading conditions. Also, using the CBR as a measure of strength, mixes of RCA with up to 25% of CDRA showed higher strength than virgin aggregates. Aggregate blends have been found common in the literature to improve the properties of RCA. It was commonly found in the literature that RCA can exhibit higher strength than virgin aggregates (see e.g., Poon et al., 2006; Arulrajah, 2014; Arisha et al., 2018; Arshad, 2019; Zhang et al., 2021; Ramirez, 2018).

Reza et al. (2020) studied the performance of RCA and non-RCA pavement through the international roughness index, pavement quality index and surface rating. That study evaluated the long-term performance of RCA in concrete pavements in Minnesota for pavement base applications. The performance of 211 miles of RCA concrete pavement was compared with conventional pavement sections with similar conditions. The pavement sections with similar

construction practices and traffic were used to compare the performance and costs. Pavements with RCA required major concrete pavement rehabilitation in 27 years and non-RCA after 32 years. Even though RCA concrete pavements were found to require major concrete pavement rehabilitation several years before, the conventional concrete pavements lifecycle cost analysis showed that RCA pavements are more economically viable than their traditional alternatives. This trend is primarily caused by the significant difference between the cost of RCA and virgin aggregates. It is worth considering that RCAs are typically produced in-place or close to the project, significantly reducing hauling costs.

In Oklahoma, during the 1980s, ODOT built several sections of jointed plain concrete pavement (JPCP) and continuously reinforced concrete pavement (CRCP) that contained RCA as coarse aggregate. The long-term performance was evaluated through visual inspections, modulus of elasticity, compressive strength, splitting tensile strength, and falling weight deflectometer testing by Mukhopadhyay et., al (2018). It was observed that JPCP pavements built with RCAs exhibited relatively lower performances than conventional JPCP sections. However, CRCP sections built with RCA exhibited relatively good performance. This behavior was supported by the idea that CRCP provides better protection of the base from erosion. In that study, the quality of RCA was defined as source dependent. It was also mentioned that the allowable number of contaminants varies from state to state. It was noted that RCA from recycling plants generally exhibited a lower quality than those recycled in-place. In the production of RCA in recycling plants, concrete of different types and from different sources is crushed, so the materials are mixed. Comparatively, recycling in-place is generally produced from one quality of concrete. According to agency experience, recycled aggregates from plants generated poor quality RCAs,

and it was suggested that the durability index (DI) (AASHTO T 210) be used as one of the screening tools for RCA (Mukhopadhyay et al. 2018).

2.3. DOT Specifications for Pavement Base Construction

The standard specifications for highway construction are intended to establish minimum acceptable limits to control the quality of the construction materials. A review of the standard specifications of 50 states revealed that currently, 41 states use RCA as a base material in their specifications. Figure 2-2 shows the states that mention using RCA in aggregate bases. The most commonly assessed physical properties were specific gravity, absorption, and gradation (AASHTO M 147, 2017). However, the requirements for compliance vary across states. Some states, such as Texas and California, allow RCA use alone, whereas others require that the RCA be blended with virgin aggregates.

The characteristics of a base layer are described in Section 703 of the standard specifications of ODOT. It is mentioned that RCA is allowed as coarse aggregate for the base layer. The gradation requirements for aggregate base materials specified by ODOT are classified into four types: Type A, Type B, Type C, and Type D (ODOT, 2019). For Types A, B, and C, the plasticity index must be less than six and the liquid limit be less than 25. Also, for all types of aggregates, materials passing a #200 (75μm) sieve must not be greater than two-thirds of the materials passing a #40 (425μm) sieve. Additionally, even though the department allows for blending different aggregates, no aggregates with plasticity above eight can be used. The standard specification allows for using gravel, stone, disintegrated granite, crushed concrete, and combinations of coarse aggregates for pavement bases. For Type A and Type B gradations, at least 40% of the material retained on a #4 (4.75mm) sieve should be uniformly graded and mechanically crushed particles with at least one fractured face. For Type C and Type D

gradations, 100% of the material retained on a #4 (4.75mm) sieve should be uniformly graded and mechanically crushed particles with at least two fractured faces. Type C gradation should also contain no more than 15% natural sand. Regarding durability, the coarse aggregate retained on a 3/8" (9.5mm) sieve should have less than 50% wear from the LA abrasion test as described in AASHTO T 96 (AASHTO, 2002). Also, a durability index (DI) of at least 40, according to AASHTO T 210 (AASHTO, 2015), is required for the finer and coarser parts of the aggregate.

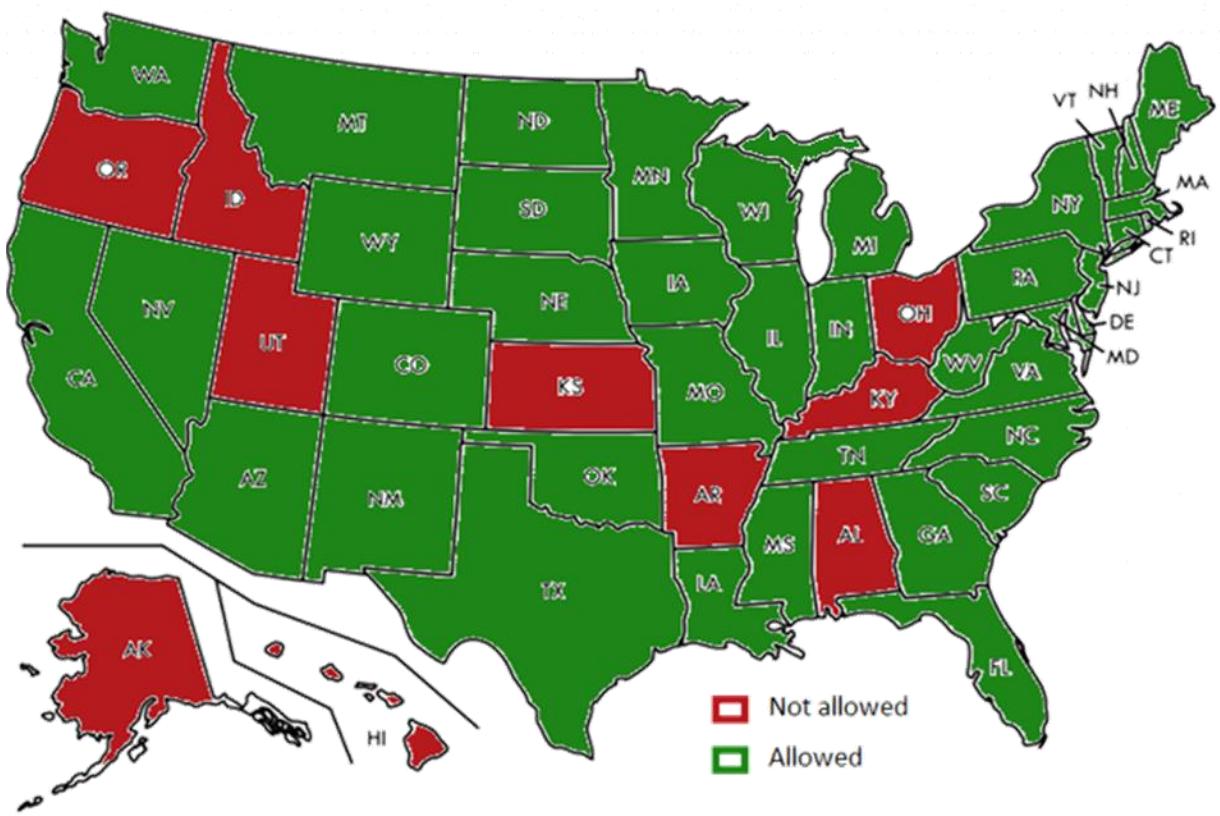

Figure 2-2: States allow RCA as a base material

It is evident from the literature review that state DOTs use different methods to ensure the quality of their aggregate bases. The following is a summary of the primary requirements:

Contaminants:

- Texas DOT's requirement for maximum allowable deleterious material is 1.5% when tested in accordance with Tex-413-A (TxDOT, 2014). Also, the aggregate should be free from reinforcing steel and other objectionable materials.
- The Missouri DOT test method TM71 (MoDOT, 2021) is required for measuring the number of contaminants. The maximum allowable contaminants are limited to 2%.
- Louisiana DOT requires the contractors to quantify harmful materials following the DOTD TR 119 (LaDOTD, 2020) test method.
- According to Colorado DOT specifications, recycled materials should be free from any vegetable matter, clumps, or balls of clay (see CDOT, 2021).
- Minnesota DOT requires that the maximum amount of wood, plant matter, plastic, plaster, and fabric be limited to 0.3% (see MoDOT, 2021).

Gradation:

- Texas DOT requires that recycled materials follow Type D aggregate gradation (see TxDOT, 2014).
- Louisiana DOT has gradation requirements for RCAs in the specification (see LaDOTD, 2016).
- Also, Massachusetts DOT included gradation recommendations for RCAs in their specification (see MoDOT, 2021).

LA Abrasion Loss:

- Colorado DOT requires that aggregate loss in LA abrasion testing be less than 50% for use in pavement bases (see CDOT, 2021).

- Massachusetts DOT requires that aggregate loss in LA abrasion testing be less than 50% for use in pavement bases (see MoDOT, 2021).

- The Louisiana DOT requires that the loss in the LA abrasion machine be less than 40% (see LaDOTD, 2016).

Durability Index:

- California DOT requirements for durability index differ for different aggregate classes. California DOT requires that, for Class 2 aggregates, the durability index (DI) by California test 229 (Caltrans, 2011) and a sand equivalent test by California test 217 (Caltrans, 2011) should have a minimum value of 35 and 25, respectively. Also, for Class 3 aggregates, the sand equivalent test by California test 217 (Caltrans, 2011) is required to have a minimum value of 21.

Others:

- Louisiana DOT requires that the soundness be less than 15% when used as a pavement base. The magnesium sulfate soundness test should be performed following the AASHTO T 104 (AASHTO, 2020) test method.

- Texas DOT requires that the sulfate content of the subgrade soils be tested where the aggregate base will be placed. The colorimetric test method should be performed following the Tex-145-E (TxDOT, 2005).

2.4. Properties of RCA

2.4.1 Particle Size Distribution of RCA

The sieve analysis or particle size distribution, also known as the gradation test, is used to determine the distribution of particles by size. A mechanical sieving machine is commonly used to separate the aggregate by size following the AASHTO T 27 test method (AASHTO, 2012). After the aggregate samples pass through a series of sieves, the weight retained is recorded and frequently displayed as the amount of material passing each sieve.

The gradation of the aggregate base is an essential characteristic of the aggregate as it has a significant impact on resilient modulus, permeability, and durability (Alexandria, 2013). for the upper limit (UL) and lower limit (LL) gradations, Ghabchi et al. (2013) evaluated the effect of gradations on permeability (k) and resilient modulus (M_r) of aggregates commonly used in Oklahoma. It was found that a denser gradation resulted in lower permeability (k) and higher resilient modulus (M_r) values than less dense samples. Also, Khoury et al. (2010) studied the effect of gradation, including compaction energy, on the M_r and k values of aggregates in Oklahoma. For all the aggregate types assessed, the upper limit gradations showed higher values of maximum dry density (MDD). In addition, the UL gradation tended to have a lower permeability or hydraulic conductivity. Therefore, denser material with higher values of MDD is expected to show lower permeability values.

2.4.2 Abrasion Loss of RCA from Los Angeles (LA) Abrasion Test

The LA abrasion test is used as an indicator of the relative quality of the aggregate as described in AASHTO T 96 (AASHTO, 2002). The LA abrasion test is widely used to evaluate the resistance of aggregates to abrasion and impact forces (Papagiannakis & Masad, 2008).

Khoury et al. (2010) mentioned that the abrasion resistance of aggregate is essential during construction as well as during the service life of the pavement. It is understood that dynamic loads induced by heavy traffic require that the aggregate quality be sufficient to endure such loads.

Arulrajah et al. (2012) studied the properties of RCA for base and subbase applications in terms of particle size distribution, modified Proctor compaction, specific gravity, water absorption, California bearing ratio and used the LA abrasion test as a measure of the quality of the aggregate. It was found that the RCA specimens satisfied the allowable limits of the LA abrasion test set by the state of Victoria, Australia.

2.4.3 Durability Loss of RCA

The durability index (DI) is used by ODOT to measure the relative resistance of an aggregate to produce detrimental particles (AASHTO T 210, 2015). The durability of the finer part (D_f) and coarser part (D_c) of the aggregates can be determined by the AASHTO T210 test method. This test provides a rapid evaluation of the quality of an aggregate source by determining the resistance to generating claylike particles in the presence of water by mechanical degradation methods (Papagiannakis & Masad 2008). Olorunsogo et al. (2002) highlighted the significance of the durability of materials used in pavement construction. According to Wu et al. (1998), the DI test has primarily been used in the western states for identifying weathered basalt containing interstitial montmorillonite that would not contribute to strength but swelling and shrinking when used as an unbound aggregate base.

Hveem (1964) studied several aggregates from California and determined the D_f and D_c values for each. Table 2-1 lists the values obtained from that study as a measure of construction

quality controls. These values are expected to help determine the relative quality of the recycled concrete aggregates with respect to virgin aggregates. It was emphasized to wash the aggregates prior to testing to discard the fines from the sample. Therefore, the original fines present in the samples will not have any effect on the durability index for either the finer part or coarser part. The fines produced during the testing were generated from interparticle abrasion during the agitation period prescribed in the test procedure.

Table 2-1: Durability of virgin aggregate bases (after Hveem, 1964)

Aggregate gradation (% passing)					Durability index (DI)	
1 1/2”	3/4”	#4	#30	#200	Durability of coarser part (D_C)	Durability of finer part (D_F)
93	72	38	22	4	87	86
100	99	56	36	9	80	80
100	96	51	28	8	87	78
98	81	38	16	4	78	74
100	69	42	25	7	85	70
97	73	46	21	9	66	68
93	78	53	25	6	67	66
98	84	57	25	10	63	69
100	94	48	26	7	59	65
100	81	37	17	9	67	57
97	71	41	22	10	62	57
97	91	74	31	14	54	51
100	96	55	30	11	59	48
100	96	56	31	8	59	44
98	81	48	22	10	52	40
97	74	39	24	10	40	43
99	85	45	25	9	35	28

2.4.4 Texture and Angularity of RCA

The texture and angularity of an aggregate can be determined with the aggregate imaging system (AIMS). The AIMS device was designed to scan and take images of the aggregate using a built-in camera and video microscope. The angularity and texture of an aggregate can be determined using these images and the classification charts developed by Masad and Fletcher (2005).

Particle angularity and texture were found to affect the engineering behavior of the aggregate. According to Randolph et al. (2000), aggregate surfaces with rough textures will provide more resistance to the flow of water than smoother textures. According to Khoury et al. (2010), a rough surface texture provides the fines places to grip, producing stronger bonds and promoting stability; however, a rougher surface would decrease the void spaces causing reduced permeability. Khoury et al. (2010) noted that larger particles play a significant role in evaluating the permeability of open-graded bases, focusing on the texture and angularity of the coarser particles. It was observed that the permeability increased due to an increase in the angularity of an aggregate for an open-graded base layer. However, as the percentage of fines increased, the gradation became denser, and permeability was affected by other properties rather than angularity alone.

2.4.5 Moisture-Density Relationship (OMC and MMD) of RCA

The stability of an aggregate base depends significantly on its density. The moisture-density relationship is used to determine the optimum moisture content (OMC) and maximum dry density (MDD) of an aggregate. To determine OMC and MDD, the modified Proctor test is commonly used, as described in AASHTO T 180 (AASHTO, 2019). Density relates to

permeability, specific gravity, unit weight, degree of compaction, and water content of the layer (Alexandria, 2013). Also, Hoff (2004) reported that density relates to the degree of compaction and water content of a layer during construction.

Guthrie et al. (2007) studied several blends of virgin aggregates with different percentages of reclaimed asphalt pavement (RAP). According to Guthrie et al. (2007), the use of RAP caused a decrease in MDD and OMC. The study concluded that since the aggregate particles in RAP are covered with asphalt, the specific gravity would decrease. Also, the asphalt-coated aggregates were expected to have reduced capacity for water absorption. Similarly, Edil et al. (2012) studied RAP and RCA blends from 8 different states and concluded that even though the MDD varies in a narrow range for RAP and RCA, the OMC of RAP is lower than that of RCA.

Poon and Chan (2006) examined the potential use of RCAs and crushed clay brick blends as aggregate in unbound base layers. The OMC and MDD values of RCAs, crushed clay brick blends, and virgin aggregates were determined. Virgin aggregates were found to have the highest MDD, followed by RCA and crushed clay bricks. For the OMC, the trend was reversed, with clay bricks having the highest water absorption, followed by RCA and virgin aggregate.

Khoury et al. (2010) reported that the MDD of aggregates increased with increasing compaction effort and percentage of fines. In their study of aggregate bases in Oklahoma, Khoury et al. (2010) found that the MDD was an important factor affecting the performance of unbound layers. The study showed that as compaction effort increased, the MDD of the aggregate increased, resulting in a denser packing of the aggregate and a reduction in void ratios. The presence of fines in the aggregate also contributed to an increase in MDD. These findings suggest that the selection of the proper compaction effort and percentage of fines is important in

achieving a dense and stable pavement layer that can withstand traffic loads and other environmental stresses.

2.4.6 Resilient Modulus Test (M_r) of RCA

The structural stiffness of a base layer can be evaluated in the laboratory by using the resilient modulus (M_r) test. Researchers have commonly used the AASHTO T 307 test method to determine the M_r of soil (Titi et al., 2006; Khoury et al., 2010; Alexandria, 2013; Arshad et al., 2017). Typically, specimens for M_r testing are compacted at MDD with moisture contents of OMC and OMC +2% to simulate the conditions during construction. Hoff (2004) found that samples compacted to the same density through different methods can significantly vary in strength. Hoff (2004) compared the modified Proctor method to a vibratory hammer, vibratory table, and gyratory compactor. Also, the M_r values increased with increasing compaction effort.

Tian et al. (1998) used AASHTO T 294-94 test procedure to assess the impact of gradation and moisture content on resilient modulus values under laboratory conditions. Using the range of gradation suggested by the ODOT's standard specifications for highway construction, three gradations, namely upper limit, lower limit, and intermediate gradation, were selected for testing. It was observed that the M_r values changed significantly due to changes in gradation. The maximum variability in M_r was 50% between the intermediate gradation and upper limit gradation. Also, moisture content significantly impacted the M_r values; moisture content values 2% above the OMC produced changes in M_r of more than 20%. Zaman et al. (1994) studied the M_r of six commonly used aggregates as base and subbase layers in Oklahoma. Tests were performed to assess the impact of gradation, compaction method (vibratory compactor and modified Proctor), specimen size, and test procedure (AASHTO T 92-91I and T 294-92I) on the M_r values. Although gradation impacted M_r values, the effect was less

significant than the stress state. For the same gradation and bulk stress, the M_r values varied between 20% and 50%.

Several researchers have compared the M_r values between RCA and virgin aggregates to determine if RCAs could exhibit comparable performance. For example, Bozyurt et al. (2012) studied the resilient modulus of RAP and RCA as unbound base layers in Minnesota. It was noted that the RCA showed the lowest plastic strain during M_r testing. Gabr et al. (2013) studied the resilient modulus of RCAs from two different sources and a virgin aggregate. Based on the results of this study, it was recommended that RCAs could be used as base materials when compacted at 98% of the MDD. In terms of M_r and permanent strain, the RCA aggregates were found to have improved M_r values compared to those of virgin aggregate. Nataatmadja et al. (2001) observed that RCA could have higher M_r values than virgin aggregates under low deviatoric stress. Similarly, several other studies reported higher M_r values of RCAs than those of virgin aggregates (see e.g., da Conceição Leite et al., 2011; Gabr and Cameron, 2012).

2.4.7 Hydraulic Conductivity (k) of RCAs

The hydraulic conductivity or permeability (k) measures the water flow through an aggregate sample. The permeability can be determined by laboratory testing using the constant head or falling head permeability test (Das, 2018).

Cedergren (1994) observed that regular pavement construction practices with slow-draining materials were responsible for the early deterioration of pavement structures in the U.S. It was mentioned that although concerns over water in the pavement structure have been ignored in the past 30-40 years in the U.S., excellent drainage could easily triple the service life of a pavement. It was also noted that open-graded drainage layers in pavement bases should have a

coefficient of permeability (k) between 3.5 cm/sec (10,000 ft/day) and 35 cm/sec (100,000 ft/day). Several researchers have studied the effect of permeability on the performance of pavement bases across the U.S. For example, Randolph et al. (2000) mentioned that permeable bases have become more prevalent in design as adequate draining was found essential for ensuring the long-term service life of a pavement. Several permeability values were determined for aggregates present in pavement sections in Ohio, along with the resilient moduli of the studied aggregates.

Randolph et al. (2000) found that the following factors affect permeability: temperature, void ratio, particle size distribution, shape and texture, and degree of saturation. As temperature increases, the density of the fluid and viscosity reduces, causing an increase in permeability (k). The degree of compaction of the aggregate base can have a considerable effect on the particle distribution and arrangement of voids within the compacted layer, thereby considerably impacting the permeability. Particle size distribution, shape, and texture have also been found to affect permeability. The particle size impacts the arrangements of voids among and between particles. Smaller particles are expected to leave smaller and disconnected voids, causing resistance to water flow. Also, elongated surfaces or irregular particles create flow paths that are more resistant to flow. Similarly, particles with rougher textures will provide more resistance to flow.

Liang et al. (2006) studied the mechanical properties of aggregate base materials accepted by Ohio DOT. Mechanical properties of drainable bases were determined in terms of resilient modulus, strength, durability, permeability, and permanent deformation under cyclic loading. Additionally, instrumented pavement sections were built with different drainable base materials and compared with the laboratory permeabilities. It was concluded that a k value of

around 3,000 ft/day should be required for a drainable base layer, according to Cedergren (1974). Based on a previous recommendation, Liang et al. (2006) found that some aggregates used by Ohio DOT produced unsatisfactory permeability results.

In Oklahoma, Khoury et al. (2010) assessed the permeability of aggregate bases. Permeability tests were conducted using the falling head permeability test (ASTM D 5084). It was found that the coefficient of permeability (k) of an unbound layer depends on a range of factors, including gradation, shape, abrasion, compaction, viscosity of the fluid, and degree of saturation. Compaction effort was inversely proportional to permeability because denser packing caused by higher compaction efforts reduces the void ratios, causing difficulties for water flow. The angular material was found to promote larger permeability values. Khoury et al. (2010) reported that the permeability of the open-graded layer increased due to increased angularity.

Poon et al. (2006) studied the self-cementing properties of fine recycled concrete aggregates (FRCA) and their effects on unbound bases in terms of compressive strength, pH value, leaching and permeability. Also, the x-ray diffraction test was used to identify the components of the FRCA that are responsible for the self-cementing properties. The results of the study showed that the self-cementing properties of FRCA can considerably improve the strength and stiffness of unbound base materials in time. The properties of FRCA were influenced by the cement content, age, the water-cement ratio, and particle size distribution. Based on the laboratory results, the self-cementing properties of FRCA in the samples were attributed to the amount of unhydrated cement and C_2S presented in the adhered mortar. Also, the permeability of FRCA was observed to be negatively impacted by the self-cementing properties. A reduction in permeability was observed with the increase in curing time.

2.5. RCA Performance with AASHTOWare Pavement ME

Zhang et al. (2021) studied the long-term performance of pavement bases constructed with RCA and RAP. Aggregate blends of recycled materials and virgin aggregates were studied for an eight year period with seasonal freezing in Minnesota. The seven sections used in that study included four warm mix asphalt (WMA) sections of 127 mm thickness and three hot mix asphalt (HMA) sections of 102 mm thickness. Falling weight deflectometer (FWD) tests were used to determine the M_r values. Seasonal deflections and M_r data were obtained. It was found that the climatic variations affected the performance more critically than traffic loading in terms of long-term performance. Also, replacing virgin aggregate bases with 100% or 50% of RCA improved the stiffness of the base layer in the long run. It was also observed that the M_r values varied significantly in different seasons. The base layer with RCA performed better than those with RAP. The aggregate bases that replaced virgin aggregates with 50% and 100% of RCA and 100% RAP increased the overall base layer M_r values. The international roughness index (IRI) and rut depths were used to measure the ride quality of the pavement. Even though there were variations in layer moduli, the IRI and rutting showed that the ride quality did not experience any significant changes.

Kim et al. (2011) compared the performance of concrete pavements with RCA and virgin aggregate bases in Iowa. The performances of these sections were investigated in terms of pavement condition index (PCI) and IRI. The assessment was done on sections used for 10 to 34 years. The results indicated comparable performance of RCA bases and subbases constructed with virgin aggregates. All studied RCA sections performed adequately. However, the RCA test sections were found to have a few longitudinal and transverse cracks. These distresses likely resulted from lane-to-shoulder separation and lane-to-shoulder drop-off.

2.6. RCA Costs as a Base Layer

Aggregate bases built with RCA have been found to produce savings in terms of aggregate costs. According to Guthrie et al. (2007), using RAP and RCA can produce high-quality aggregate bases while resulting in significant cost savings. According to that study, the use of recycled materials could lead to a cost savings of 25 to 50% compared to traditional (virgin) aggregates. Reza et al. (2020) studied several RCA sections produced in Minnesota from a long-term perspective. In that study, the performance of a virgin aggregate base was compared with that of an RCA base under similar conditions. The performance of these sections was evaluated in terms of IRI, pavement quality index and surface rating. Through life cycle cost analysis (LCCA), it was found that the RCA sections were the most economical, even though the RCA section required complete pavement rehabilitation a few years earlier.

Ram et al. (2011) utilized the LCCA techniques to quantify the economic and environmental impact of using recycled materials in Michigan. Different pavement types, with and without cementitious materials in pavement concrete, were included. Also, RCA was considered in the base layers, with (bound layer) and without cementitious materials (unbound layer). The sections were divided into three categories according to the traffic intensity represented by the annual average daily traffic (AADT) expected for each section. Traffic Level 1 had an AADT of fewer than 6,000 vehicles, Level II had an AADT of 6,000-10,000 vehicles, and Level III had more than 10,000 vehicles with an annual growth rate of 2-3%. The cost was evaluated at the present age and grouped into four categories depending on the age of the pavement (less than 20, 20-24 years, 25-29 years and 30 years or greater) and up to 50 years for all future maintenance activities based on Michigan DOT standards. (MDOT, 2005). The distress index curve was used for preservation strategies and to establish a serviceability limit. For this

project, a distress index of 25 was considered the threshold for the HMA overlays, and a threshold of 50 was considered for complete reconstruction. According to the LCCA, pavement sections built using RCA aggregates in the concrete pavement (RCA concrete) exhibited similar costs in terms of LCCA compared to those containing virgin aggregate at low traffic levels (Traffic Level I). However, sections with higher traffic levels failed prematurely, most needing complete reconstruction in about 20 years. A few sections of RCA as a base layer were studied for Traffic Level I, showing exceptional costs in terms of LCCA for low traffic levels (Ram et al., 2011). It was noted that recycling in-place would reduce the economic and environmental impacts due to the extraction of material and transportation.

3. CHAPTER THREE: MATERIALS AND METHODS

The locally available RCA materials and virgin aggregate used in this study are described in Section 3.1. Section 3.2 outlines the laboratory testing methods employed to characterize the aggregates, while Section 3.3 discusses the methods used to evaluate pavement performance in terms of pavement distresses. Finally, Section 3.4 details the life cycle cost analysis (LCCA) method used in this study.

3.1. Materials Used in the Study

In this study, RCAs from various sources and a virgin aggregate were evaluated. As discussed in the previous chapter, the quality of RCAs can vary significantly depending on the source and production practices. RCAs produced in recycling plants contain concrete of different qualities, as well as contaminants from the rubble. Conversely, RCAs generated in-place are obtained by crushing concrete from a single quality of concrete from an existing concrete road. Consequently, RCAs are expected to have different qualities depending on the quality of the source materials. For instance, RCAs produced by local demolition waste handlers in Oklahoma have provided poor quality material in the past, with a significant presence of clay particles (Mukhopadhyay et al., 2018). The RCAs used in this study contained contaminants such as tiles, wood, plastics, and rubber, which can negatively affect the quality of aggregate bases. Therefore, it is important to carefully evaluate the source and quality of RCAs before using them in the construction of new pavements and reconstruction of existing pavements.

Oklahoma DOT standard specifications (ODOT, 2019) recommend using one of four types of gradation (ODOT Types A, B, C, and D) to construct an unbound aggregate base. The literature indicated significant variations in strength due to changes in gradation (Zaman et al.,

1994; Tian et al.,1998; Khoury et al., 2010). To reduce the variability of test results, aggregates with ODOT Type A gradation were used in this study. Since Type A gradation has significant variability in particle size distribution, aggregate blends similar to the upper limit and lower limit of ODOT Type A gradations were prepared for evaluation. The durability loss of the aggregates caused by placement and compaction was simulated using the LA abrasion machine. The properties used to characterize the aggregates are listed in Section 3.2. Figure 3-1 and Table 3-1 present the gradation range for ODOT Type A gradation.

Table 3-1: ODOT gradation Type A UL and LL

Sieve sizes	Sieve sizes (mm)	Upper limit Type A (%passing)	Lower limit Type A (%passing)
3/4”	19	100	40
3/8”	9.5	75	30
No. 4	4.75	60	25
No. 10	2	43	20
No. 40	0.425	26	8
No. 200	0.075	12	4

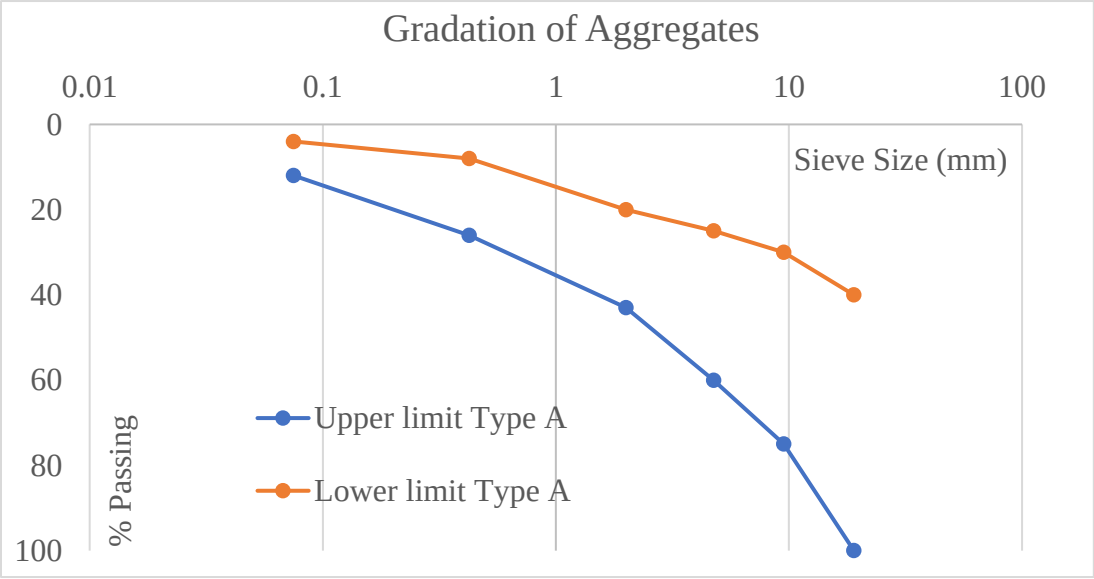

Figure 3-1: ODOT gradation Type A UL and LL

Recycled aggregates were collected from a plant-based source (RCA-2) and two recycled in-place (RCA-1 and RCA-3) construction sites in Oklahoma. Also, a commonly used virgin limestone aggregate (VLA-1) was collected from Davis, Oklahoma. The RCAs used in this study represent possible candidates for the construction of new pavements and reconstruction of existing pavements. The following section presents a brief description of the collected materials. The collected aggregates can be seen in Figure 3-2. The following naming conventions were used in this thesis:

i. Recycled concrete aggregate (RCA-1): produced in-place from Interstate 40
ii. Recycled concrete aggregate (RCA-2): produced in a recycling plant from TJ Campbell Construction, Oklahoma
iii. Recycled concrete aggregate (RCA-3): produced in-place from SH 69, Calera, Oklahoma
iv. Virgin limestone aggregate (VLA-1): produced in Davis, Oklahoma

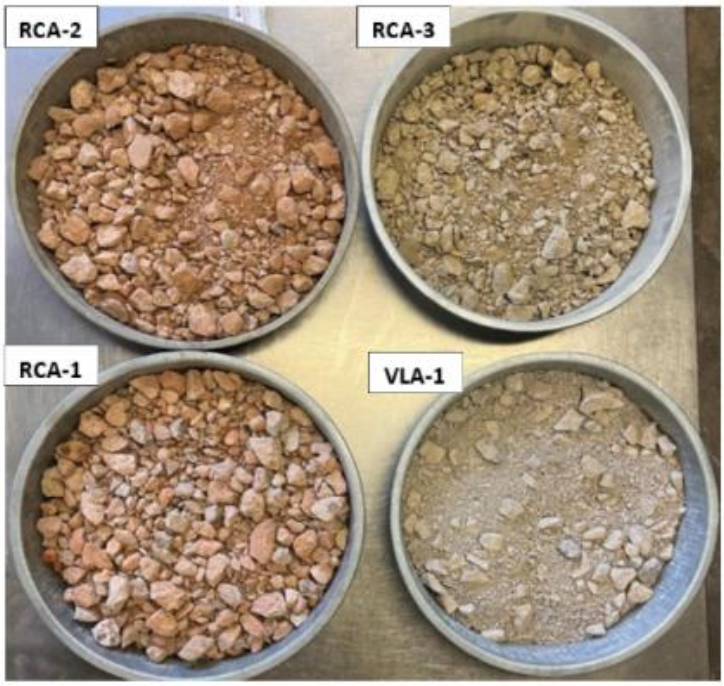

Figure 3-2: Aggregate sources used (as received)

3.1.1 Recycled Concrete Aggregates (RCA-1, RCA-2, RCA-3)

Among the three RCAs, one was collected from a plant-based source (RCA-2), and the other two (RCA-1 and RCA-3) from recycled in-place construction sites in Oklahoma. The RCAs from the recycled-in-place construction sites are expected to be of higher quality because of the strict quality control during the construction of pavements as required by ODOT. The RCA-2 aggregate was collected from a local recycling plant. As a result, the quality of the RCA is expected to be negatively impacted. Also, the RCA-2 is expected to have more contaminants than the other RCA aggregates. As discussed previously, it is common to find tiles, wood, clay particles and other contaminants in RCAs from recycling plants.

Additionally, to understand the changes caused by field placement and compaction, a field compacted recycled concrete aggregate was needed. Therefore, field compacted RCA-3 was collected from the reconstruction of US-69 in Calera, Oklahoma. The field compacted sample was defined as CRCA-3. The aggregate was used to estimate the number of LA abrasion cycles that would be representative of placement and compaction in the field.

3.1.2 Virgin Limestone Aggregate Used (VLA-1)

The virgin limestone aggregate (VLA-1) was collected from the aggregate quarry in Davis, Oklahoma. The virgin aggregate is expected to be free of visible contaminants, unlike the RCAs used in this study.

3.2. Experimental Methodology

Laboratory testing in this study included the following: gradation, wash loss, optimum moisture content (OMC) and maximum dry density (MDD), Los Angeles (LA) abrasion test, permeability (k), durability index (DI), and resilient modulus (Mr). The LA abrasion machine

was used to simulate different levels of degradation of the aggregate caused by placement and compaction. The samples prepared were conditioned in the LA abrasion machine for 0, 100, 300, and 500 cycles. Wash loss, OMC, MMD, and LA abrasion losses were determined with no conditioning to represent the initial state of the aggregate.

Figure 3-3 shows the workflow diagram, and Table 3-2 presents the test matrix used in this study. The standards used for conducting these tests are mentioned in the test matrix. Also, descriptions of the test methods are provided in the following sections.

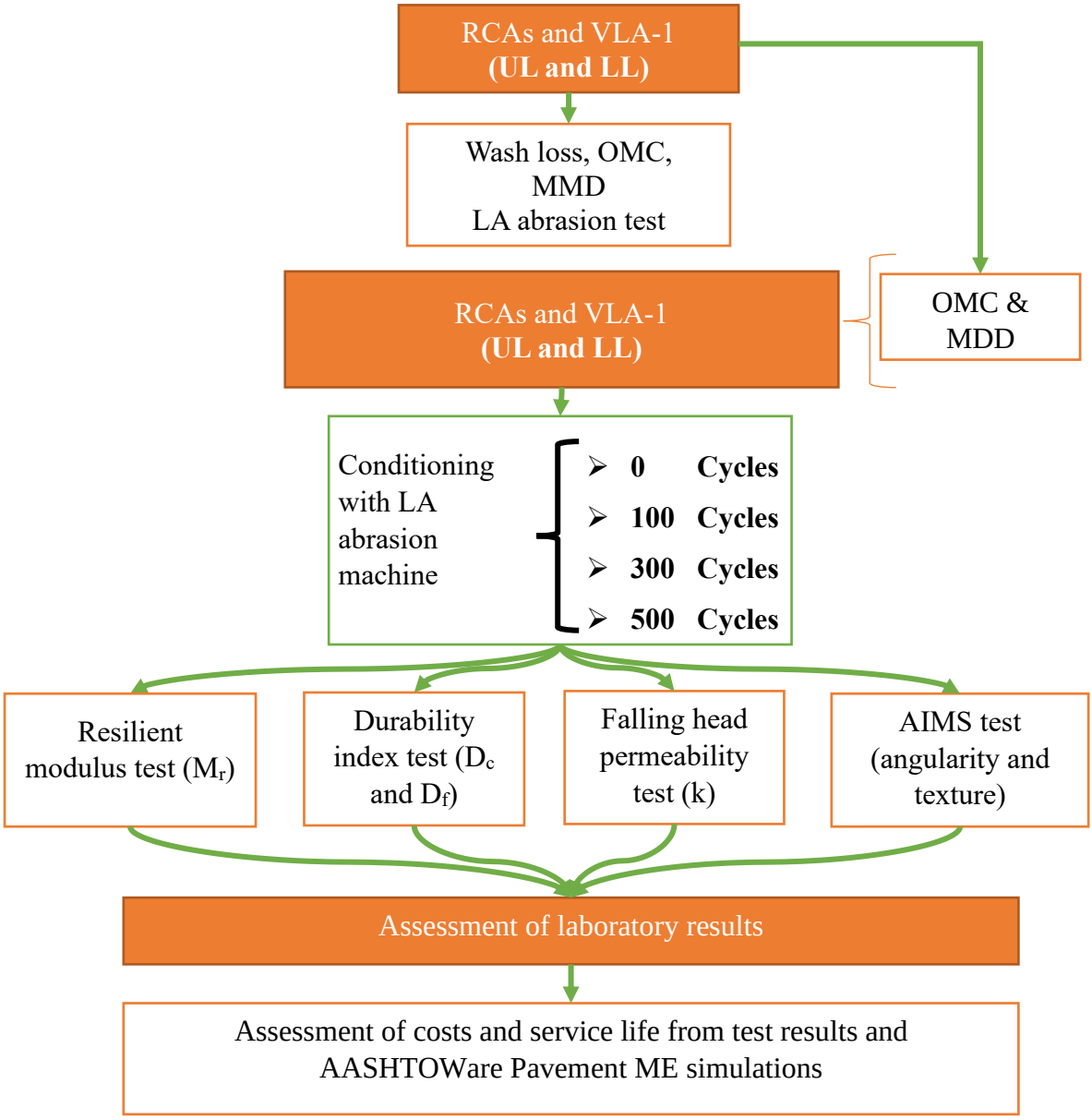

Figure 3-3: Work-flow diagram of the study

Table 3-2: Test matrix

Test method		*Particle size distribution*	*Durability*		*Density*	*Strength and stability*	*Hydraulic conductivity*	*Service life and performance*
		Changes in gradation and aggregate shape indices	Evaluation of durability of recycled aggregates (DI)	Los Angeles (LA) abrasion test	Modified Proctor for (OMC) and (MDD)	Evaluation of the effect of construction on resilient modulus (M_r)	Falling head permeability test (k)	Service life and performance
		AASHTO T27 and AIMS	AASHTO T 210	AASHTO T 96	AASHTO T180	AASHTO T 307	ASTM D 5084	AASHTO Pavement ME
RCA-1 / RCA-2 / RCA-3 / VLA-1	UL-LA0	X	X	X	X	X	X	X
	LL-LA0	X	X	X	X	X	X	X
	UL-LA100	X				X	X	
	LL-LA100	X				X	X	
	UL-LA300	X				X	X	
	LL-LA300	X				X	X	
	UL-LA500	X				X	X	
	LL-LA500	X				X	X	

3.2.1 Particle Size Distribution

Samples for each aggregate were prepared for the upper limit and lower limit of ODOT's type A gradation and conditioned in the LA abrasion machine (0, 100, 300, and 500 cycles). The gradation of the conditioned samples was evaluated to determine the expected changes in gradation following placement and field compaction. For the sieve analysis of the fine and coarse aggregates, the samples were tested as described in AASHTO T 27 (AASHTO, 2012). The following sieve sizes were used for the gradation test: 3/4", 3/8", #4, #10, #40, and #200 (Figure 3-4).

Figure 3-4: Mechanical sieving machine

3.2.2 X-Ray Diffraction (XRD)

X-ray diffraction (XRD) is a nondestructive test used for the characterization of crystalline materials. This test can provide information on structures, phases, preferred crystal orientations, average grain size, crystallinity, strain, and crystal defects (Bunaciu et al., 2015). The test was performed on RCA-3 and VLA-1 to provide information on the minerals found in the aggregate and aid in understanding their behavior. A monochromatic beam of x-rays is utilized to generate x-ray diffraction peaks, which are scattered at particular angles from every set of lattice planes in each sample. Each unique x-ray diffraction pattern is used for the rapid identification of minerals present within a rock or soil sample. From the x-ray diffraction pattern, the atomic arrangements in a given material can be used to determine the minerals used because the characteristic of its crystal structure will describe a unique mineral. The XRD data can also determine the proportion of the different minerals in a sample. Using monochromatic Cu Kα radiation at 40 kV and 44 mA, the Rigaku powder XRD device was employed to conduct the XRD tests. The scan range spanned 2° to 70° at a scan rate of 0.002° per second and with a detector count time of 2 seconds/step. First, the samples are prepared by breaking aggregate particles into small pieces and then turned into fine powder using a micronizer. After being evenly spread onto a glass slide (Figure 4-5(a)), the powder samples were placed inside the XRD equipment for testing (Figure 4-5(b)). The test results and profile fitting were processed using the XRD spectra using the Jade 2010 software.

3.2.3 Los Angeles (LA) Abrasion Test

The LA abrasion test measures the resistance to degradation of the mineral aggregate, providing an indicator of the relative quality of the aggregate as described in AASHTO T 96 (AASHTO, 2002). The pavement base must resist the degradation caused by placement,

vibratory compaction during construction, environmental conditions, and dynamic loads caused by traffic. Therefore, resistance to wear is important for pavement design, construction, and performance. The test involves placing a specific number of steel balls inside a rotating drum that rotates at a speed of 30-33 revolutions per minute. For the ODOT Type A gradation, the test requires 11 steel spheres. The samples consisted of 5,000 grams (g) of material, with 2,500 g retained between sieve sizes 3/4" and 1/2", and another 2,500 g retained between sieve sizes 1/2" and 3/8". The drum rotates for 500 cycles, and the material retained on the #12 sieve is washed, weighed and compared to the initial weight. The percentage loss is then calculated as a measure of durability loss for the aggregate. Additionally, the LA abrasion machine was used to condition the aggregate sample for 100, 300 and 500 cycles before testing in accordance with the test matrix in Table 3-2. A photograph of the LA abrasion machine used in the study is presented in Figure 3-5.

Figure 3-5: LA abrasion machine

3.2.4 Durability Index (DI)

The AASHTO T 210 (AASHTO, 2015) test method describes the durability tests of aggregates. The durability index (DI) measures the relative resistance of aggregates to produce detrimental fines when degraded. The test procedure mentions that fine dust in the aggregates presents a problem. Undesirable amounts of fines can negatively impact the quality of the aggregate. The durability test needs to be conducted on the finer part (D_f) and coarser part (D_c) of the aggregates. For D_f, the sand equivalent test was used to measure the durability of fines as specified in AASHTO T 176 (AASHTO, 2008).

3.2.5 Durability Index of Coarser Part (D_C)

For the coarse part of the aggregate, the durability testing procedure as described in AASHTO T 210 (AASHTO, 2015) was followed. The test must be conducted on the portion of the material larger than the #4 sieve. The necessary equipment included a mechanical washing vessel, collection pan, mechanical agitator, a calcium chloride solution, and distilled water. A mechanical agitator was used to cause mechanical degradation (Figure 3-6(a)). The mechanical agitator ran approximately 285 cycles per minute and agitated the sample to generate claylike fines with a lateral reciprocating motion. For the initial preparation, the coarser part of the aggregate was washed, containing a set amount of materials retained in sieve sizes 1/2", 3/8", and #4 sieve after two minutes in the agitator and dried for testing. Specifically, the material retained in sieve sizes 1/2", 3/8" and #4 sieve had a dried mass of 1,050 g, 550 g and 900 g, respectively. The material is agitated for 10 minutes with distilled water to collect the fines smaller than the #200 sieve (Figure 3-6(b)). The collected water with fines was poured over a graduated cylindrical tube and flipped 20 times to ensure proper mixing. Finally, the cylinder

was let to settle for 20 minutes before taking measurements (Figure 3-6(c)). The D_c values were determined using the height of the sediment and tables provided in the test method.

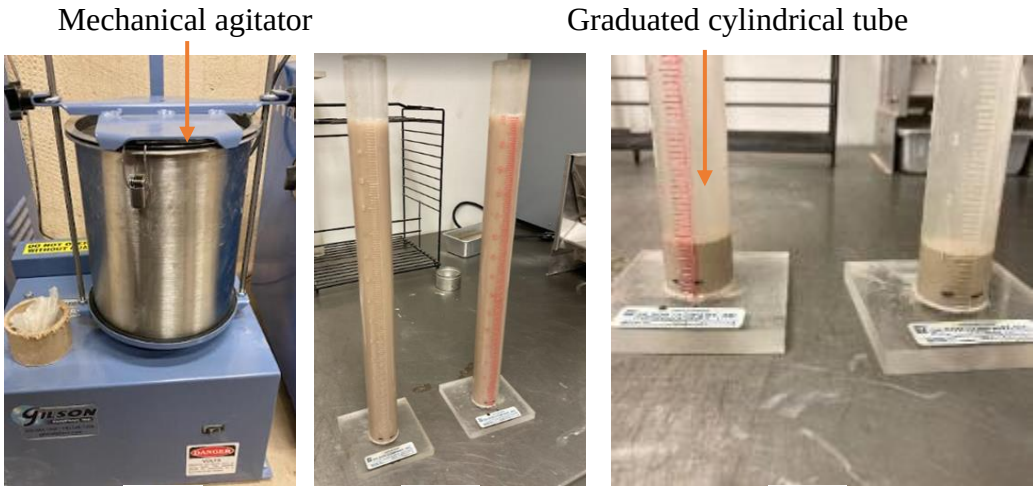

Figure 3-6: Durability of coarser part; a) mechanical agitator; b) initial state; and c) final State

3.2.6 Durability Index of Finer Part (D_F)

For the finer part of the aggregate, the sand equivalent test was conducted as described in AASHTO T 176 (AASHTO, 2008). The test must be conducted on the material passing the #4 sieve. The test needed a mechanical shaker, graduated cylinder, irrigator tube, weighted foot assembly, siphon, and stock solution. Similar to the durability of the coarser part, an equivalent sand shaker was used to generate claylike fines with a lateral reciprocating motion (Figure 3-7(a)). For the initial preparation, 500 g of the material retained in sieve sizes below #4 is separated from each gradation. After two minutes in the mechanical agitator, the aggregate was washed, discarding all the material below sieve #200 and then dried. The fine material was collected in a 3-oz tin, placed inside a graduated cylindrical tube, and filled with a working solution (Figure 3-7(c)). The cylindrical tube was placed in a sand equivalent mechanical shaker for 10 minutes. Finally, the cylindrical tube was left undisturbed for 20 minutes to allow

settlement before the measurements were taken, the weighted foot assembly was used to identify the sand reading (Figure 3-7(d)). The durability of fines was then calculated as the percentage of sand over clay.

(a) (b) (c) (d)

Figure 3-7: Durability of finer part; a) sand equivalent shaker; b) working solution; c) cylindrical tube; and d) weighted foot assembly

3.2.7 Aggregate Imaging System (AIMS)

The aggregate imaging system (AIMS) is an automated computer unit designed for measuring the shape, angularity, and texture of an aggregate. The system can measure aggregates ranging in size from 37.5 mm to 150 mm. It includes an aggregate measurement tray with grid points at specific distances along the x and y axes. The square tray is placed above a light-

emitting diode system with a light ring mounted on the lenses, a camera, and a video microscope with an optem zoom 160 video microscope (Figure 3-8). The camera moves along specified grid locations in x, y, and z directions, and the movement is controlled by a closed loop direct current servo. The texture and angularity of the aggregates can be determined by analyzing the captured images. The first step was to calibrate the instrument, followed by placing a coarse aggregate sample on the tray. From the captured images, the texture and angularity were analyzed using classification charts developed by Masad and Fletcher (2005).

Figure 3-8: AIMS setup

According to Masad and Fletcher (2005), the angularity was classified as polished for angularity values from 0 to 165, smooth for values from 165 to 275, low roughness for values from 275 to 350, and moderate roughness for values from 350 to 460. For texture, the aggregates were classified as rounded for values from 0 to 2,100 and sub-rounded for values from 2,100 to 4,000. The angularity and texture were obtained from the AIMS test for the coarser portion of the material. The material retained in 3/4", 3/8" and #4 sieve sizes were used for the lower limit gradation. For the upper limit gradation, the material retained in 3/8" and #4 sieve sizes were

used. AIMS test was conducted on aggregates with and without conditioning to assess the expected changes during field placement and compaction.

3.2.8 Moisture-Density Relationship (OMC and MMD)

The moisture-density relationship was determined for each aggregate type and gradation by the modified Proctor test. The moisture density relationships were used to determine the OMC and MDD of the aggregates. The modified Proctor test was conducted on at least four moisture contents for each aggregate using a manual compactor of 10 lb and a free fall height of 18 in. as described in AASHTO T 180 (AASHTO, 2019). The samples were compacted in 5 layers with 56 blows using a manual compactor in a 6 in. mold. Figure 3-9 shows a photograph of the compaction of the specimen using a manual modified Proctor compactor hammer.

Figure 3-9: Modified Proctor test

3.2.9 Resilient Modulus Test (M_r)

The resilient modulus test was conducted following the method described in AASHTO T 307 (AASHTO, 2021). Using the OMC for the upper and lower limits of aggregates with no conditioning, samples were prepared for the resilient modulus testing with 0, 100, 300, and 500 cycles of conditioning in the LA abrasion machine to simulate the durability loss caused by placement and compaction. The M_r tests were carried out according to the test matrix in Table 3-2. The repeated load triaxial test is one of the most commonly used methods for determining M_r values (Titi et al., 2006). In the repeated triaxial test, the compacted specimen was subjected to cyclic stress (haversine-shaped load pulse) and static confining pressure in a triaxial chamber. A load pulse duration of 0.1 sec followed by a rest period of 0.9 sec was used for resilient modulus testing using a servo-controlled hydraulic actuator (MTS).

(a) (b)

Figure 3-10: Resilient Modulus test; (a) specimen compaction; and (b) setup for test

Two linear variable differential transducers (LVDTs) were mounted externally to measure the recoverable deformation. The cylindrical split mold has a diameter of 6.0 in. and a height of 12 in., with a thick rubber membrane placed inside to avoid collapse. The samples were

compacted in 6 layers with 112 blows per layer using an automatic mechanical compactor in the split steel mold with the rubber membrane (Figure 3-10(a)). The specimen was placed on the MTS loading platform and the mold was carefully extruded. An additional rubber membrane was placed over the sample to cover possible holes punctured in the membrane during compaction. On both sides of the specimen, filter papers and a 0.5 in. porous stone were placed and then sealed with o-rings. The triaxial cell was placed over the specimen and sealed. Figure 3-10(b) shows the setup used for M_r testing. At the beginning of the test, the sample was conditioned by applying a load equivalent to maximum axial stress of 15 psi and confining stress of 20 psi for 750 repetitions. After conditioning, the resilient modulus test followed the loading sequences shown in Table 3-3.

Table 3-3: Loading sequences of resilient modulus test (AASHTO T 307, 2021)

Sequence No	Chamber confining pressure (psi)	Maximum axial stress (psi)	Cyclic stress (psi)	Constant stress (psi)	No. of load applications
Conditioning	15.0	15.0	13.5	1.5	500-1,000
Sequence 1	3.0	3.0	2.7	0.3	100
Sequence 2	3.0	6.0	5.4	0.6	100
Sequence 3	3.0	9.0	8.1	0.9	100
Sequence 4	5.0	5.0	4.5	0.5	100
Sequence 5	5.0	10.0	9.0	1.0	100
Sequence 6	5.0	15.0	13.5	1.5	100
Sequence 7	10.0	10.0	9.0	1.0	100
Sequence 8	10.0	20.0	18.0	2.0	100
Sequence 9	10.0	30.0	27.0	3.0	100
Sequence 10	15.0	10.0	9.0	1.0	100
Sequence 11	15.0	15.0	13.5	1.5	100
Sequence 12	15.0	30.0	27.0	3.0	100
Sequence 13	20.0	15.0	13.5	1.5	100
Sequence 14	20.0	20.0	18.0	2.0	100
Sequence 15	20.0	40.0	36.0	4.0	100

3.2.10 Hydraulic Conductivity (k)

The hydraulic conductivity or aggregate permeability (k) can be determined in the laboratory following ASTM D 5084 (ASTM, 2016). The falling head permeability test measures the water flow through an aggregate sample connected to a standpipe. The standpipe measures the amount of water passing through the soil and the water head. Before starting the test, the sample was saturated with the standpipe filled with water. The test was initialized by allowing water to flow through the sample until the water reached a given limit. The time required to drop the water levels were recorded along with the temperature. As described in ASTM D5084 (ASTM, 2016), the head loss of the specimen should be less than 75% of the initial head loss during the hydraulic conductivity test. Khoury et al. (2010) observed that for permeability testing, using a rigid wall permeameter could result in erroneous measurements of k. Therefore, the test was conducted using a flexible wall permeameter with confining air pressure of 10 psi to avoid short-circuiting the drainage path. For the falling head permeability test, specimens were compacted with the modified Proctor method at OMC to simulate field conditions.

The permeameter consisted primarily of a steel cylinder with a diameter of 6.25 in. and a height of 6.5 in., a bottom mold, a long vertical cylinder with an attached scale for reading the measurements, a pressure gauge, air pressure connection, water connections to the cylinder, and a reservoir tank (Figure 3-11). The mold contained a thick 0.025 in. rubber membrane held in place by o-rings, providing an air-tight seal. It was essential to verify that the setup was air-tight to ensure the accuracy of the test. Additionally, to complete the setup, the following was needed: two porous cylindrical stones, each having a diameter of 6 in. and thickness of 0.5 in., rubber gaskets, a stopwatch, and hose clamps.

The permeability of the aggregate base was calculated using ASTM D 5084 (ASTM, 2016). The change in height with time was recorded. The velocity (v) and hydraulic gradient (i) values were then calculated and plotted on a graph. The falling head approach employed by Fwa et al. (1998) (see Equation 1) was used in the analysis of the permeability results:

$$v = k_1 * i^n \qquad (1)$$

where:

v = specific discharge velocity in ft/day (cm/sec),

k_1 = coefficient of permeability in ft/day (cm/sec), and

n = experimental coefficient (unit less).

(a) (b) (c) (d)

Figure 3-11: Permeability test; (a) compacted samples and extrusion; (b) rubber membrane with o-rings; (c) porous stones; and (b) permeability set-up

A power trend line was fitted through the points in the graph of v versus i. The coefficient of permeability values was then corrected for temperature using Equation (2) and finally reported at a temperature of 20˚C.

$$k_{20°C} = (\frac{n_{T°C}}{n_{20°C}})k_{T°C} \qquad (2)$$

Where:

$k_{T°C}$ and $k_{20°C}$ = coefficient of permeability at T˚C and 20˚C, respectively,

And,

$n_{T°C}$ and $n_{20°C}$ = viscosity (N.m^{-2}.sec) of water at temperatures T˚C and 20˚C, respectively.

3.3. Performance and Service Life with AASHTOWare Pavement ME

AASHTOWare Pavement ME software is used to design pavement using a mechanistic-empirical design approach. The performances of flexible and rigid pavements in terms of pavement distresses were evaluated using AASHTOWare Pavement ME software based on traffic, climate, and material properties determined through laboratory testing. The performance threshold values should reflect policies regarding acceptable pavement conditions for each state and are used to judge the adequacy of the pavement (AASHTO, 2020). The performance thresholds for the pavement sections are described below. Two pavement sections were evaluated for this study, namely SH-48 (flexible pavement) and SH-33 (rigid pavement).

The aggregate bases were modeled with different aggregate base options (RCA-1, RCA-2, RCA-3, and VLA-1) for both flexible and rigid pavement sections. The upper limit gradation of the aggregates was used for this evaluation. Different layers considered for the analysis can be seen in Figure 3-12. The analysis was done by varying the M_r values to assess the performance

of the aggregate bases with RCA-1, RCA-2, RCA-3 and VLA-1 aggregates. The M_r values used for the simulation were obtained from laboratory testing. A design life of 20 years, annual average daily traffic (AADT) of 4,000, and the same climate conditions were considered in the simulations.

(a) SH-48 flexible pavement (b) SH-33 rigid pavement

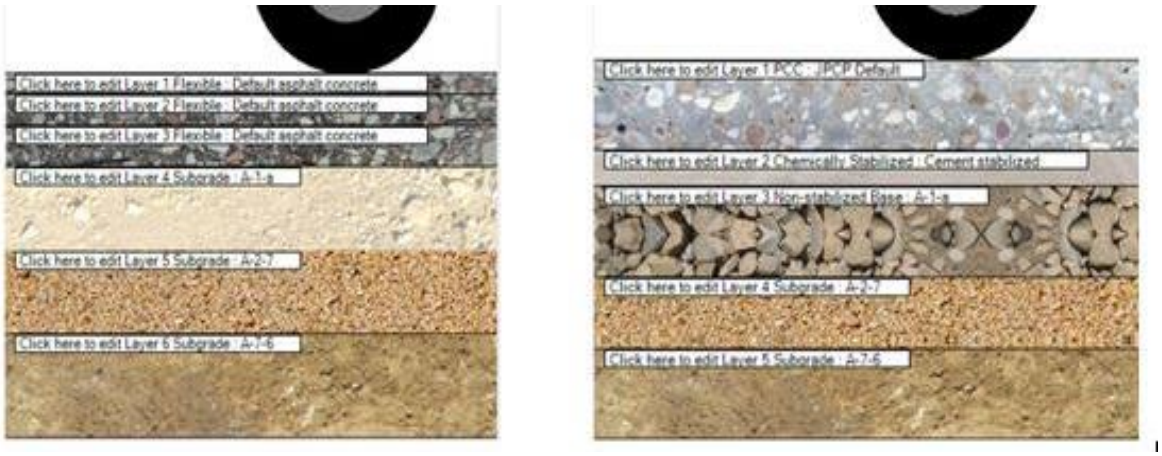

Figure 3-12: Pavement sections; (a) SH-48; and (b) SH-33

Flexible Pavement (SH-48)

The section SH-48 pavement consisted of three asphalt layers with a total thickness of 9 in. A granular aggregate base (RCA-1, RCA-2, RCA-3, and VLA-1) with a thickness of 8 in. was used below the three asphalt layers. Finally, an 8 in. thick stabilized subgrade was placed above the natural subgrade. Rutting, top-down, and bottom-up fatigue cracking were used to assess the performance of aggregate bases. According to the mechanistic-empirical pavement design guide (AASHTO, 2020), for an urban principal arterial roadway, the threshold for total rutting is 0.50 in., top-down fatigue cracking is 20% lane area, and bottom-up fatigue cracking is 20% lane area. The values considered for M_r, gradation, and thickness of each layer are listed In Table 3-4.

Table 3-4: Properties of SH-48 pavement section

	Thickness (in.)	Elastic/Resilient modulus (psi)	Gradation
Asphalt layer 1	2	Default	S4
Asphalt layer 2	3	Default	S3
Asphalt layer 3	4	Default	S3
Aggregate base	8	23,200 (RCA-1) 12,800 (RCA-2) 23,386 (RCA-3) 18,350 (VLA-1)	Type A
Stabilized subgrade	8	10,000	A-2-7
Subgrade	Semi-infinite	8,000	A-7-6

Rigid Pavement (SH-33)

The SH-33 pavement section consisted of a 10 in. Portland cement concrete (PCC) and a 4 in. cement stabilized base. A granular aggregate base (RCA-1, RCA-2, RCA-3, and VLA-1) with a thickness of 8 in. was used below the two superior layers. Finally, an 8 in. stabilized subgrade was placed above the natural subgrade.

Table 3-5: Properties of SH-33 pavement section

	Thickness (in.)	Elastic/Resilient modulus (psi)	Gradation
PCC	10	4,200,000	-
Cement stabilized base	4	2,000,000	-
Aggregate base	8	23,200 (RCA-1) 12,800 (RCA-2) 23,386 (RCA-3) 18,350 (VLA-1)	Type A
Stabilized subgrade	8	10,000	A-2-7
Subgrade	Semi-infinite	8,000	A-7-6

The international roughness index (IRI)(in./mile), mean joint faulting (in.), and transverse cracking (% slabs) were used to assess the performance of aggregate bases. From the mechanistic-empirical pavement design guide (AASHTO, 2020), for an urban principal arterial

roadway, the threshold for terminal IRI is 200 in./mile, mean joint faulting is 0.2 in., and transverse cracking is 15% slabs area. The values considered for $M_{r,}$ gradation, and thickness of each layer are listed in Table 3-5.

3.4. Costs Analysis

The life cycle cost analysis (LCCA) of the flexible pavement section SH-48 was performed based on the AASHTOWare Pavement ME simulations. The distress target values used for the LCCA were obtained from the recommended values in AASHTOWare Pavement ME software (version 2.5.5). Target failure values for pavement distress were established; for rutting, a value of 0.75 in. was used. For both top-down and bottom-up fatigue cracking, the target value was assumed to be 25% of the lane area. The year reaching 75% of the target value for each distress was identified from the AASHTOWare Pavement ME simulations for estimating costs. As a maintenance strategy for the pavement section, only two strategies were considered: crack filling every five years and milling and overlay when the distresses approached 75% of the target value. The initial and maintenance costs were converted to net present worth with a discount rate of 3%.

4. CHAPTER FOUR: LABORATORY TEST RESULTS

The stiffness, durability, and hydraulic properties of some commonly used RCAs and virgin aggregates in Oklahoma were assessed in this study. As discussed in Chapter 3, the aggregate properties, namely gradation, aggregate shape indices (angularity and texture), LA abrasion, OMC, and MDD, presence of contaminants were addressed. Additionally, the resilient modulus (M_r), permeability (k), and durability indices (D_f and D_c) of selected RCAs were compared to those of a virgin aggregate. Furthermore, x-ray diffraction (XRD) tests were conducted on RCA-3 and VLA-1 to determine the mineral compositions. The performance in terms of pavement distresses and costs of pavement bases using recycled and virgin aggregates were compared using the AASHTOWare Pavement ME simulations in Chapter 5. The findings of this study are expected to provide valuable information on the use of RCAs in the construction of new pavements and reconstruction of existing pavements.

4.1. Initial Gradation (as Received) of Different Aggregates

Gradation is one of the requirements in ODOT as well as other state DOTs specifications for selecting aggregate base materials (see e.g., Texas DOT, 2014; Colorado DOT, 2021; California DOT, 2018; Missouri DOT, 2021; Louisiana DOTD, 2026; Massachusetts DOT, 2020). Figure 4-1 presents the initial gradations of RCA-1, RCA-2, RCA-3, and VLA-1 aggregates. It was observed that the VLA-1 aggregate had an initial gradation that fell around the middle of the upper and lower limits of Type A aggregate base. Comparatively, the RCA-1 aggregate went beyond or outside of the lower limit gradation for sieve sizes #4 and #10, and RCA-3 followed the lower limit gradation for sieve sizes #10, #40, and #200. These differences in the aggregate gradations likely resulted from the breaking mechanisms used to produce these aggregates since the type of crusher used will affect the gradation and quality of the RCA

produced (Cavalline et al., 2022). The gradations of the VLA-1 and RCA-2 aggregates were close to the upper limit gradation. However, the gradations of the RCA-1 and RCA-3 aggregates were closer to the lower limit gradation. The source and quality of the material produced differences in gradation due to conditioning of the aggregates using different cycles (0, 100, 300, and 500 cycles) in the LA abrasion machine (Appendix B, see Figure B-1 to Figure B-8). Also, as discussed subsequently, gradation is one of the influencing factors for resilient modulus and coefficient of permeability – two design parameters used in AASHTOWare Pavement ME.

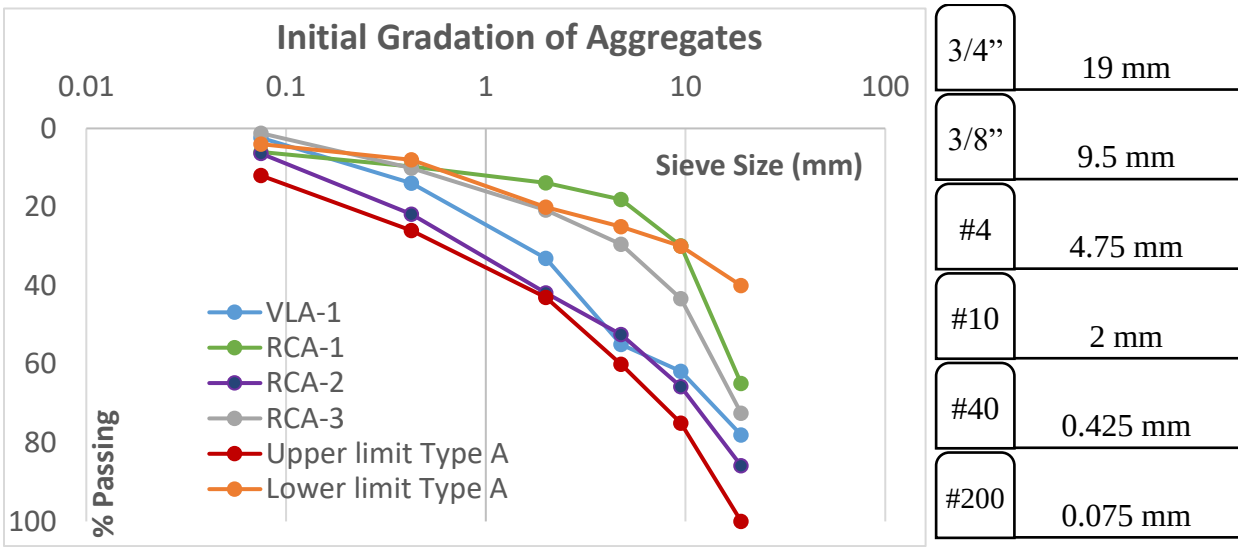

Figure 4-1: Initial gradation (as received) of RCA-1, RCA-2, RCA-3, and VLA-1 aggregates

4.2. Wash Loss and Contaminants of Different Aggregates

Recycled concrete aggregates often contain foreign materials or contaminants. Fine particles can adhere to the surface of the aggregates. The wash loss test was performed to compare the amount of loss of fine particles in each of the selected aggregates. The results are summarized in Table 4-1. It is seen that the VLA-1 and RCA-3 aggregates show relatively less wash losses, indicating good quality aggregates regarding wash loss. However, the RCA-1 and RCA-2 aggregates had significantly higher wash losses. For example, for sieve #10, RCA-2 had

the highest wash loss of 7.3% compared to 4.9% for RCA-1, 1.68% for RCA-3, and 1.23% for VLA-1 aggregates. The RCA-2 aggregate produced in a recycling plant had numerous clay clumps that could not be removed through washing. The RCA produced in recycling plants contains bricks, tiles and other contaminants that come with the rubble and may negatively affect the quality of the material. However, high quality aggregate is expected from known sources like highways and airfield pavements (Mukhopadhyay et al., 2018). Therefore, it is expected that RCAs produced in recycling plants like RCA-2 would exhibit poor behavior compared to those produced in-place from existing highway pavements (RCA-1 and RCA-3). The RCA-1 aggregate exhibited a higher wash loss than the virgin aggregate. The RCA-1 aggregate had clay clumps, indicating possible contamination with the underlying soil.

Table 4-1: Percent wash loss of different aggregates

Size	%Loss due to washing with water			
	VLA-1	RCA-1	RCA-2	RCA-3
3/4”	0.64	1.45	1.63	0.69
3/8”	0.50	1.29	1.51	0.15
#4	0.94	3.12	3.56	0.93
#10	1.23	4.86	7.30	1.68

Contaminants were found in all RCAs and the level of contaminants varied among the RCAs. The RCA-3 had the least contaminants, mostly plastic fibers and asphalt-coated aggregates (Figure 4-2), whereas RCA-2 had the most contaminants, including clay clumps, tiles, glass, twigs, and plastics (Figure 4-3). The RCA-1 had some twigs and mostly clay clumps (Figure 4-4). Considering all aggregate sources, RCA-2 contained higher contamination compared to the other aggregates. Comparatively, the VLA-1 and RCA-3 showed significantly less contamination. From the contamination point of view, it is expected that RCA-2 will have a higher potential for durability loss than the other aggregates since it has a considerably higher

wash loss. It is important to note that clay like particles are frequently present in recycled aggregates produced in recycling plants and can negatively affect their performance (Mukhopadhyay et al., 2018) and should be carefully evaluated in order to ensure their suitability for use in the construction of new pavements and reconstruction of existing pavements.

The contaminants present in RCAs can be harmful to the performance of an aggregate base. Therefore, limiting the level of contamination or presence of foreign particles is necessary to ensure desired performance. As discussed in Chapter 2, several DOTs have specified the amounts of contaminants allowed in their aggregate base. It is expected that RCAs produced in-place will be of higher quality than plant produced RCAs and will have fewer contaminants (Mukhopadhyay et al., 2018, Cavalline et al., 2022). The results support the relatively clean environment used to produce RCAs in-place where fewer foreign contaminants are expected. Aggregates produced in-place, such as RCA-3 and RCA-1, are expected to have fewer detrimental contaminants.

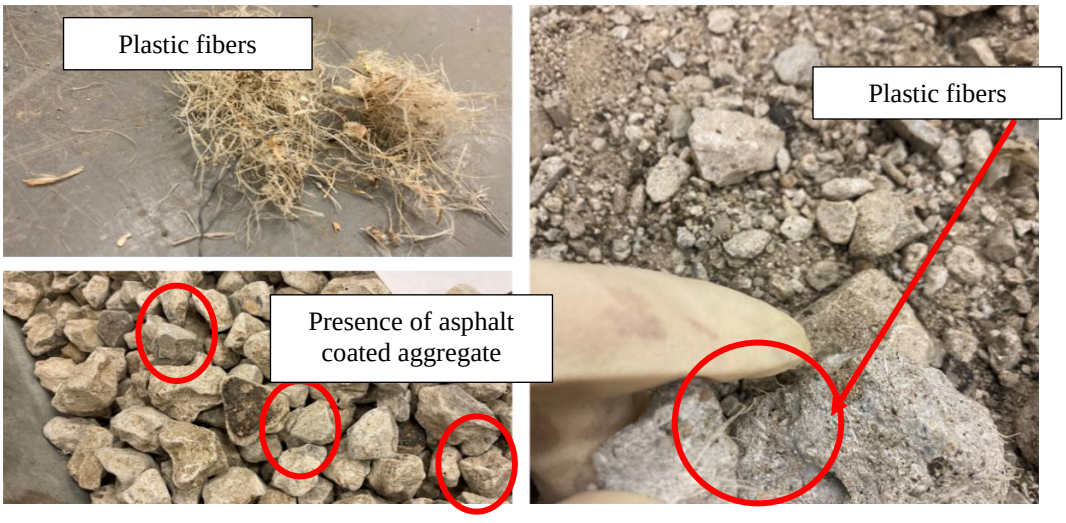

Figure 4-2: Contaminants in RCA-3

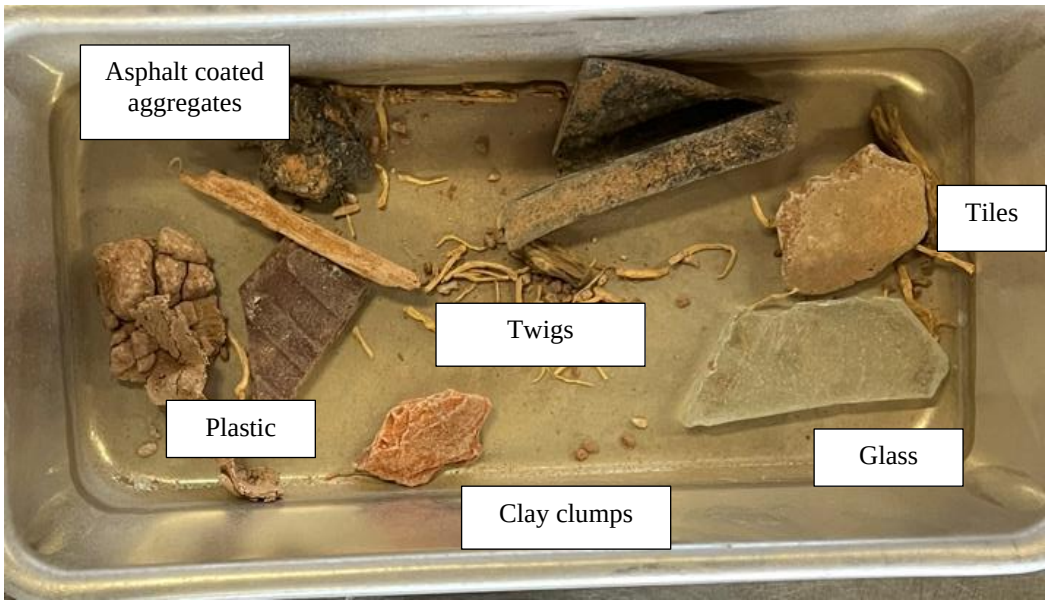

Figure 4-3: Contaminants in RCA-2

Figure 4-4: Contaminants in RCA-1

4.3. Elemental Analysis of Aggregates (XRD)

X-ray diffraction (XRD) tests were used to determine the mineralogical compositions of the VLA-1 and RCA-3 aggregates. Due to limited resources and logistics, the XRD tests were not pursued for the RCA-1 and RCA-2 aggregates. The XRD spectra for VLA-1 and RCA-3 aggregates can be found in Appendix E (see Figure E-1 to Figure E-2). The mineralogical

compositions of the VLA-1 and RCA-3 aggregates are presented in Table 4-2. It was observed that the RCA-3 aggregate mainly contains dolomite (80.8%) and limestone (12.1%). The VLA-1 aggregate is composed of limestone (78.1%), arcanite (17.5%), and quartz (4.4%). Typically, dolomite exhibits higher hardness than limestone. As a result, RCA-3 (produced in-place) is expected to exhibit less loss due to abrasion, impact, environmental and traffic loading than limestone aggregate (VLA-1).

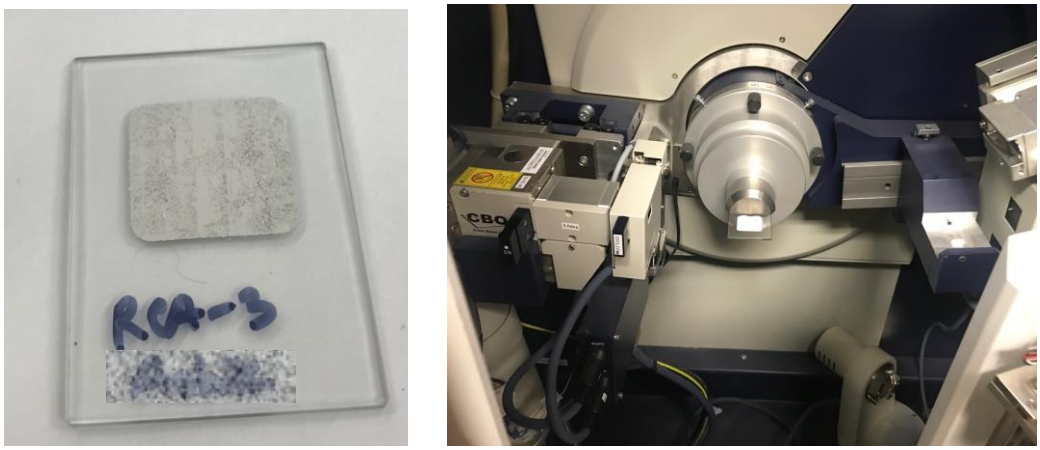

Figure 4-5: (a) Powder XRD sample and (b) XRD test setup

Table 4-2: Elemental analysis of aggregates

RCA-3				VLA-1			
Mineralogical composition		Oxides		Mineralogical composition		Oxides	
Dolomite ($MgCa(CO_3)_2$)	80.8%	CaO	31.4%	Calcite ($CaCO_3$)	78.1%	CaO	48.8%
Calcite ($CaCO_3$)	12.1%	K_2O	0.6%	Arcanite (K_2SO_4)	17.5%	K_2O	9.4%
Sanidine-high ($KAlSi_3O_3$)	3.6%	SiO_2	2.3%	Quartz (SiO_2)	4.4%	SO_3	8.0%
Graphite (C)	3.5%	Al_2O_3	0.7%			SiO_2	4.4%
		MgO	17.7%			CO_2	34.4%
		CO_2	56.7%				

4.4. LA Abrasion Losses at Different Cycles

In order to use aggregate as a pavement base, state DOTs have established different requirements to ensure quality and durability. For example, ODOT requires a maximum loss of 50% in the LA abrasion test (ODOT, 2019). As can be seen in the test results summarized in Table 4-3, the RCA-3 aggregate showed lower abrasion losses for all the conditioning cycles. Abrasion losses of RCA-3 and VLA-1 aggregates were similar. Comparatively, the RCA-1 and RCA-2 aggregates exhibited higher abrasion losses than the virgin aggregate.

As mentioned in Chapter 2, previous studies have found RCAs to have higher abrasion losses than virgin aggregates (see e.g., Gabr and Cameron, 2012; da Conceição Leiteet al., 2011). The quality of the material, however, is expected to affect the resistance to abrasion. From Table 4-3, RCA-3 and VLA-1 had similar values in the LA abrasion for all the aforementioned cycles. At 100 cycles, all the RCA-3 and VLA-1 aggregates exhibited similar losses. For 300 and 500 cycles, RCA-1 and RCA-2 had significantly higher losses than RCA-3 and VLA-1. The presence of clay clumps and contaminants found on RCA-1 and RCA-2 are thought to be responsible for the higher values of abrasion losses. For RCA-1 and RCA-2, it was observed that the sample for the LA abrasion had many clay clumps that would easily be abraded by the steel spheres causing a significant impact in the LA abrasion values since all the aggregates passing the #12 sieve need to be discarded according to the test procedure. The RCA-3 aggregate used for this study was expected to have improved behavior because of the high quality (fewer foreign particles) of RCA obtained from highway pavements. A low abrasion loss of VLA-1 and RCA-3 indicates that these aggregates are expected to have higher resistance to degradation caused by abrasion. Other aggregates produced in-place exhibiting qualities similar to RCA-3 are expected to perform well in the LA abrasion test.

Table 4-3: Abrasion loss of different aggregates

Aggregates	LA abrasion cycles		
	100 cycles (%)	300 cycles (%)	500 cycles (%)
VLA-1	11.0	17.3	29.2
RCA-1	11.4	28.2	42.8
RCA-2	12.0	26.7	38.4
RCA-3	10.9	12.5	23.2

4.5. Moisture-Density Relations of Different Aggregates

The moisture-density relationships were determined using the modified Proctor method. Specifically, the optimum moisture content (OMC) and the maximum dry density (MDD) values were determined using this test for the upper and lower limit gradations of all aggregates. Table 4-4 includes a summary of these results. It was observed that all the RCAs had higher OMCs than the virgin aggregate. Also, the MDDs of all RCAs were lower than those of the virgin aggregate (VLA-1). Also, an oversized aggregate correction was needed for the lower limit gradation for all aggregates. The moisture-density relationships of all aggregates are graphically illustrated in Appendix A (see Figure A-1 to Figure A-8).

For the upper limit gradation, the OMC of RCA-1, RCA-2, and RCA-3 were 6.3%, 8.7%, and 10.0%, respectively. Comparatively, for the same gradation (UL), the OMC for the VLA-1 aggregate was 5.1%. The MDD for the UL of the VLA-1 aggregate was 144.4 pcf, whereas, for the RCAs, the MDD ranged from 118.6 pcf to 121.3 pcf. For the lower limit gradation, the OMC values of RCA-1, RCA-2, and RCA-3 were 5.6%, 7.2%, and 8.3%, respectively. Comparatively, for the same gradation (LL), the OMC for the VLA-1 aggregate was 2.7%. The MDD for the LL of the VLA-1 aggregate was 156.1 pcf, whereas, for the RCAs, the MDD ranged from 127.3 pcf to 134.4 pcf. The RCAs used in this study were produced by crushing existing concrete structures. The coarser part of the aggregate is primarily composed of aggregate with attached

cement mortar which can absorb more water and increase the water demand. Also, these concrete coated aggregates are porous, allowing more water to penetrate them, reducing their density, and allowing the material to hold more water. Other researchers have found a similar trend where the OMC of RCA is higher, and the MDD is lower than that of virgin aggregates (see e.g., Park, 2003; Poon and Chan, 2006; Gabr and Cameron, 2012; Arulrajah et al., 2013).

Table 4-4: OMC and MDD of different aggregates

	Upper limit				Lower limit			
	VLA-1	RCA-1	RCA-2	RCA-3	VLA-1	RCA-1	RCA-2	RCA-3
OMC (%)	5.1	6.3	8.7	10.0	2.7	5.6	7.2	8.3
MDD (pcf)	144.4	118.6	126.3	121.3	143.0	120.7	1230.	122.1
MDD* (pcf)	-	-	-	-	156.1	131.2	134.4	127.3

* After oversized correction

4.6. Angularity and Texture of Different Aggregates

The angularity and texture of all aggregates were determined using the AIMS test. For the upper limit gradation, the AIMS test was performed on the aggregate retaining on 3/8” and #4 sieves. For the lower limit gradation, the AIMS test was performed on the aggregate retaining on 3/4”, 3/8”, and #4 sieves.

The average textures of the aggregates with no conditioning are presented in Table 4-5 and Table 4-6 for the upper limit and lower limit gradations, respectively. For the upper limit gradation, the texture of VLA-1 was higher than RCA-1 and RCA-2 but lower than RCA-3. In all cases, the aggregates of larger sieve sizes had higher texture (Table 4-5). For the lower limit gradation, RCA-3 values were higher than VLA-1, except for sieve size 3/4”. Also, RCA-1 had a lower texture than VLA-1, as seen in Table 4-6. However, for the aggregates with no conditioning, the average textures were similar in magnitude. The differences in properties are thought to be caused by the crushing mechanism used to produce these aggregates. Cavalline et

al. (2022) mentioned that the crushing equipment and operational practices had impacts on the angularity and texture of RCAs.

Table 4-5: Average texture for the upper limit for aggregates with no conditioning

Aggregate conditioning	Average texture (UL)							
	Retaining on 3/8" sieve				Retaining on #4 sieve			
	VLA-1	RCA-1	RCA-2	RCA-3	VLA-1	RCA-1	RCA-2	RCA-3
0 cycle	242.5	197.2	209.8	255.1	184.4	160	175.7	205.4

* 0 <Polished < 165 < Smooth < 275

Table 4-6: Average texture for the lower limit for aggregates with no conditioning

Aggregate conditioning	Average texture (LL)								
	Retaining on 3/4" sieve			Retaining on 3/8" sieve			Retaining on #4 sieve		
	VLA-1	RCA-1	RCA-3	VLA-1	RCA-1	RCA-3	VLA-1	RCA-1	RCA-3
0 cycle	367.7	220.5	316.5	247.5	197.2	255.1	191.9	160	205.4

* 0 <Polished < 165 < Smooth < 275 < Low Roughness < 350

The average angularities of the aggregates are presented in Table 4-7 and Table 4-8 for the upper limit and lower limit gradations, respectively. Regarding gradient angularity for the upper limit gradation, The RCA-2 aggregate exhibited the lowest angularity among all three aggregates. For aggregates retaining on the 3/8" sieve, however, the angularity of the RCA-1 was 3,117.1, which was higher than the VLA-1 (Table 4-7). For the lower limit gradation, the angularity of the VLA-1 was higher than the RCA-1 for aggregates retaining on 3/4" and #4 sieves. Also, the angularity of RCA-3 was lower than VLA-1 for all sieve sizes in both the upper limit and lower limit gradations. Similar to texture, the angularities were similar in magnitude and classified as sub-rounded. As mentioned previously, the crushing mechanism and operational practices used to produce these aggregates are thought to be responsible for this trend.

Table 4-7: Average gradient angularity for the upper limit for aggregates with no conditioning

Aggregate conditioning	Average gradient angularity (UL)							
	Retaining on 3/8" sieve				Retaining on #4 sieve			
	VLA-1	RCA-1	RCA-2	RCA-3	VLA-1	RCA-1	RCA-2	RCA-3
0 cycle	2,937.5	3,117.1	2,823.3	2,847.4	3,386.2	3,330.3	3,154.0	2,945.8

* 2,100 < Sub-rounded < 4,000

Table 4-8: Average gradient angularity for the lower limit for aggregates with no conditioning

Aggregate conditioning	Average gradient angularity (LL)								
	Retaining on 3/4" sieve			Retaining on 3/8" sieve			Retaining on #4 sieve		
	VLA-1	RCA-1	RCA-3	VLA-1	RCA-1	RCA-3	VLA-1	RCA-1	RCA-3
0 cycle	2,920.5	2,701.5	2,532.2	2,864.4	3,117.1	2,847.4	3,386.2	3,330.3	2,945.8

* 2,100 < Sub-rounded < 4,000

4.7. Resilient Modulus of Different Aggregates

Previous studies have used different models to correlate the resilient modulus of aggregate bases with stress levels (Khoury et al., 2010). These models were based on different independent variables, such as confining pressure (σ_3), deviatoric stress (σ_d), bulk stress (θ), and octahedral stress (τ_{oct}). The bulk stress (θ) model, presented in Equation (3), has been used widely for unbound aggregate bases (Andrei et al., 2004). In this study, this model was used to represent the M_r of aggregate bases as a function of θ. A Bulk stress (θ) of 15 psi was used to calculate the design resilient modulus for aggregate bases, as recommended in the AASHTO 1993 design (Huang, 2004).

$$M_r = k_1 \theta^{k_2} \qquad (3)$$

where:

M_r = resilient modulus, and

k_1, k_2 = model parameters

Table 4-9 compares the design resilient modulus values of all aggregates with no conditioning. The design resilient modulus values for the VLA-1 aggregate were found to vary between 19,089 psi and 11,378 psi for the upper and lower limit gradations, respectively, with an average of 15,234 psi. The average resilient modulus for the RCA-3 aggregate was 22,912 psi (23,386 psi for UL to 22,437 psi for LL), for RCA-1 was 18,088 psi (23,200 psi for UL to 12,975 psi for LL), and for RCA-2 was 11,800 psi (12,800 psi for UL to 10,800 for LL). The RCA-3 and RCA-1 aggregates exhibited higher M_r values than the corresponding values for the VLA-1 aggregate for the upper and lower limit gradation. Based on these results, RCA-1 and RCA-3 are expected to perform better than the VLA-1 aggregate as pavement bases. Regarding RCA-2, the M_r values were found to be lower than those of VLA-1, RCA-1, and RCA-3 aggregates. The reduced strength of RCA-2 was believed to be caused by the inferior quality of source materials. The RCA-2 was produced in a recycling plant with concrete of different qualities and varying amounts of contaminants. The high M_r values observed for the RCA-3 likely resulted from the proper control of quality during the construction of the highway pavement section. Also, RCA-1 exhibited higher M_r values than the virgin aggregates. Both of these aggregates (RCA-1 and RCA-3) were produced on-site from existing highway pavements with high quality materials, producing high quality recycled aggregates. Other researchers have reported M_r of recycled aggregates to be higher or comparable to that of a virgin aggregate (see e.g., Bennert et al., 2000; da Conceição Leite et al., 2011; Gabr and Cameron, 2012). The M_r values for each loading sequence and the design M_r values for the aggregates for the upper and lower limit gradations are shown in Appendix C (see Table C-1 to Table C-16).

Table 4-9: Design resilient modulus values of all aggregates

Aggregate type	Gradation	Limit	K_1	K_2	Design resilient modulus (psi)	Average M_r
VLA-1	ODOT Type A	Upper	7,402.60	0.35	19,089	15,234
		Lower	3,807.80	0.4	11,378	
RCA-1		Upper	7,037.50	0.44	23,200	18,088
		Lower	4,160.80	0.42	12,975	
RCA-2		Upper	5,108.5	0.34	12,800	11,800
		Lower	3,659.9	0.4	10,800	
RCA-3		Upper	8,385.7	0.38	23,386	22,912
		Lower	6,604.7	0.45	22,437	

Changes in Resilient Modulus of Aggregates (0, 7, and 30 days)

During the testing stage, it was observed that the RCA-3 samples became hardened after resilient modulus (M_r) testing. It was hypothesized that the fine particles in the RCA and additional fine particles generated by the compaction process acted as the cementing agent in the presence of water during the sample preparation process. Therefore, samples with the CRCA-3 aggregate were prepared and tested after 0, 7, and 30 days at their OMCs to observe changes in M_r over time. The samples were sealed and left undisturbed in a sealed container at room temperature. The moisture content was conserved by maintaining the saturation level inside the container. Figure 4-6 shows the behavior relative to M_r values of RCA-3 after 0, 7, and 30 days of curing at OMC. It can be seen that, as time progressed, the strength increased steadily. For comparison, the design M_r values are summarized in Table 4-10. The design M_r values were positively affected by curing time. The design M_r values were 23,308 psi at 0 days, 27,011 psi at 7 days, and 29,723 psi at 30 days of curing. Therefore, recycled aggregates having similar characteristics to RCA-3 are expected to increase in strength over time. It is believed that this behavior is due to the reaction of unhydrated cement particles in the presence of moisture. As finer particles are generated during aggregate placement and compaction in the field, the stiffness

of the base may increase. However, the opposite trend is expected for drainage (Poon et al., 2006).

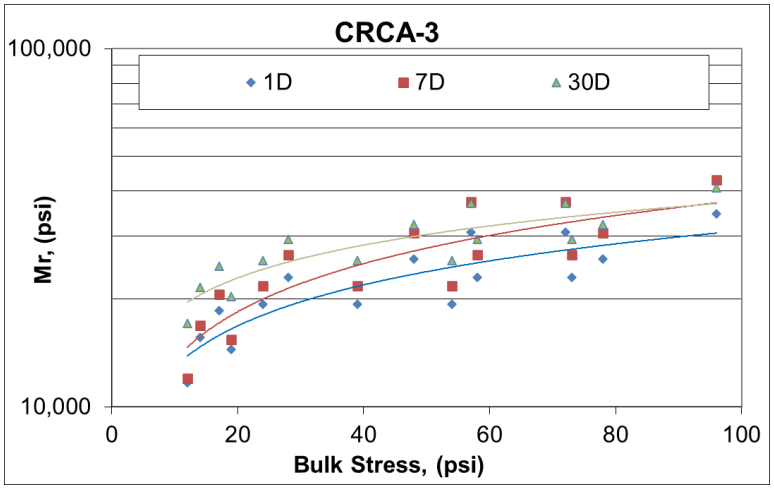

Figure 4-6: Resilient modulus of the CRCA-3 aggregates after 0, 7, and 30 days

Table 4-10: Design resilient modulus values of the CRCA-3 after 0, 7, and 30 days

Aggregate type	Gradation	Time	K_1	K_2	Design resilient modulus (psi)
C.RCA-3	ODOT Type A (As received)	1D	7,698.78	0.42	23,308
		7D	7,362.51	0.49	27,011
		30D	12,242.63	0.34	29,723

4.8. Durability index of Different aggregates

Foreign particles can be detrimental to the performance of aggregate bases. Therefore, ODOT and several other state DOTs use the durability index (DI) to measure the relative resistance of the aggregate to produce detrimental clay like particles. ODOT specifications require a minimum DI of 40 for both the finer part (D_f) and coarser part (D_c) of aggregates.

For the coarser part (D_c), the test requires only a set amount of each sieve size. Specifically, the material retained in sieve sizes 1/2”, 3/8”, and #4 sieve with a dried mass of

1,050 g, 550 g, and 900 g, respectively. Therefore, the upper and lower limit gradations have the same results. From Table 4-7, the durability index of the coarser part (D_c) met the minimum requirement of 40. It was observed that the coarser part mostly contained crushed concrete clumps, which were expected to perform well. Furthermore, the durability indices of the coarser part (D_c) of RCA-2 and RCA-3 were comparable to that of VLA-1. The RCA-2, RCA-3, and VLA-1 aggregates had D_c values of 71, 78, and 73, respectively. The D_c value of RCA-3 was higher than VLA-1, suggesting a greater resistance to durability issues. In contrast, RCA-1 had the lowest value of D_c, suggesting a lower resistance to durability issues than the virgin aggregate. However, all of the values are considerably above the threshold limit of 40 suggested by ODOT.

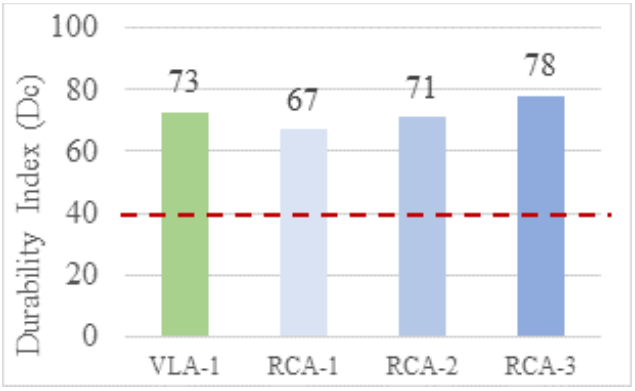

Figure 4-7: Coarse aggregate durability indices of different aggregates

For the finer part (D_f), the test required taking a representative sample from each selected gradation. Therefore, the results obtained for the upper and lower limit gradations were different. Figure 4-8(a) and Figure 4-8(b) summarize the durability indices for the finer part of the upper limit and lower limit gradation of the aggregates, respectively. It was observed that the RCA-1 (34 for the UL and 29 for the LL) and RCA-2 (26 for the UL and 23 for the LL) did not satisfy the ODOT minimum requirement of 40 for the durability of the upper limit and lower limit gradations. However, VLA-1 (72 for the UL and 75 for the LL) and RCA-3 (60 for the UL and

55 for the LL) met the requirements for both the upper and lower limit gradations of the aggregate. During testing, it was observed that both RCA-1 and RCA-2 contained clay clumps that remained even after washing. Controlling the amount of these contaminants is essential to maintaining the quality of RCA bases. From the aforementioned results, it is evident that the fine aggregate durability test could be used as a screening tool to ensure the quality of recycled aggregate. Mukhopadhyay et al. (2018) mentioned the durability of the finer part (D_f) was a useful screening tool since most RCAs had difficulties passing this test.

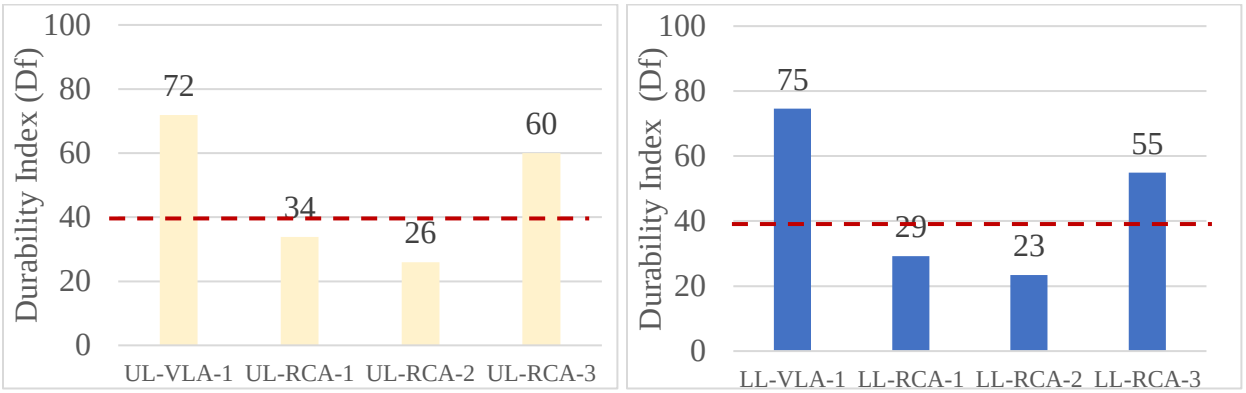

(a) (b)

Figure 4-8: Fine aggregate durability for (a) upper and (b) lower limits gradation of different aggregates

4.9. Permeability of Different Aggregates

The permeability values of all four aggregates with no conditioning are summarized in Table 4-11 and Table 4-12 for the upper and lower limit gradations, respectively. The permeability of the aggregates for the upper and lower limit gradations showed no specific trend. However, the values were similar in magnitude for the upper and lower limit gradations. The reason for this behavior can be attributed to the fact that aggregate gradation remained consistent (in the UL and LL, respectively), and no significant differences in shape indices (angularity and

texture) were observed without conditioning. The permeability curves for all aggregates are exhibited graphically in Appendix F (see Figure F-1 to Figure F-13).

Performing a falling head permeability test can be challenging due to a number of factors. One of the main difficulties is that the rubber membrane used in the test can be punctured by the compacted aggregates, which can cause the test to fail. In addition, during the testing process, new drainage paths can be created, resulting in a sudden increase in head loss that can render the test data inappropriate for estimating permeability values. This was observed during the test, where a steep increase in head loss was noted, making the test results invalid. Moreover, the type of mold used for compacting samples can pose additional challenges. The sample can be damaged or cracked during extrusion from the mold, creating additional drainage paths that would affect the permeability of the samples. To obtain accurate results, it was of paramount importance to carefully monitor the testing process and take measures to minimize these potential sources of error.

Table 4-11: Permeability of aggregates for upper limit gradations with temperature correction

UL	k		n	T (°c)
	cm/s	ft/day		
VLA-1	3.40E-03	9.65	1.98	21.2
RCA-2	4.06E-03	11.52	0.35	20.4
RCA-3	2.88E-03	8.15	0.75	23.2

Table 4-12: Permeability of aggregates for lower limit gradations with temperature correction

LL	k		n	T(°c)
	cm/s	ft/day		
VLA-1	9.38E-03	26.59	1.28	21.0
RCA-1	1.03E-02	29.09	0.83	21.0
RCA-3	5.85E-03	16.60	1.25	25.0
C.RCA-3	6.03E-03	17.09	0.89	21.2

4.10. Changes in Gradation and Shape Parameter Corresponding to Field Compaction

Degradation during the service life of aggregate bases can be divided into two stages, namely loss during construction (specifically during vibratory compaction) and loss during the service life from vehicular traffic and environmental conditions. The gradation of the aggregate base is known to significantly impact the behavior of pavement bases. The changes in gradations and shape parameters due to varying number of LA abrasion cycles were used to estimate the changes in properties during construction (specifically placement and compaction). For this purpose, the upper and lower limit gradations of the aggregates were conditioned using the LA abrasion machine with 100, 300, and 500 cycles. After each set of cycles, the changes in gradation and shape parameters (angularity and texture) were determined. First, changes in gradation and shape indices due to laboratory compaction (modified Proctor) were determined and used to estimate expected changes during placement and compaction in the field. Compaction energy was used as a basis for this estimation. Finally, the results from a field compacted aggregate (CRCA-3) were compared to the uncompacted aggregate (RCA-3) to verify the results estimated through laboratory compaction.

The compaction energy used in preparing an aggregate sample according to the modified Proctor method was estimated as 56,000 lbf-ft/ft^3 as described in ASTM D1557-12 (ASTM, 2021). The compaction energy used by a vibratory roller ranges from 27,200 to 55,750 lbf-ft/ft^3 (DYNAPAC CA250D technical data sheet), with an average of 41,400 lbf-ft/ft^3 for each pass. Three passes of this vibratory roller were assumed to provide the optimum compaction, with a corresponding energy of 124,200 lbf-ft/ft^3. Thus, the compaction effort for three passes of a vibratory roller requires about twice the energy required for the compaction effort used in the

laboratory based on the modified Proctor method. This equivalency was used in correlating laboratory compaction with placement and compaction in the field.

The changes in the gradation of the RCA-1 aggregate for the upper limit gradation with different LA abrasion cycles and after laboratory compaction are presented in Figure 4-9. From Figure 4-9, it was observed that the gradation after compaction in the modified Proctor test is similar to the gradation after 100 cycles in the LA abrasion test. The changes in the gradations for the remaining aggregates are graphically presented for the upper and lower limit in Appendix B (see Figures B-1 to Figure B-8). Similar results were observed for the other aggregates as well. Therefore, it is hypothesized that field compaction can be equivalent to 200-300 cycles in the LA abrasion test since the compaction effort in the field is approximately twice compared to laboratory compaction. The hypothesis is later verified using RCA-3 and CRCA-3. Table 4-13 summarizes the changes in texture, and Table 4-14 summarizes the changes in angularity of aggregates retaining on 3/8" and #4 sieves for the upper limit gradation of the VLA-1, RCA-1, and RCA-2 aggregates with different LA abrasion cycles and after laboratory compaction. For the lower limit gradation, Table 4-15 summarizes the changes in texture and Table 4-16 summarizes the changes in angularity of aggregates retaining on 3/4", 3/8" and #4 sieves of the VLA-1, RCA-1, and RCA-2 aggregates with different LA abrasion cycles and after laboratory compaction. From the AIMS test results, the angularity values of aggregates after the modified Proctor compaction were similar to that for the 100 cycles in a LA abrasion machine. Therefore, it can be concluded that the field placement and compaction cause durability change equivalent to 200-300 cycles in a LA abrasion machine since the compaction effort in the field is approximately twice compared to laboratory compaction.

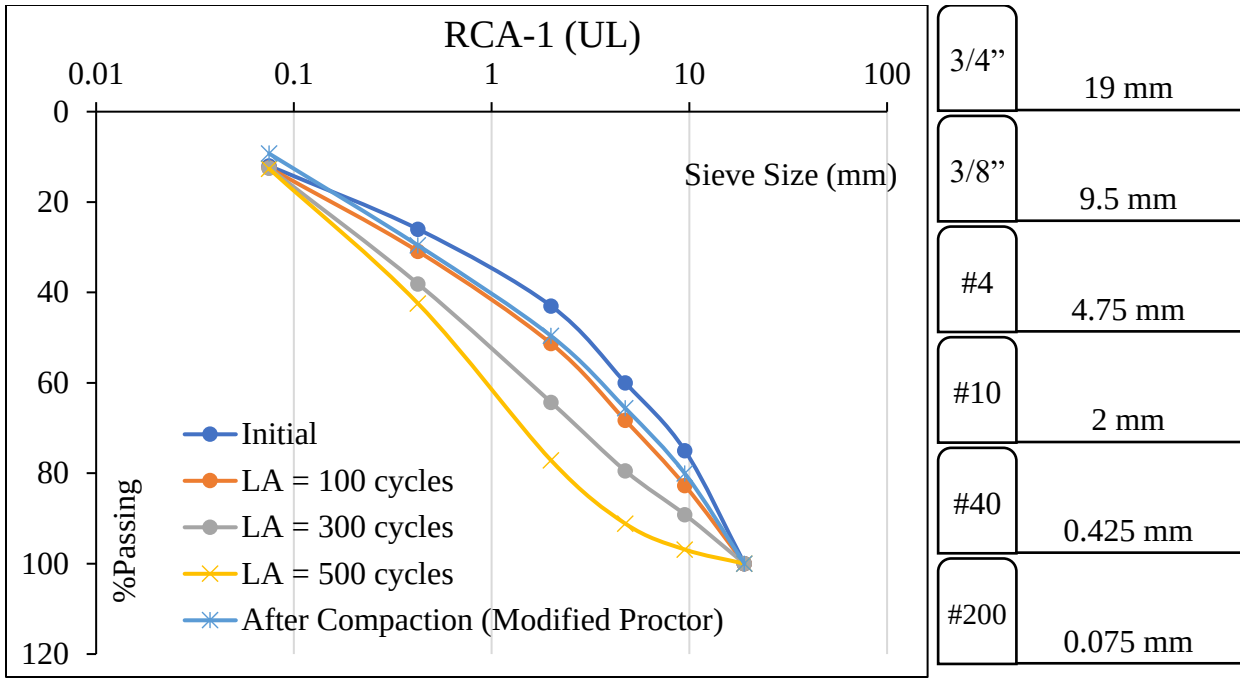

Figure 4-9: Change in gradation of RCA-1 (UL) with different LA abrasion cycles and laboratory compaction

Table 4-13: Changes in texture with different LA abrasion cycles and laboratory compaction for the UL gradation

Aggregate conditioning	Average texture (UL)					
	Retaining on 3/8” sieve			Retaining on #4 sieve		
	VLA-1	RCA-1	RCA-2	VLA-1	RCA-1	RCA-2
0 cycle	242.5	197.2	209.8	184.4	160.0	175.7
100 cycles	295.3	173.7	196.0	238.0	139.9	152.7
300 cycles	281.8	163.5	196.2	219.4	151.9	152.2
500 cycles	298.9	163.4	208.3	228	156.5	158.1
After compaction	245.8	188.5	203.5	175.9	152.3	160.3

* 0 <Polished < 165 < Smooth < 275

Table 4-14: Changes in angularity with different LA abrasion cycles and laboratory compaction for the UL gradation

Aggregate conditioning	Average gradient angularity (UL)					
	Retaining on 3/8" sieve			Retaining on #4 sieve		
	VLA-1	RCA-1	RCA-2	VLA-1	RCA-1	RCA-2
0 cycle	2,937.5	3,117.1	2,823.3	3,386.2	3,330.3	3,154.0
100 cycles	2,521.0	2,757.4	2,561.0	2,706.1	2,811.9	3,100.2
300 cycles	2,118.4	2,476.1	2,576.0	2,392.6	2,748.8	2,528.4
500 cycles	1,963.5	2,436.1	2,161.4	2,371.6	2,439.5	2,568.6
After compaction	2,316.9	2,921.3	2,731.3	2,649.5	2,785.9	2,968.6

*0 <Rounded <2,100 < Sub-rounded < 4,000

Table 4-15: Changes in texture with different LA abrasion cycles and laboratory compaction for the LL gradation

Aggregate conditioning	Average texture (LL)					
	Retaining on 3/4" sieve		Retaining on 3/8" sieve		Retaining on #4 sieve	
	VLA-1	RCA-1	VLA-1	RCA-1	VLA-1	RCA-1
0 cycle	367.7	220.5	247.5	197.2	191.9	160.0
100 cycles	371.9	221.5	280.9	166.6	208.6	143.8
300 cycles	377.4	191.4	308.8	170.4	232.8	141.6
500 cycles	360.8	193.0	298.9	164.4	245.8	158.3
After compaction	363.4	198.2	260.5	182.5	220.5	152.7

* 0 <Polished < 165 < Smooth < 275

Table 4-16: Changes in angularity with different LA abrasion cycles and laboratory compaction for the LL gradation

Aggregate conditioning	Average gradient angularity (LL)					
	Retaining on 3/4" sieve		Retaining on 3/8" sieve		Retaining on #4 sieve	
	VLA-1	RCA-1	VLA-1	RCA-1	VLA-1	RCA-1
0 cycle	2,920.5	2,701.5	2,864.4	3,117.1	3,386.2	3,330.3
100 cycles	2,134.0	2,252.8	2,587.6	2,605.5	3,055.9	3,044.4
300 cycles	2,057.6	2,037.4	2,149.1	2,444.5	2,610.6	2,852.2
500 cycles	1,990.1	1,877.0	1,963.5	2,157.9	1,963.5	2,662.2
After compaction	2,338.4	2,185.3	2,426.3	2,552.6	2,927.3	2,895.6

*0 <Rounded <2,100 < Sub-rounded < 4,000

In addition to using energy as a basis, LA abrasion cycles were correlated to field placement and compaction by comparing the properties (gradation and shape indices) of uncompacted (RCA-3) and a field compacted aggregate (CRCA-3). Figure 4-10 shows the as-received gradations of RCA-3 and CRCA-3. The upper and lower limits of the ODOT Type A gradations are shown as a reference (Figure 4-10). As expected, the CRCA-3 aggregate exhibited a finer gradation than RCA-3 due to field placement and compaction. The changes in gradation of the RCA-3 aggregate varied from 1.5% to 22.5% for different sieve sizes, as seen in Table 4-17. The most affected sieve sizes were 3/4", 3/8", #4 and #10, with a change of 15.9%, 22.5%, 18.3% and 12.1%, respectively.

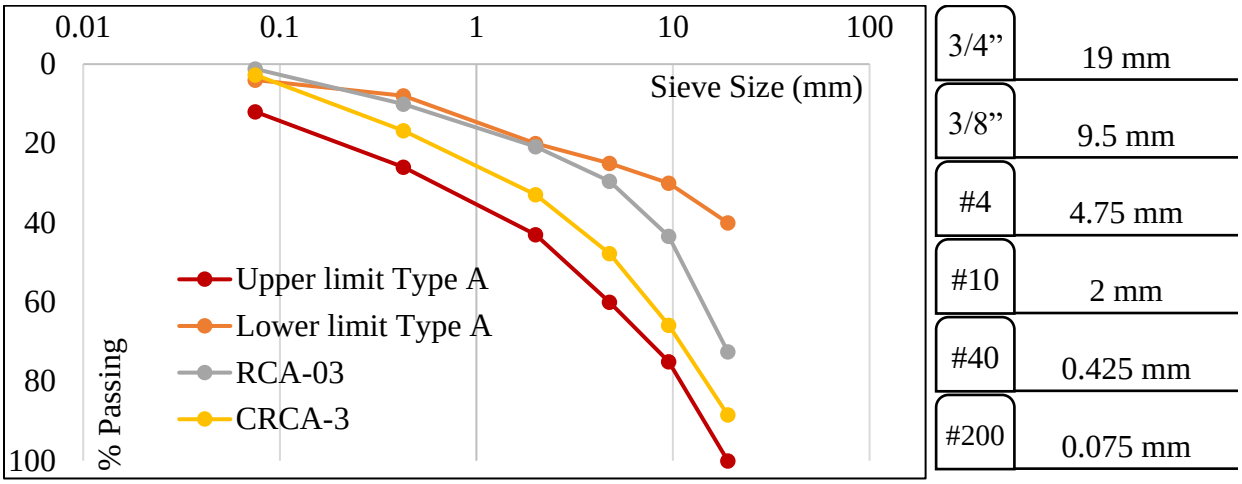

Figure 4-10: RCA-3 gradation after field placement compaction

Table 4-17: Changes in gradation due to field placement and compaction

Sieve Sizes	Upper limit Type A (%passing)	Lower limit Type A (%passing)	RCA-3 (%passing)	CRCA-3 (%passing)	Difference (%)
3/4"	100	40	72.5	88.4	15.9
3/8"	75	30	43.4	65.8	22.5
#4	60	25	29.5	47.7	18.3
#10	43	20	20.8	32.9	12.1
#40	26	8	10.1	16.8	6.7
# 200	12	4	1.2	2.7	1.5

To simulate the impact of field placement and compaction, laboratory samples were prepared for the upper and lower limit gradations of RCA-3. The samples were then subjected to mechanical degradation under different cycles in the LA abrasion machine (100, 300, and 500 cycles). Figure 4-11 and Figure 4-12 show the changes in gradations of the RCA-3 for the upper and lower limit gradations, respectively. Because of the degradation caused by the LA abrasion cycles, the aggregate became finer with increased LA abrasion cycles. For the upper limit gradation of the RCA-3 aggregate (Figure 4-11), approximately 300 cycles in the LA abrasion machine are expected to produce changes in the gradation similar to field placement and compaction. For the lower limit gradation of the RCA-3 aggregate (Figure 4-12), approximately 200 cycles in the LA abrasion machine are expected to produce changes in the gradation similar to field placement and compaction. It can be concluded that field placement and compaction caused changes in angularity and texture equivalent to 200-300 cycles in the LA abrasion machine.

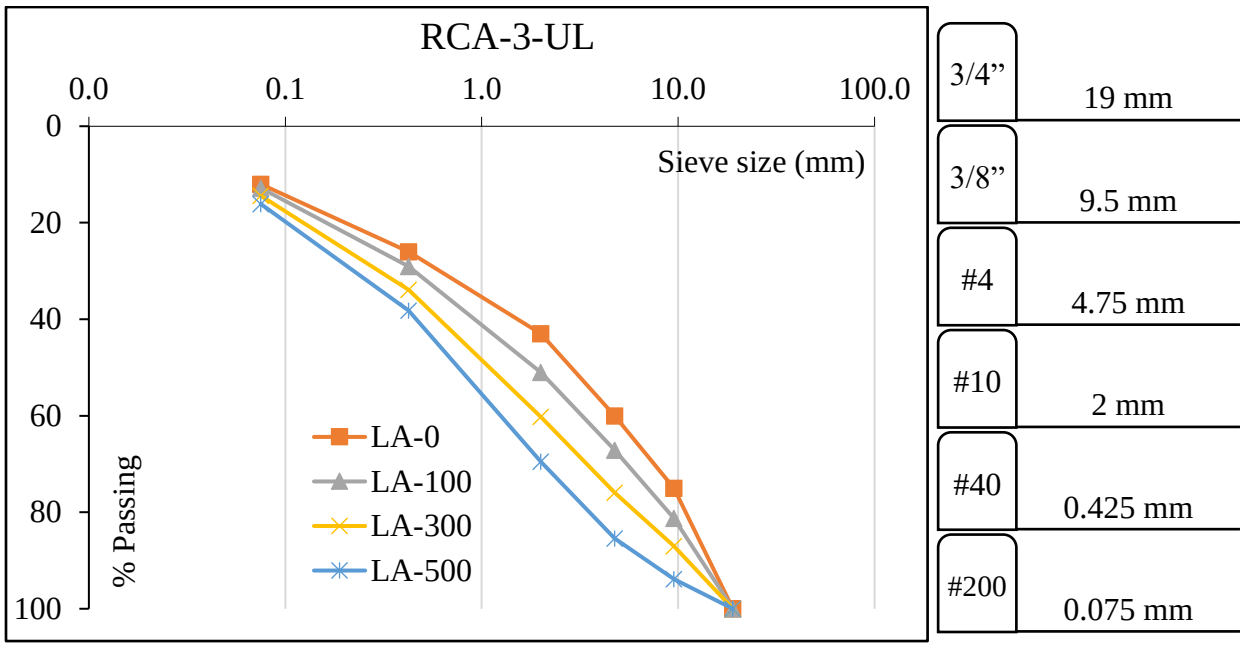

Figure 4-11: Changes in gradation of RCA-3 in the UL

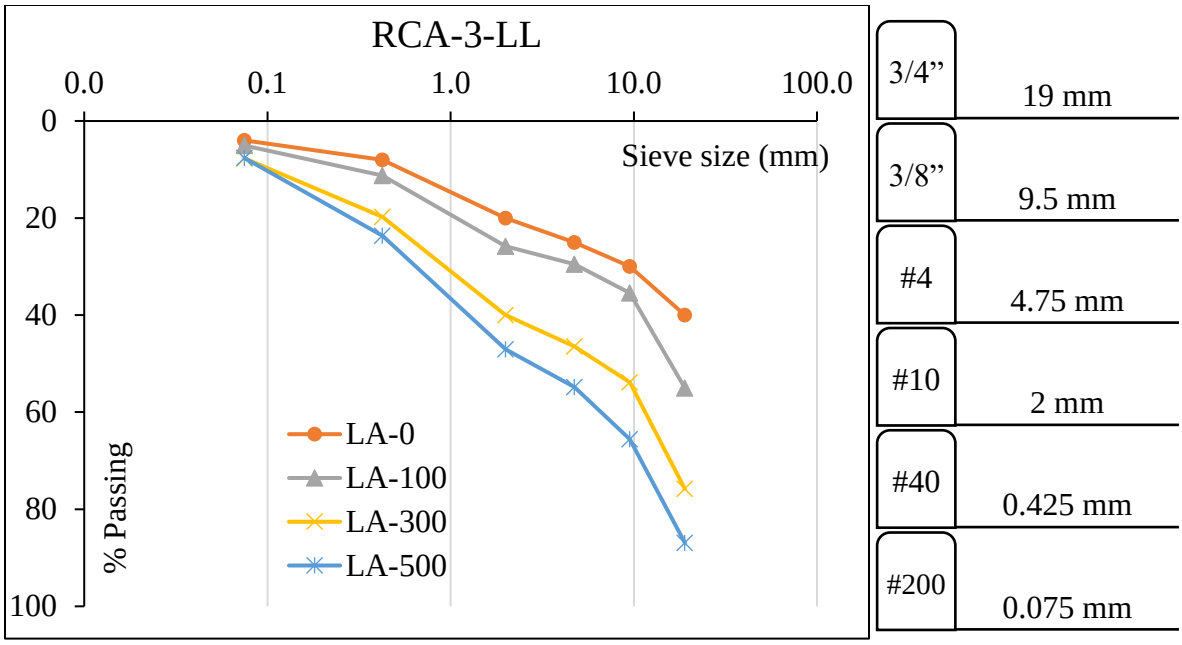

Figure 4-12: Changes in gradation of RCA-3 in the LL

Additionally, the angularity and texture of CRCA-3 aggregate were used to determine the changes in these properties that could be expected after field placement and compaction. Table 4-18 and Table 4-19 show the values of angularity and texture for the upper and lower limit gradations of RCA-3 compared to the values obtained for CRCA-3 to assess the changes in angularity caused by placement and compaction. For the texture, 200-300 cycles of conditioning in the LA abrasion machine were similar to field placement and compaction for the upper and lower limit gradation (Table 4-18 and Table 4-19). For the angularity, approximately 100- 200 cycles of conditioning in the LA abrasion machine were similar to field placement and compaction for the upper and lower limit gradations (Table 4-18 and Table 4-19). It can be concluded that field placement and compaction caused changes in angularity and texture equivalent to 100-300 cycles in the LA abrasion machine. This trend was not verified for the other aggregate since the field compacted aggregate could only be obtained for RCA-3.

Table 4-18: Angularity and texture of RCA-3 for the UL gradation

Aggregate conditioning	Retaining on 3/8” sieve		Retaining on #4 sieve	
	Average texture	Average gradient angularity	Average texture	Average gradient angularity
0 cycle	255.1	2,847.4	205.4	2,945.8
100 cycles	237.0	2,593.3	215.1	2,812.2
300 cycles	223.9	2,371.1	193.0	2,779.8
500 cycles	220.3	2,339.6	181.3	2,618.7
CRCA-3	235.0	2,736.2	211.1	2,833.9

Table 4-19: Angularity and texture of RCA-3 for the LL gradation

Aggregate Conditioning	Retaining on 3/4” Sieve		Retaining on 3/8” Sieve		Retaining on #4 Sieve	
	Average texture	Average gradient angularity	Average texture	Average gradient angularity	Average texture	Average gradient angularity
0 cycle	316.5	2,532.2	255.1	2,847.4	205.4	2,945.8
100 cycles	311.7	2,375.2	245.9	2,632.7	272.6	2,643.5
300 cycles	299.7	2,174.2	237.7	2,584.2	234.2	2,910.5
500 cycles	284.2	1,966.8	229.5	2,417.7	234.3	2,569.1
CRCA-3	304.0	2,389.3	235.0	2,736.2	211.1	2,833.9

4.11. Evaluation of Aggregates with LA Abrasion Cycles

Changes in Durability Index (DI)

The RCA-3 aggregate was used to assess the change in durability, as measured by D_c and D_f, with the number of conditioning cycles in the LA abrasion machine. Table 4-20 lists the D_c and D_f of the RCA-3 aggregate evaluated after 0, 100, 300, and 500 conditioning cycles. The D_c and D_f values remained unchanged or increased with the LA abrasion cycles for both the upper and lower limit gradations. With increased conditioning cycles, the concrete mortar adhered to

the aggregates was abraded, exposing the aggregate. As noted previously, RCA-3 contained dolomitic aggregate known for its hardness, causing an increase in durability. Recycled concrete aggregates produced from highways pavements, similar to RCA-3, are expected to exhibit higher durability for both the finer part and coarser part of the aggregate compared to RCAs produced in recycling plants containing different types of concrete mixes and an abundance of contaminants. The CRCA-3 aggregate had lower values of durability indices than the RCA-3 aggregate because of the changes that the material experienced during placement and compaction. The additional fines adhered to the aggregate are thought to be responsible for this trend.

Table 4-20: Durability indices of RCA-3 aggregates after different LA abrasion cycles

Aggregate	D_f	Aggregate	D_c
RCA-3-UL-LA0	60	RCA-3-UL-LA0	78
RCA-3-UL-LA100	86	RCA-3-UL-LA100	80
RCA-3-UL-LA300	83	RCA-3-UL-LA300	82
RCA-3-UL-LA500	86	RCA-3-UL-LA500	82
RCA-3-LL-LA0	55	RCA-3-LL-LA0	78
RCA-3-LL-LA100	74	RCA-3-LL-LA100	79
RCA-3-LL-LA300	72	RCA-3-LL-LA300	78
RCA-3-LL-LA500	76	RCA-3-LL-LA500	79
CRCA-3	48	CRCA-3	76

Changes in Permeability

The permeability of RCA-3 aggregate was determined for both upper limit and lower limit gradations of the aggregate subjected to different conditioning cycles. The results were used to assess the changes in permeability due to degradation. The permeability results for the upper limit and lower limit gradations are presented in Figure 4-13 and Figure 4-14, respectively. From Figure 4-13, the permeability of the lower limit gradation (16.60 ft/day) was higher than that of the upper limit gradation (8.15 ft/day) samples with no conditioning. The lower limit gradation was significantly coarser than the upper limit. For upper limit gradation, the aggregate is thought

to have denser packing of the aggregate reducing the water flow, thus reducing the drainage capability.

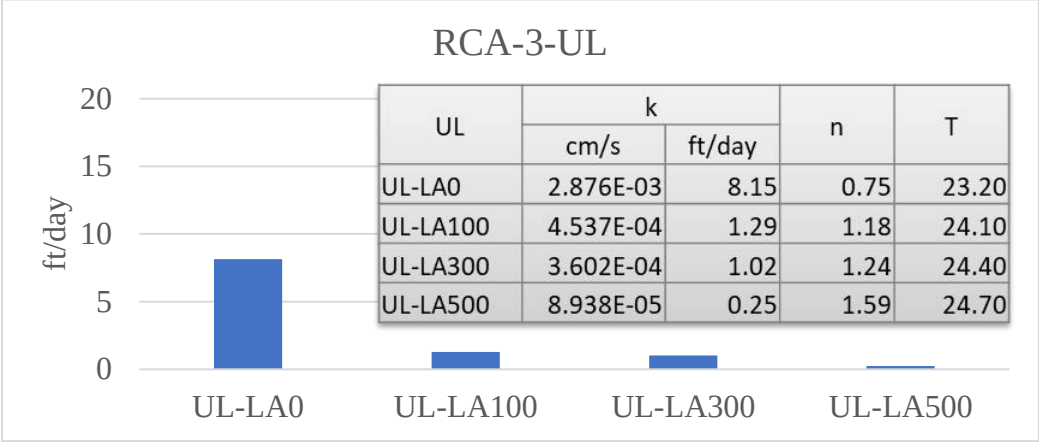

UL	k		n	T
	cm/s	ft/day		
UL-LA0	2.876E-03	8.15	0.75	23.20
UL-LA100	4.537E-04	1.29	1.18	24.10
UL-LA300	3.602E-04	1.02	1.24	24.40
UL-LA500	8.938E-05	0.25	1.59	24.70

Figure 4-13: Permeability of the upper limit of RCA-3 at different conditioning cycles

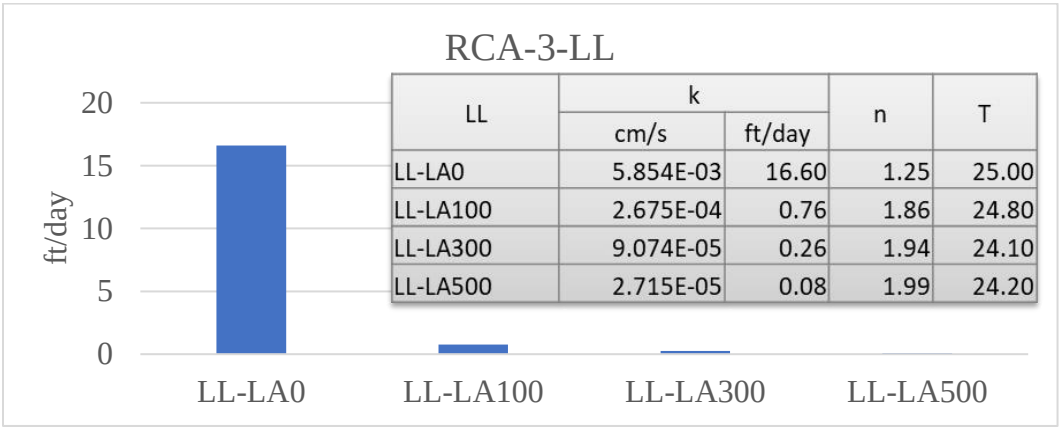

LL	k		n	T
	cm/s	ft/day		
LL-LA0	5.854E-03	16.60	1.25	25.00
LL-LA100	2.675E-04	0.76	1.86	24.80
LL-LA300	9.074E-05	0.26	1.94	24.10
LL-LA500	2.715E-05	0.08	1.99	24.20

Figure 4-14: Permeability of the lower limit of RCA-3 at different conditioning cycles

From Figure 4-13, the permeability of the lower limit gradations varied from 16.60 ft/day to 0.08 ft/day and for the upper limit gradations from 8.15 ft/day to 0.25 ft/day. The permeability of aggregates subjected to conditioning was reduced significantly due to the fines produced during conditioning. The degradation of the aggregate and production of fines made the flow path more tortuous and caused a reduction in flow, as expected. It is evident from these results

that a significant reduction in permeability should be expected due to placement and compaction in the field. Currently, ODOT does not have any requirement for the permeability of aggregate bases considering construction. Instituting such requirements is expected to enhance pavement performance relative to drainage.

Changes in Resilient Modulus of Aggregates

The resilient modulus values were determined for all sequences, and the design resilient modulus was calculated using Equation (3) for all aggregates. The design resilient modulus was calculated for each aggregate sample after 0, 100, 300 and 500 cycles of conditioning in the LA abrasion machine. Among all aggregates used in this study, the RCA-2 aggregate had the lowest values of M_r for both the upper limit and lower limit gradations. However, RCA-1 and RCA-3 were found to have higher M_r values than the VLA-1 aggregate for both the upper and lower limit gradations.

The resilient modulus values of RCA-3 for the upper limit gradation after different conditioning cycles are presented in Table 4-21 and Figure 4-15. Based on the results, generally, resilient modulus values are reduced with an increase in abrasion cycles for the upper limit gradation. However, for the RCA-3 aggregate, a slight increase in M_r is seen after 100 conditioning cycles. The conditioning cycles caused the gradation to become finer, negatively affecting the M_r values. This trend is thought to be caused by the rearrangement of particles, gradation changes, and changes in angularity and texture during compaction. The RCA-3 and CRCA-3 aggregates had similar M_r values with no conditioning, indicating that the changes in shape indices (angularity and texture) that CRCA-3 experienced during field placement and compaction did not significantly affect the M_r values.

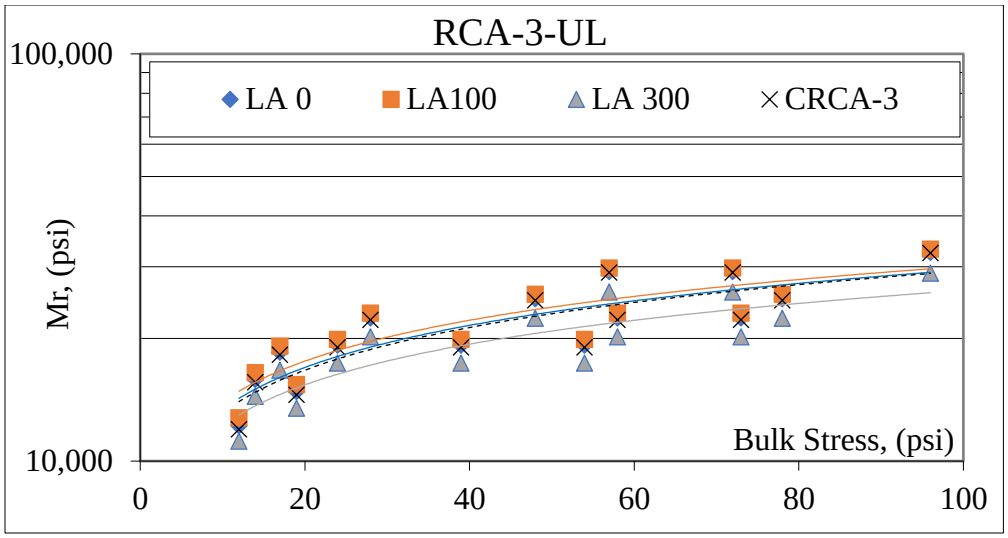

Figure 4-15: Resilient modulus plots of the upper limit RCA-3 and CRCA-3 aggregates

Table 4-21: Resilient moduli of the upper limit RCA-3 and CRCA-3 aggregates

Aggregate	RCA-3			CRCA-3
Column #	LA0	LA100	LA300	LA0
Parameter	Predicted resilient modulus (M_r)			
Unit	psi			
Sequence 1	12,215	12,779	11,186	11,963
Sequence 2	15,883	16,491	14,424	15,622
Sequence 3	18,519	19,143	16,737	18,262
Sequence 4	14,823	15,421	13,491	14,563
Sequence 5	19,273	19,900	17,397	19,018
Sequence 6	22,471	23,101	20,186	22,231
Sequence 7	19,273	19,900	17,397	19,018
Sequence 8	25,058	25,679	22,433	24,834
Sequence 9	29,217	29,810	26,030	29,030
Sequence 10	19,273	19,900	17,397	19,018
Sequence 11	22,471	23,101	20,186	22,231
Sequence 12	29,217	29,810	26,030	29,030
Sequence 13	22,471	23,101	20,186	22,231
Sequence 14	25,058	25,679	22,433	24,834
Sequence 15	32,580	33,138	28,927	32,430

For the lower limit gradation, Table 4-22 and Figure 4-16 show that M_r values decreased with the abrasion cycles for the lower limit gradation. Loss of durability, changes in gradation and loss of angularity and texture were possible causes for this reduction in M_r values. For the

lower limit gradations, CRCA-3 had a similar M_r as RCA-3 with no conditioning. Therefore, similar to the upper limit gradation, changes in angularity and texture did not significantly affect the resilient modulus.

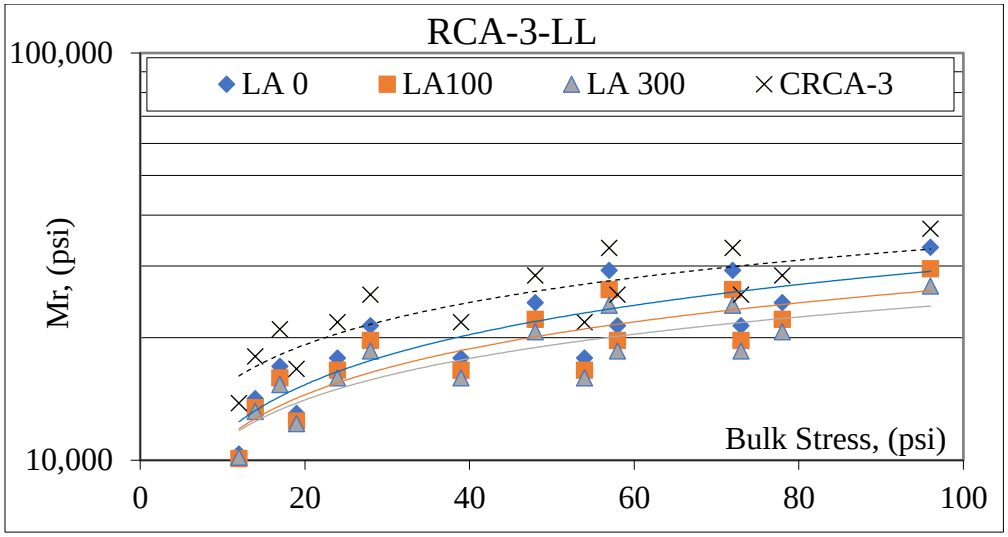

Figure 4-16: Resilient modulus plots of the lower limit RCA-3 and CRCA-3 aggregates

Table 4-22: Resilient moduli of the lower limit RCA-3 and CRCA-3 aggregates

Aggregate	RCA-3			CRCA-3
Column #	LA0	LA100	LA300	LA0
Parameter	Predicted resilient modulus (M_r)			
Unit	psi			
Sequence 1	10,343	10,091	10,156	13,790
Sequence 2	14,145	13,450	13,160	17,958
Sequence 3	16,987	15,912	15,314	20,959
Sequence 4	13,027	12,471	12,293	16,753
Sequence 5	17,815	16,622	15,929	21,817
Sequence 6	21,394	19,664	18,537	25,462
Sequence 7	17,815	16,622	15,929	21,817
Sequence 8	24,363	22,155	20,642	28,412
Sequence 9	29,258	26,210	24,020	33,159
Sequence 10	17,815	16,622	15,929	21,817
Sequence 11	21,394	19,664	18,537	25,462
Sequence 12	29,258	26,210	24,020	33,159
Sequence 13	21,394	19,664	18,537	25,462
Sequence 14	24,363	22,155	20,642	28,412
Sequence 15	33,317	29,529	26,748	37,000

The design M_r values were calculated for all aggregates subjected to conditioning cycles, as displayed in Table 4-23. For the upper limit gradation, the RCA-1 aggregate shows a considerably high M_r value (23,200 psi) with no conditioning cycle. However, the M_r values reduced substantially after 100 cycles (11,600 psi). This reduction may be explained by the RCA-1 having the highest abrasion loss in the LA abrasion test. These changes in M_r values may be detrimental to the aggregate base as the resilient modulus of this aggregate is expected to reduce considerably during construction. For the upper limit, the VLA-1 and RCA-1 aggregates exhibited a reduction in M_r values after 100, 300, and 500 conditioning cycles compared to the initial M_r (no conditioning). Also, the RCA-3 aggregate showed a similar trend except for the M_r at 300 cycles, which was higher than the initial M_r (0 cycles) for the upper limit gradation. For the lower limit gradation, it was observed that, for VLA-1 and RCA-1 aggregates, the M_r values increased with conditioning cycles. The M_r values after 100, 300, and 500 cycles are higher than the initial M_r (0 cycle). For the lower limit gradation, the RCA-3 aggregate exhibited a reduction in M_r values reduced when subjected to 100 and 300 conditioning cycles compared to the initial M_r values (0 cycle). However, after 500 cycles, an increase in M_r was observed for this aggregate. The M_r values for all aggregates in the upper and lower limit gradations for all loading sequences are shown in Appendix C (Table C-1 to Table C-6) for all conditioning cycles. From the results, it was observed that for the upper limit gradation after conditioning, the aggregates mostly exhibited a reduction in M_r values. Changes in gradation (additional fines produced by conditioning) and loss of angularity and texture are possible causes for this reduction in M_r values. However, the lower limit gradation exhibited the opposite trend. The aggregates mostly exhibited an increase in M_r values. The lower limit gradation is significantly coarser than the upper limit gradation, and it is thought that the changes in gradation (additional

fines produced by conditioning) caused the aggregate to reconfigure in a tighter configuration causing an increase in M_r values.

Table 4-23: Design resilient modulus of aggregates with conditioning

Type A (UL)					Type A (LL)				
ID	LA abrasion cycles	K_1	K_2	Design M_r (psi)	ID	LA abrasion cycles	K_1	K_2	Design M_r (psi)
VLA-1	0	6,602	0.38	18,350	VLA-1	0	3,396	0.44	11,200
	100	3,096	0.50	11,975		100	7,591	0.28	11,975
	300	3,759	0.47	13,400		300	4,910	0.45	13,400
	500	3,443	0.50	13,300		500	5,512	0.39	13,300
RCA-1	0	7,038	0.44	23,200	RCA-1	0	4,161	0.42	12,975
	100	4,629	0.34	11,620		100	4,508	0.44	14,800
	300	6,617	0.27	13,750		300	6,694	0.30	15,050
	500	6,567	0.29	14,400		500	5,560	0.35	14,300
RCA-2	0	5,109	0.34	12,800	RCA-2	0	3,660	0.40	10,800
	300	6,344	0.27	13,100		300	-	-	-
	500	4,446	0.35	11,450		500	-	-	-
RCA-3	0	8,386	0.38	23,386	RCA-3	0	6,605	0.45	22,437
	100	8,868	0.37	22,708		100	6,685	0.41	20,294
	300	7,771	0.37	23,945		300	7,006	0.37	18,401
	500	9,478	0.33	18,925		500	9,217	0.44	23,315

5. CHAPTER FIVE: PERFORMANCE PREDICTION OF RCA AGGREGATE BASE USING AASHTOWARE PAVEMENT ME

5.1. Assessment of Service Life Using AASHTOWare Pavement ME Simulations

The service life of aggregate bases using recycled concrete aggregates (RCA-1, RCA-2, and RCA-3) and a virgin aggregate (VLA-1), discussed in the previous chapter, were studied using mechanistic analyses. The commonly used software by the state DOTs, AASHTOWare Pavement ME, was used for this purpose. The performance of a flexible pavement (SH-48) and a rigid pavement (SH-33) was simulated using this software. The simulation results were then used to conduct a life cycle cost analysis (LCCA) for the flexible pavement (SH-48). A design life of 20 years and annual average daily traffic (AADT) of 4,000 were considered in the simulation for the same climate conditions.

5.1.1 Performance and Service Life of Flexible Pavements (SH-48) with RCA Base

The pavement section of SH-48 consists of three asphalt layers totaling 9 in. Below the asphalt layer is an 8 in. granular aggregate base followed by an 8 in. thick stabilized subgrade. A cross-section of this pavement section is shown in Figure 3-12. The associated properties used for each layer are given in Table 3-4. As mentioned in Chapter 3, the following distresses thresholds were considered in the simulation: total rutting (0.50 in.), top-down fatigue cracking (20% lane area), and bottom-up fatigue cracking (20% lane area) (AASHTO, 2020).

The impact on performance due to the use of different aggregate base alternatives was assessed by using the M_r values obtained from the laboratory testing of each aggregate for the upper limit gradation. The effect of different aggregate bases on the service life of the flexible

pavement (SH-48) is presented in Table 5-1.

Table 5-1: Effect of aggregate types on the service life of SH-48 (flexible pavement)

Aggregate base	Base thickness (in.)	Design resilient modulus (psi)	Total pavement rutting (in.)	Top-down fatigue cracking (% Lane area)	Bottom-up fatigue cracking (% Lane area)
VLA-1 (UL)	8	18,350	0.42	14.19	18.57
RCA-1 (UL)	8	23,200	0.42	14.14	10.08
RCA-2 (UL)	8	12,800	0.43	14.28	31.90
	10	12,800	0.43	14.22	27.66
	12	12,800	0.43	14.22	23.93
	14	12,800	0.42	14.26	20.14
RCA-3 (UL)	8	23,386	0.42	14.14	9.81

The pavement rutting and top-down cracking were unaffected by the aggregate type. Rutting ranged from 0.42 to 0.43 in. and top-down fatigue cracking from 14.14% to 14.28% of lane area. It is believed that the properties of the base layer selected were appropriate for the loading conditions (traffic and climate), allowing the asphalt layer to perform well in rutting and top-down cracking even when the M_r of the bases changed (12,800 psi to 23,386 psi). However, bottom-up fatigue cracking values showed considerable differences among the base options since fatigue cracking is highly dependent on the structural support that is provided by the aggregate base. For the aggregate bases having 8 in. thickness, the lowest value for bottom-up fatigue cracking (9.81%) was obtained for RCA-3, which had the highest resilient modulus. Comparatively, VLA-1 had a bottom-up fatigue cracking of 18.57%, RCA-1 had 10.08%, and RCA-2 had 31.9% for the same layer thickness. The pavement section with RCA-1, RCA-3 and VLA-1 showed significantly lower values of bottom-up fatigue cracking than RCA-2. In order to improve the bottom-up fatigue cracking of RCA-2, the thickness of the aggregate base was increased to 14 in. using increments of 2 in. It was expected that the added thickness would reduce bottom-up fatigue cracking. For a 14 in. aggregate base, the bottom-up fatigue cracking

of RCA-2 improved to 20.14%. Both RCA-1 and RCA-3 showed better performance for all pavement distresses compared to VLA-1 for the same layer thickness.

5.1.2 Performance and Service Life of Rigid Pavements (SH-33) With RCA Base

The pavement section on SH-33 was a rigid pavement having a thickness of 10 in. (top layer). This layer of Portland cement concrete (PCC) was supported by a 4 in. thick cement stabilized base, an 8 in. thick granular base, and an 8 in. thick stabilized subgrade. A cross-section of this pavement section is shown in Figure 3-12. The properties for each layer used in the simulation are given in Table 3-5. As mentioned in Chapter 3, the following distress thresholds were considered in the simulation: terminal IRI (200 in./mile), mean joint faulting (0.2 in.), and transverse cracking (15% slabs) (AASHTO, 2020).

The service life of the pavement section with respect to the aforementioned distresses is presented in Table 5-2. From Table 5-2, pavement distresses were unaffected by the changes in aggregate base thickness. The section performed exceptionally well in terms of pavement distresses. The concrete layer, which is much stronger and stiffer than other layers, controls the overall performance.

Table 5-2: Effect of aggregate type on the performance of SH-33 (rigid pavement)

Aggregate base	Base thickness (in.)	Resilient modulus (psi)	Terminal IRI (in./mile)	Mean joint faulting (in.)	JPCP transverse cracking (% slabs)
VLA-1 (UL)	8	18,350	114.01	0.06	0.96
RCA-1 (UL)	8	23,200	113.93	0.06	0.96
RCA-2 (UL)	8	12,800	114.09	0.06	0.96
RCA-3 (UL)	8	23,386	113.93	0.06	0.96

5.2. Cost Analysis

5.2.1 Life Cycle Cost Analysis of Flexible Pavement with Different RCA Bases

As noted previously, the performance of pavement sections was simulated with AASHTOWare Pavement ME and used for the life cycle cost analysis (LCCA). The pavement distress threshold values of 0.75 in. for rutting and 25% of the lane area for both top-down and bottom-up fatigue cracking were used in the LCCA. The expected life of the flexible pavement for each distress (i.e., year reaching 75% of the target value) is given in Table 5-3. Two main strategies were considered for pavement maintenance: crack filling every five years, and milling and overlaying when the pavement distresses approached 75% of the target value (Table 5-4). Calculations for the initial cost of the pavement section are shown in Appendix G (see Table G-1 to Table G-5) for different thicknesses of the aggregate base. All the initial costs and the costs associated with maintenance were converted to net present worth for comparison with a discount rate of 3% (Table 5-5). It was observed that RCA-1 and RCA-3 were the most economical aggregate bases. Although the aggregate base thickness for RCA-2 needed to be increased from 8 in. to 14 in. to improve its performance, the cost of an 8 in. VLA-1 base was similar to that of a 14 in. RCA-2 base. However, reducing the thickness of RCA-2 to 10 or 12 inches resulted in increased costs, as shown in Table 5-5. Furthermore, our analysis revealed that both RCA-1 and RCA-3 exhibited a 5.3% reduction in net present worth compared to VLA-1.

Calculations for the initial cost of the pavement section are shown in Appendix G (see Table G-1 to Table G-5) for different thicknesses of the aggregate base. Additionally, the costs associated with the maintenance plan for each aggregate base are shown in Appendix G (see Table G-6 to Table G-12) for a period of 20 years.

Table 5-3: Performances of SH-48 with different aggregate bases

Aggregate base	Base thickness (in.)	Design resilient modulus (psi)	Total pavement rutting (in.) (year reaching 75% of target)	Top-down fatigue cracking (% lane area) (year reaching 75% of target)	Bottom-up fatigue cracking (% lane area) (year reaching 75% of target)
		Target value	0.75	25.00	25.00
		75% of Target	0.56	18.75	18.75
VLA-1 (UL)	8	18,350	0.42	14.19	18.57
RCA-1 (UL)	8	23,200	0.42	14.14	10.08
RCA-2 (UL)	8	12,800	0.43	14.28	31.90
RCA-2 (UL)	10	12,800	0.43	14.22	27.66
RCA-2 (UL)	12	12,800	0.43	14.22	23.93
RCA-2 (UL)	14	12,800	0.42	14.26	20.14
RCA-3 (UL)	0	23,386	0.42	14.14	9.81

Table 5-4: Maintenance plan for SH-48 with different aggregate bases

Aggregate base	Base thickness (in.)	Resilient modulus (psi)	Strategy 1		Strategy 2	
			Crack treatment	Frequency (years)	Mill and overlay	Year of occurrence
VLA-1 (UL)	8	18,350	Yes	5	Yes	15
RCA-1 (UL)	8	23,200	Yes	5	Yes	15
RCA-2 (UL)	8	12,800	Yes	5	Yes	10
RCA-2 (UL)	10	12,800	Yes	5	Yes	12
RCA-2 (UL)	12	12,800	Yes	5	Yes	12
RCA-2 (UL)	14	12,800	Yes	5	Yes	15
RCA-3 (UL)	8	23,386	Yes	5	Yes	15

Table 5-5: Net present worth of section SH-48 with different aggregate bases

Aggregate base	Base thickness (in.)	Resilient modulus (psi)	Net present worth (USD)
VLA-1 (UL)	8	18,350	$467,600.37
RCA-1 (UL)	8	23,200	$443,039.29
RCA-2 (UL)	8	12,800	$470,213.30
RCA-2 (UL)	10	12,800	$469,804.61
RCA-2 (UL)	12	12,800	$477,626.61
RCA-2 (UL)	14	12,800	$466,505.29
RCA-3 (UL)	8	23,386	$443,039.29

6. CHAPTER SIX: CONCLUSIONS AND RECOMMENDATIONS

6.1. Summary

In this study, laboratory tests were performed to generate data on the properties of RCAs pertaining to pavement bases. Also, the changes in gradation and shape indices (angularity and texture) due to placement and compaction were determined. The number of LA abrasion cycles corresponding to field placement and compaction was also determined. For laboratory testing, three recycled concrete aggregates (RCA-1, RCA-2, and RCA-3), one virgin aggregate (VLA-1), and a field compacted recycled aggregate (CRCA-3) were collected from different sources. The properties of the RCAs were evaluated in terms of gradation, optimum moisture content (OMC), maximum dry density (MDD), Los Angeles (LA) abrasion, aggregate shape indices (angularity and texture), durability index (D_c and D_f), permeability (k), resilient modulus (M_r) and permeability (k). Additionally, the gradation, resilient modulus, and permeability values obtained through laboratory testing were used to assess the performance of aggregate bases for a flexible pavement section (SH-48) and a rigid pavement (SH-33) section using AASHTOWare Pavement ME simulations. Finally, the simulation results were used to conduct a life cycle cost analysis (LCCA) for the flexible pavement section (SH-48).

6.2. Conclusions

From the laboratory test discussed in Chapter 4, the following conclusions were drawn:

- Changes in gradation and aggregate shape indices similar to 100-300 LA abrasion cycles are expected after field compaction.
- The resilient modulus of RCAs can improve over time due to the reaction of cementitious particles with water. Aggregates produced using similar conditions as RCA-3 can

experience an increase in M_r values over time. However, this behavior may cause a reduction in permeability values, as mentioned in the literature.

- The source and production practices of RCAs critically impact the aggregate's properties. For example, high-quality recycled aggregates are expected from recycled in-place highway pavements similar to RCA-3 and RCA-1. The properties of RCAs can vary significantly depending on the source materials and production practices, which could affect their suitability for pavement applications.
- The RCA-3 and VLA-1 aggregates exhibited similar properties in terms of gradation changes, durability indices (D_f and D_c), LA abrasion, and permeability. The high quality of the source material used for RCA-3 (produced in-place) is responsible for this behavior.
- The RCA-1 and RCA-2 aggregates had many contaminants, such as twigs, plastic, and clay clumps. Those foreign contaminants are likely responsible for higher LA abrasion losses and lower durability of fines (D_f). Both aggregates exhibited clay clumps. The RCA-1 aggregate produced in-place is thought to have been contaminated with the underlying soil. It is believed that these clay clumps caused the aggregates to perform poorly in terms of D_f values. RCA-1 and RCA-2 did not meet ODOT's requirement for D_f.
- The permeability values of RCA-3 reduced significantly with only 100 cycles of conditioning in the LA abrasion machine. Therefore, caution should be exercised since a significant reduction in permeability is expected after placement and compaction. Also, permeability values change more drastically for the lower limit gradation since the

material is coarser and the generated additional fines reconfigured in a tighter configuration.

- The RCA-1 aggregate showed a significant reduction in M_r for the upper limit gradation only after 100 cycles. The reduction in M_r values is thought to be influenced by the high LA abrasion loss and low values of the durability of fines (D_f).
- The RCA-2 aggregate produced in a recycling plant had the lowest M_r values. Therefore, caution should be exercised when using RCA from recycling plants due to the potential deterioration of pavement performance over time.
- The RCAs exhibited higher OMCs and lower MDDs compared to virgin aggregate, indicating that they require more water for the same level of compaction. The RCAs contain cement coated aggregates that are porous in nature. Therefore, more water could penetrate into the pores resulting in a reduction in density.

From the AASHTOWare Pavement ME simulations and life cycle cost analyses discussed in Chapter 5, the following conclusions were drawn:

- The influence of aggregate type was found insignificant on the performance of rigid pavement due to the dominance of the 10 in. thick concrete layer. In this case, RCA may be a valuable alternative for reducing costs. Typically, RCAs are produced close to the projects, reducing hauling costs, and are less costly than virgin aggregates. In cases where the virgin aggregates are far away from the project, the RCAs can provide a cost-effective solution for pavement construction.
- For flexible pavement sections with an aggregate base of 8 in., the RCA-1, RCA-2, RCA-3 and VLA-1 aggregates showed similar performance in rutting and top-down cracking. However, RCA-2 exhibited significantly higher bottom-up fatigue cracking than RCA-1,

RCA-3, and VLA-1. To address this issue, a thicker base layer of 14 in. of RCA-2 was used to improve bottom-up fatigue cracking.

- The LCCA showed that RCAs could be used to build aggregate bases at a lower cost compared to virgin aggregates. In the case of the RCA-2 aggregate, the base thickness had to be increased to 14 in. to improve the bottom-up fatigue cracking performance. The LCCA showed that the RCA-2 base of 14 in. could be built at a lower cost than the VLA-1 alternative. The other RCA sources (RCA-1 and RCA-3) exhibited lower costs compared to VLA-1 for the same layer thickness of 8 in.

6.3. Recommendations

Based on the data generated in this study, the following recommendations were provided on the use of recycled aggregates produced in Oklahoma:

1. To ensure the high quality of the aggregate, ODOT may require contractors to use RCAs from specified sources (e.g., highway pavement demolition projects). Caution should be practiced to avoid the contamination of the aggregate. State DOTs should avoid using RCAs from recycling operations since the M_r values obtained for RCA-2 (produced in a recycling plant) were considerably lower than RCA-1 and RCA-3 (both recycled in-place).
2. Requirements for contaminants could be required by ODOT, as done in other states, to ensure a proper quantification of pollutants. During RCA production, it may be unrealistic to have zero contaminants. The production process should be handled carefully to avoid contamination (e.g., dirt, clay clumps, etc.) of the RCA materials.
3. The properties of RCAs could be improved if blended with virgin aggregate up to a certain amount. The durability index for the coarser part (D_c) of RCA exhibited high

values. However, the durability index of the finer part (D_f) of RCA-1 and RCA-2 was lower than the amount allowed by ODOT. Further studies could consider improving the properties of the finer part of RCAs that do not meet the required D_f values. Additional studies are needed to determine the ideal blending ratio.

4. The threshold values of LA abrasion and durability indices (DI) currently used by ODOT were found appropriate. The aggregates that could potentially have issues, according to M_r testing, did not meet the requirement of the durability of the finer part (D_f) set by ODOT. State agencies may consider enforcing the durability index for the fine part (D_f) as a quality indicator for RCAs. Additionally, the wash loss test could be required with a maximum loss of 2%, as required by the Michigan DOT. In this study, the aggregates with higher than 2% losses also failed in the durability of the finer part (D_f).
5. ODOT could benefit from including the permeability of aggregate bases as a requirement during construction since it is expected to enhance pavement performance relative to drainability. After field placement and compaction, a significant reduction in permeability values should be expected.
6. Sulfate-rich soils may have heaving issues when exposed to the leaching of cementitious material from RCA. Therefore, ODOT may consider requiring sulfate tests on subgrade soils where the RCA base is planned for use, as other states require. The use of a separator fabric between the aggregate base and subgrade soil could reduce the problem.
7. The effect of the initial concrete strength on the quality of the RCA has not been studied yet. However, high strength concrete could potentially produce high quality RCAs. Therefore, additional studies should consider evaluating the impact of concrete strength over the quality of the RCA.

7. APPENDICES

APPENDIX A: MOISTURE-DENSITY RELATIONS FOR DIFFERENT AGGREGATES

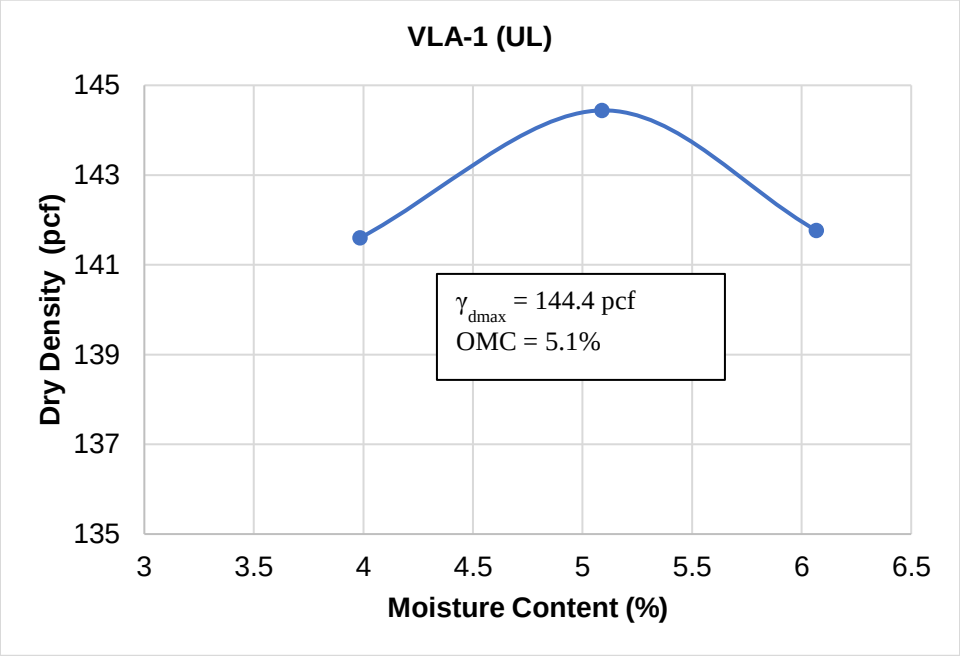

Figure A.1 Moisture-density relation for VLA-1 (UL) aggregate

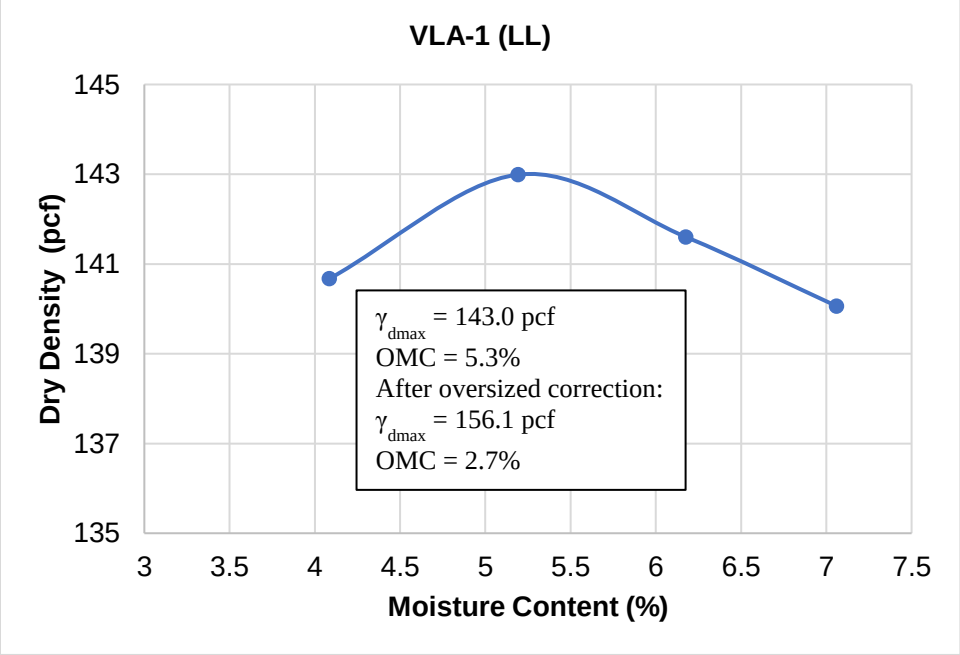

Figure A.2 Moisture-density relation for VLA-1 (LL) aggregate

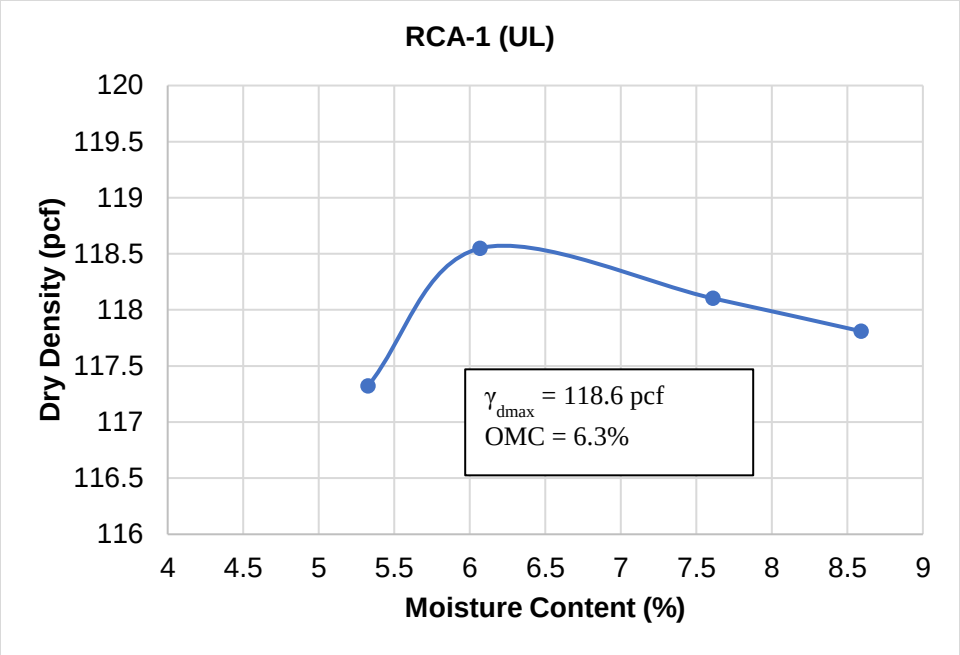

Figure A.3 Moisture-density relation for RCA-1 (UL) aggregate

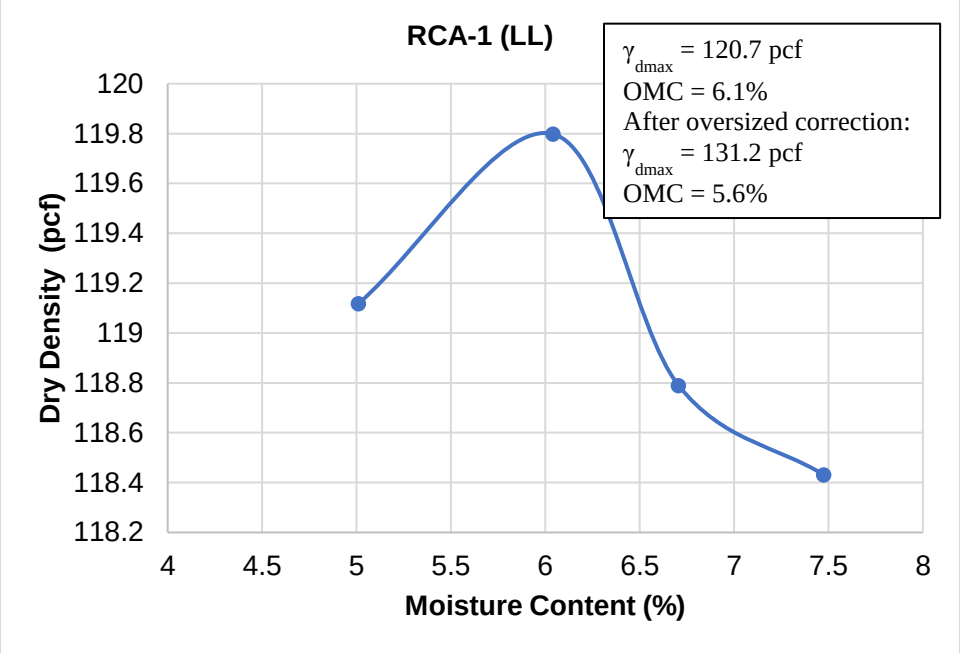

Figure B.4 Moisture-density relation for RCA-1 (LL) aggregate

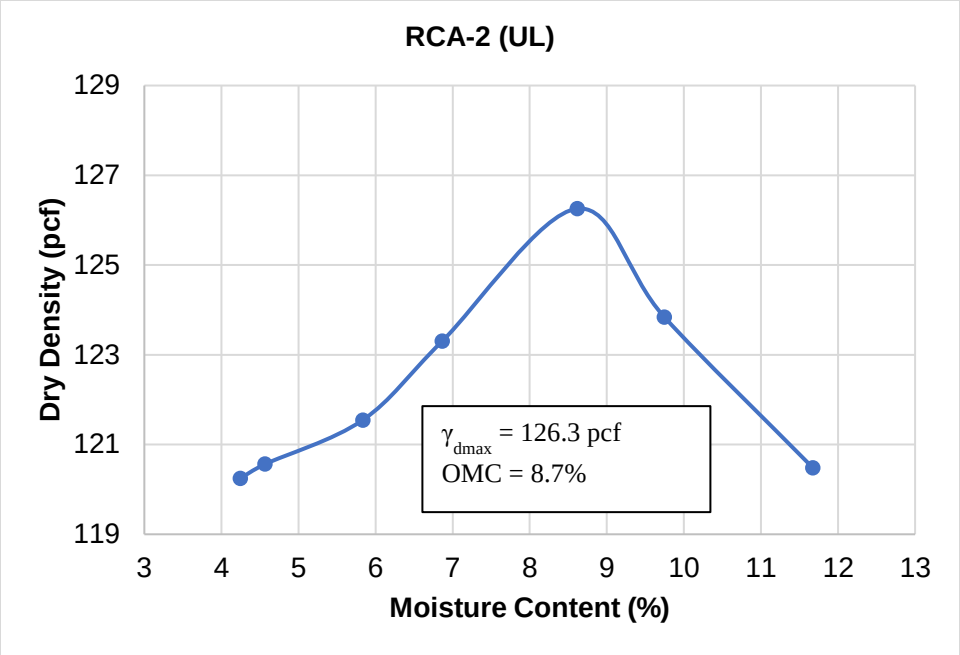

Figure A.5 Moisture-density relation for RCA-2 (UL) aggregate

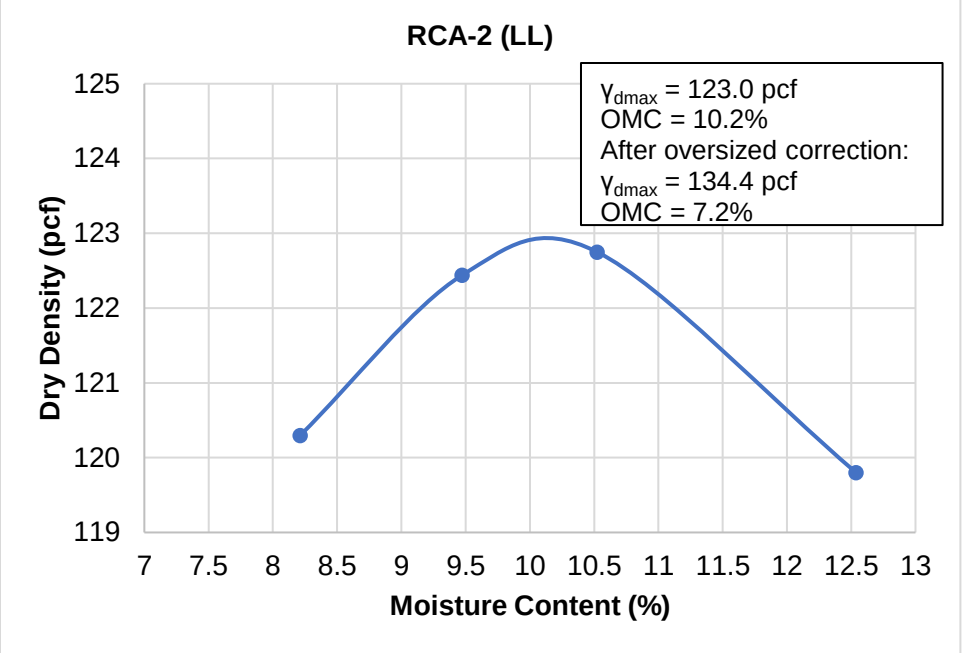

Figure A.6 Moisture-density relation for RCA-2 (LL) aggregate

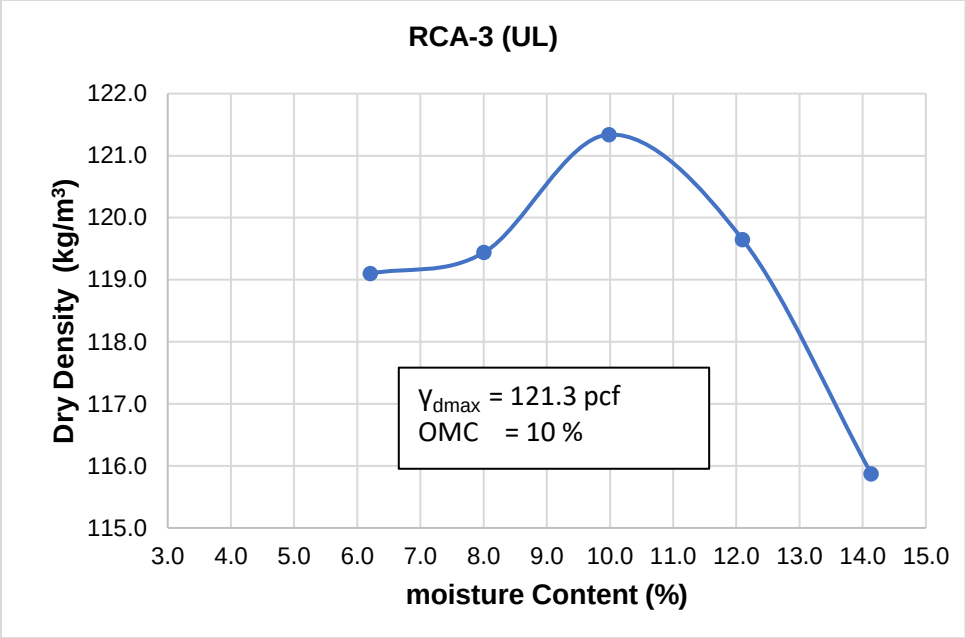

Figure A.7 Moisture-density relation for RCA-2 (UL) aggregate

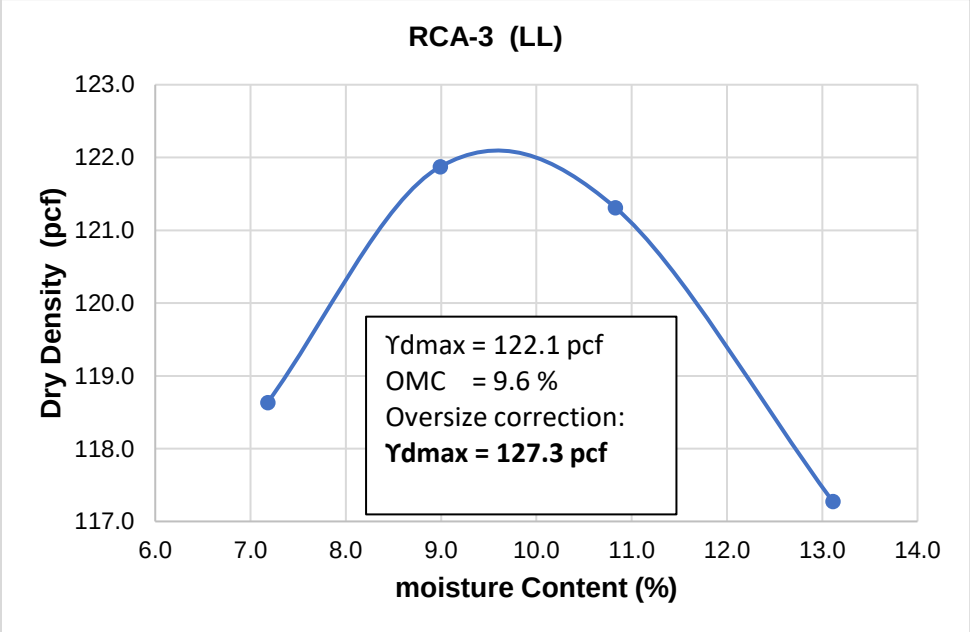

Figure A.8 Moisture-density relation for RCA-2 (UL) aggregate

APPENDIX B: CHANGES IN GRADATION WITH DIFFERENT LA ABRASION CYCLES

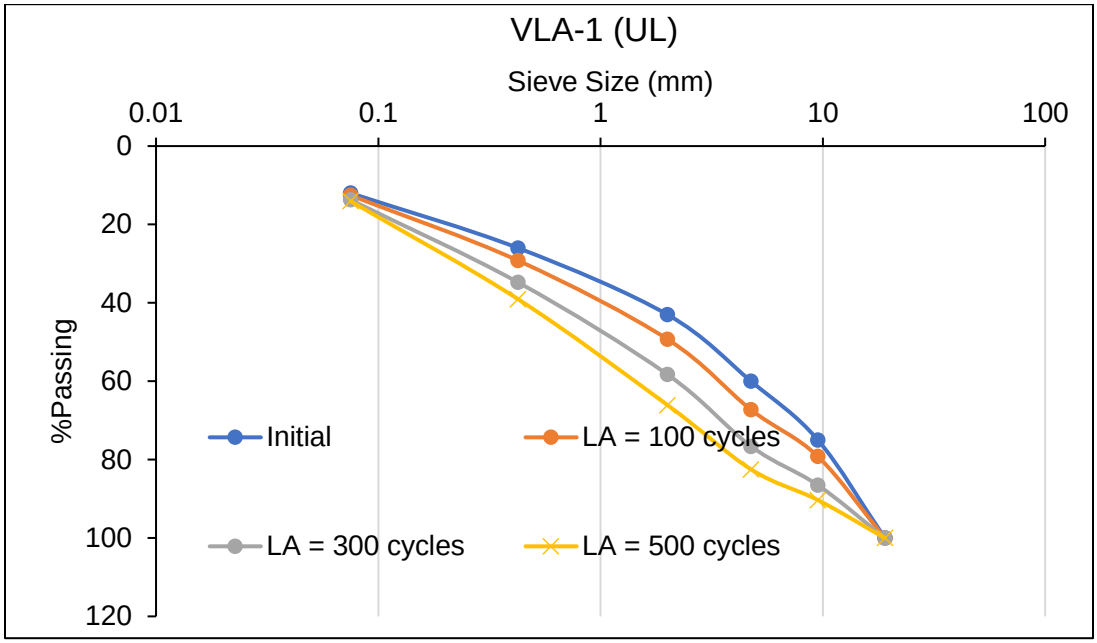

Figure B.1 Change in gradation of VLA-1 (UL) with different LA abrasion cycles

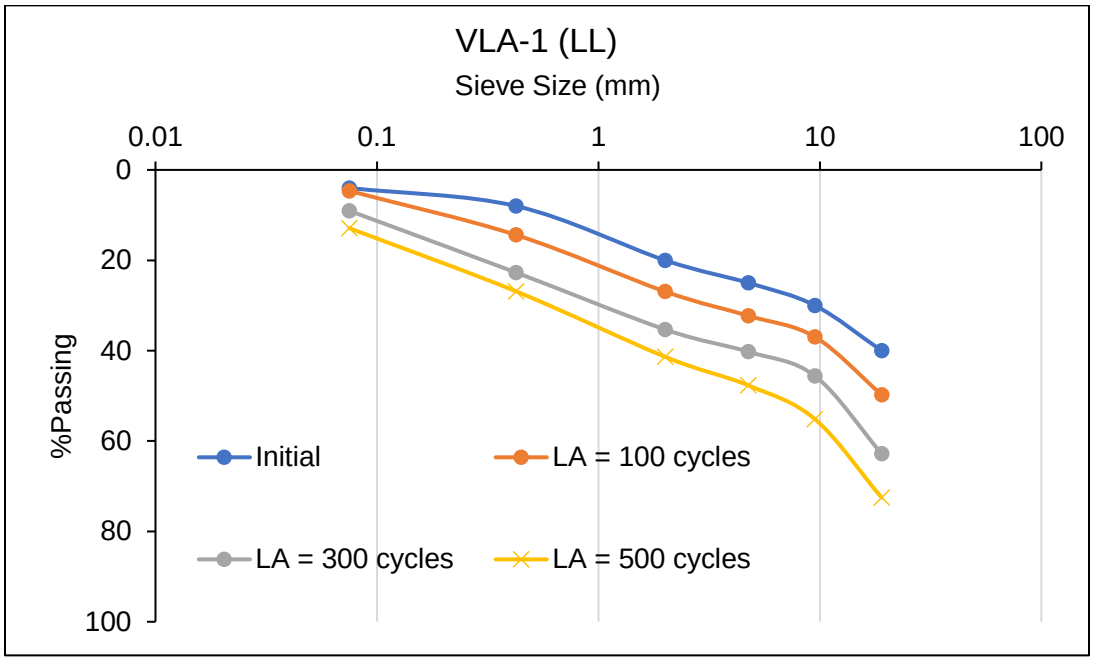

Figure B.2 Change in gradation of VLA-1 (LL) with different LA abrasion cycles

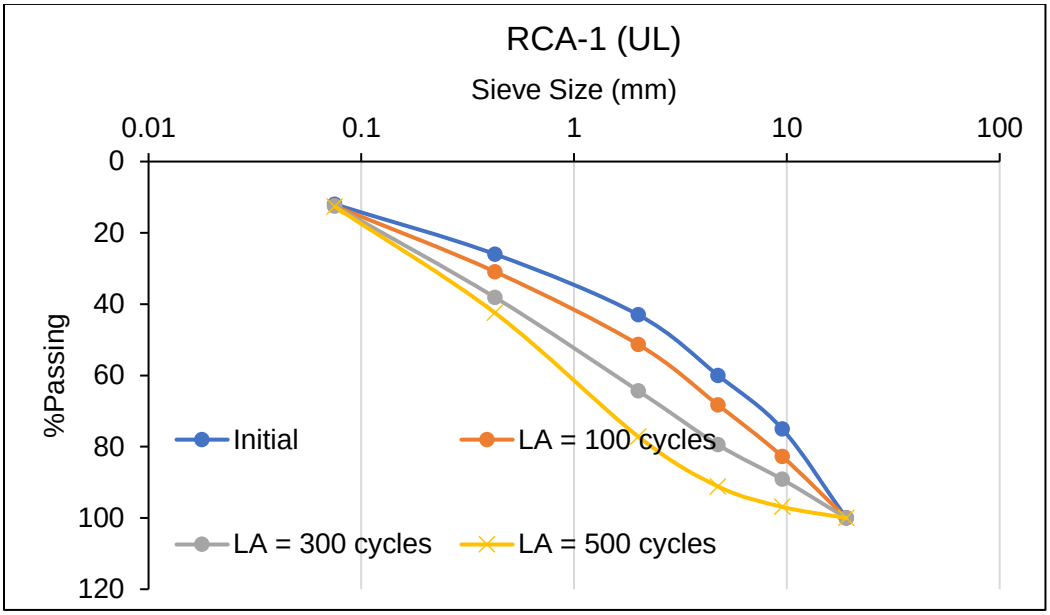

Figure B.3 Change in gradation of RCA-1 (UL) with different LA abrasion cycles

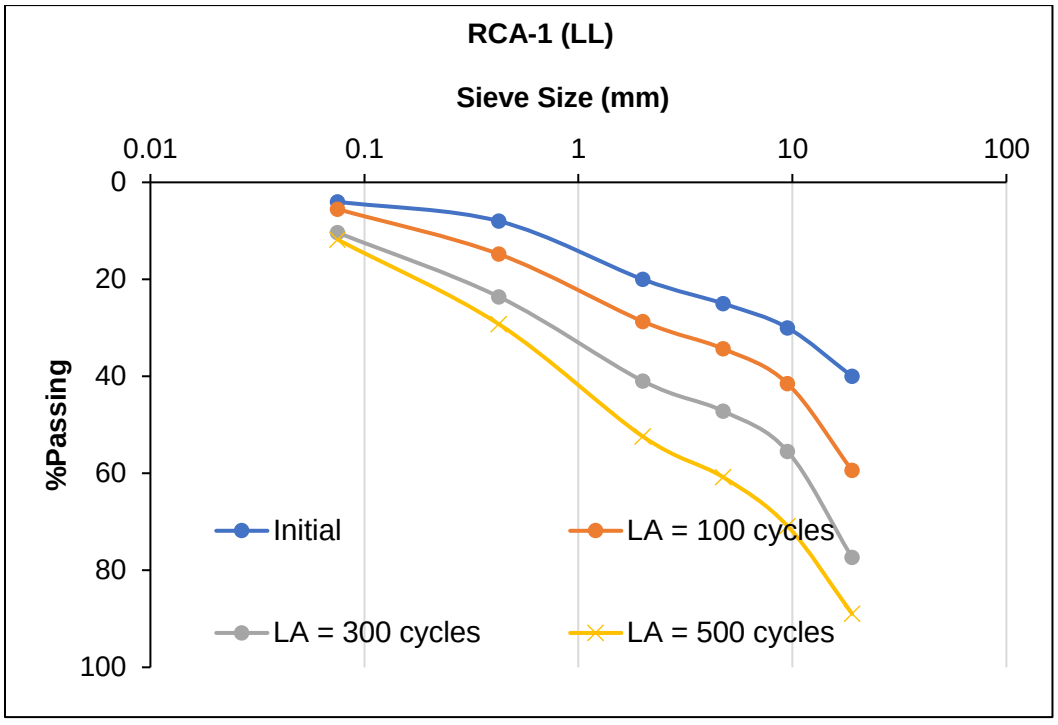

Figure B.4 Change in gradation of RCA-1 (LL) with different LA abrasion cycles

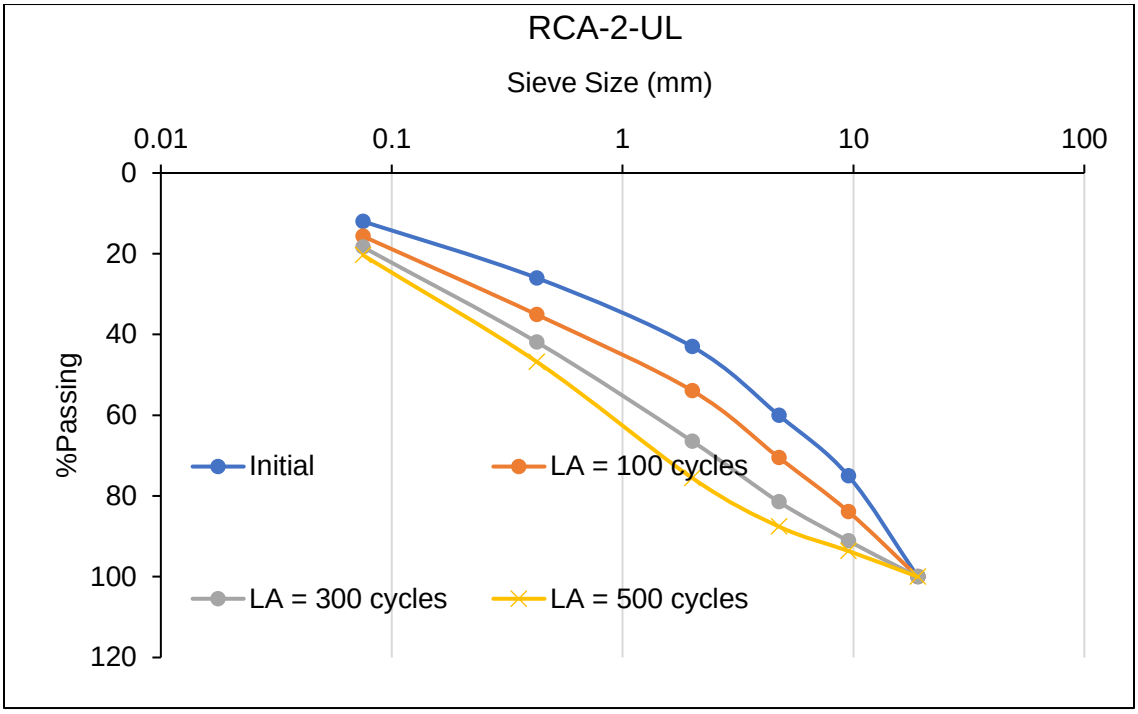

Figure B.5 Change in gradation of RCA-2 (UL) with different LA abrasion cycles

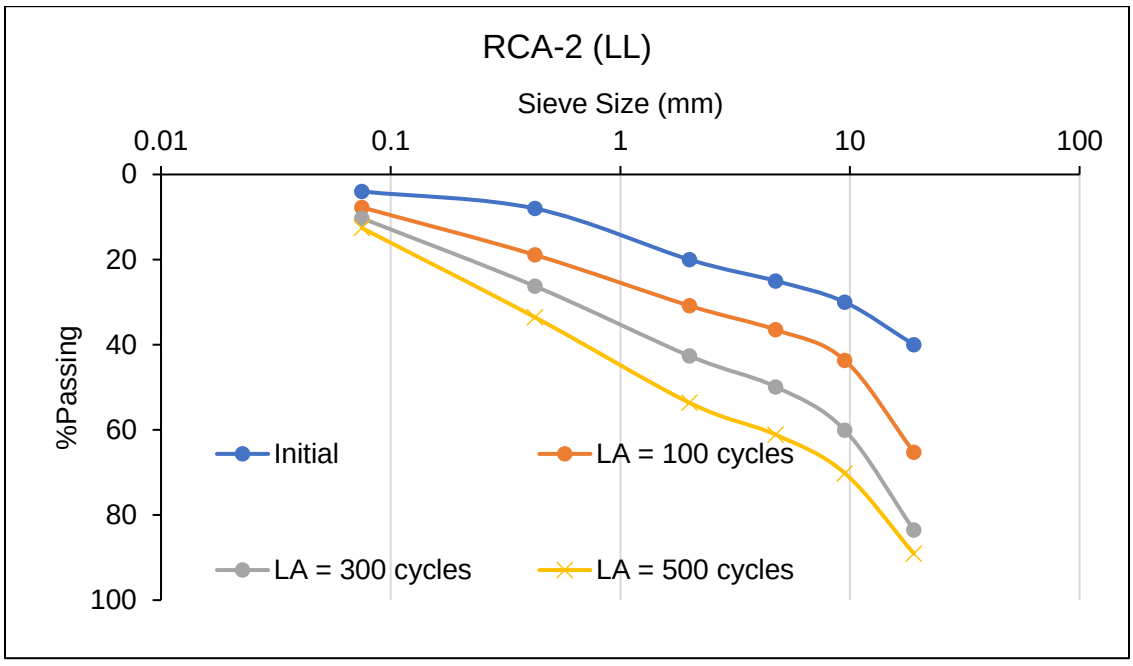

Figure B.6 Change in gradation of RCA-2 (LL) with different LA abrasion cycles

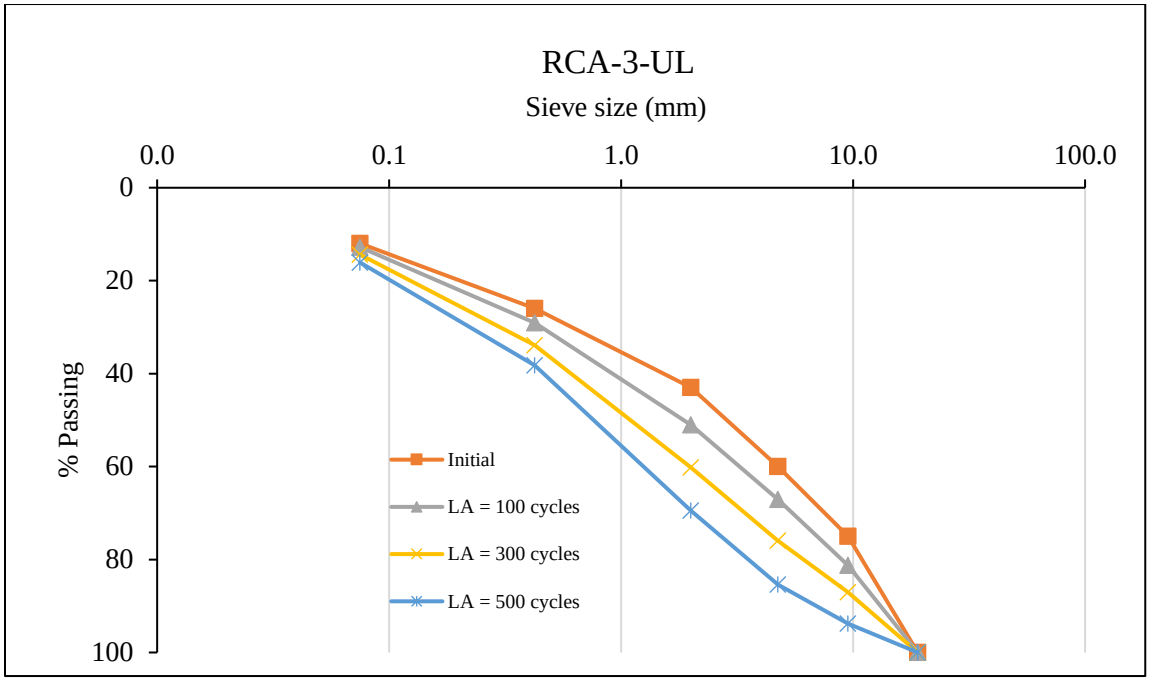

Figure B.7 Change in gradation of RCA-2 (LL) with different LA abrasion cycles

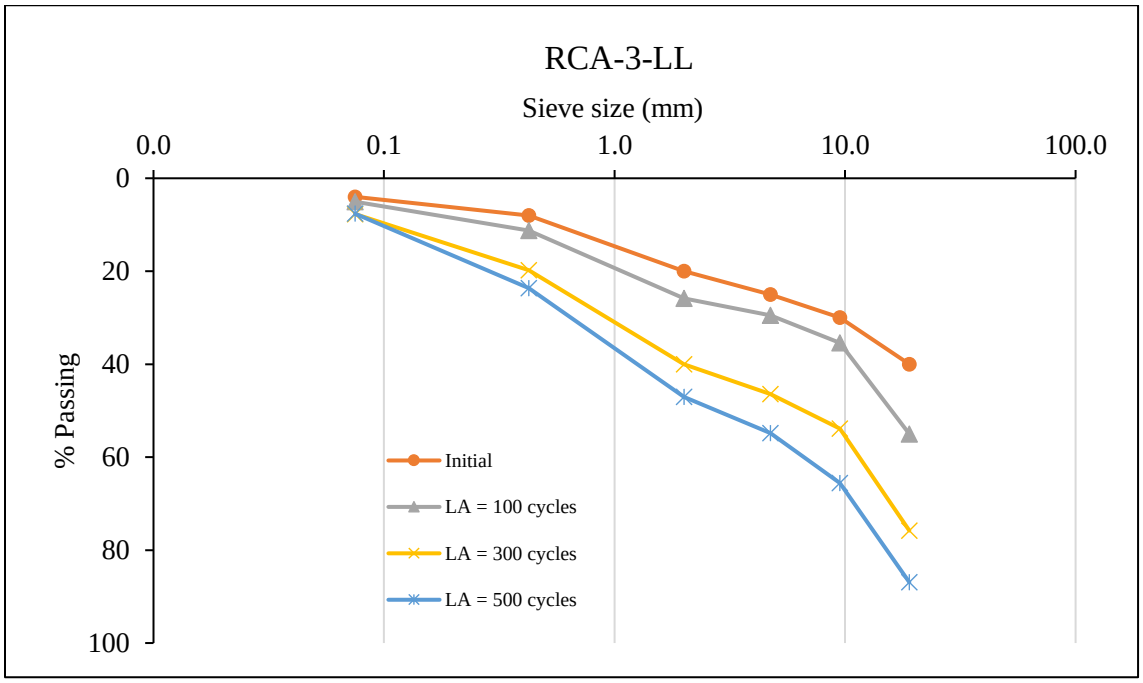

Figure B.8 Change in gradation of RCA-2 (LL) with different LA abrasion cycles

APPENDIX C: CHANGES IN RESILIENT MODULUS WITH DIFFERENT LA ABRASION CYCLES

Table C-1 Resilient modulus of the VLA-1 aggregate (upper limit) after conditioning with different la abrasion cycles

Sequence No	Chamber confining pressure (psi)	Maximum axial stress (psi)	Bulk stress (psi)	Resilient modulus (psi)			
				VLA-1 (upper limit)			
				0 cycle	100 cycles	300 cycles	500 cycles
Sequence 1	3	3	12	17,362	9,252	9,614	9,516
Sequence 2	3	6	14	18,744	13,528	14,562	13,921
Sequence 3	3	9	17	21,577	15,564	17,400	16,395
Sequence 4	5	5	19	19,554	12,324	14,023	12,855
Sequence 5	5	10	24	23,203	16,896	18,671	17,504
Sequence 6	5	15	28	25,997	20,355	22,271	21,113
Sequence 7	10	10	39	23,367	16,851	18,930	19,749
Sequence 8	10	20	48	30,785	23,963	26,071	26,840
Sequence 9	10	30	57	35,528	28,864	31,401	31,352
Sequence 10	15	10	54	24,076	16,229	18,975	19,936
Sequence 11	15	15	58	27,880	20,437	22,910	22,926
Sequence 12	15	30	72	37,426	31,205	32,295	32,196
Sequence 13	20	15	73	28,499	20,815	23,065	22,970
Sequence 14	20	20	78	33,027	25,420	27,258	26,670
Sequence 15	20	40	96	42,116	35,726	37,397	36,420

Table C-2 Model parameters and design resilient modulus of the VLA-1 aggregate (upper limit) after conditioning with different LA abrasion cycles

Aggregate type	Gradation	LA abrasion cycles	K_1	K_2	Design resilient modulus (psi)
VLA-1	ODOT Type A (UL)	0	6,602.2	0.38	18,350
		100	3,095.7	0.50	11,975
		300	3,758.9	0.47	13,400
		500	3,442.8	0.50	13,300

Table C-3 Resilient modulus of the VLA-1 aggregate (lower limit) after conditioning with different LA abrasion cycles

Sequence No	Chamber confining pressure (psi)	Maximum axial stress (psi)	Bulk stress (psi)	Resilient modulus (psi)			
				VLA-1 (lower limit)			
				0 cycle	100 cycles	300 cycles	500 cycles
Sequence 1	3	3	12	9,488	11,753	12,563	13,818
Sequence 2	3	6	14	12,029	15,043	16,876	16,327
Sequence 3	3	9	17	13,352	18,145	20,766	19,345
Sequence 4	5	5	19	11,094	14,053	15,878	16,303
Sequence 5	5	10	24	14,188	19,400	22,424	20,561
Sequence 6	5	15	28	17,025	23,536	27,059	24,212
Sequence 7	10	10	39	14,857	18,738	22,589	21,007
Sequence 8	10	20	48	20,090	26,183	29,456	28,390
Sequence 9	10	30	57	25,582	30,088	33,871	33,574
Sequence 10	15	10	54	13,623	16,486	22,020	19,711
Sequence 11	15	15	58	17,225	20,985	27,577	23,879
Sequence 12	15	30	72	25,593	29,992	39,201	34,125
Sequence 13	20	15	73	16,947	19,931	27,719	24,090
Sequence 14	20	20	78	20,307	24,169	33,064	28,468
Sequence 15	20	40	96	29,724	28,184	40,391	37,079

Table C-4 Model parameters and design resilient modulus of the VLA-1 aggregate (lower limit) after conditioning with different la abrasion cycles

Aggregate type	Gradation	LA abrasion cycles	K_1	K_2	Design resilient modulus (psi)
VLA-1	ODOT Type A (LL)	0	3,395.9	0.44	11,200
		100	7,590.8	0.28	11,975
		300	4,909.9	0.45	13,400
		500	5,512.2	0.39	13,300

Table C-5 Resilient modulus of the RCA-1 aggregate (upper limit) after conditioning with different LA abrasion cycles

Sequence No	Chamber confining pressure (psi)	Maximum axial stress (psi)	Bulk stress (psi)	Resilient modulus (psi)			
				RCA-1 (upper limit)			
				0 cycle	100 cycles	300 cycles	500 cycles
Sequence 1	3	3	12	21,265	11,188	11,843	11,995
Sequence 2	3	6	14	27,565	11,887	13,932	13,775
Sequence 3	3	9	17	29,371	13,627	15,632	14,937
Sequence 4	5	5	19	21,729	11,988	13,681	13,283
Sequence 5	5	10	24	33,359	14,381	16,227	15,255
Sequence 6	5	15	28	35,287	16,760	18,776	16,542
Sequence 7	10	10	39	38,254	14,208	15,938	15,255
Sequence 8	10	20	48	44,269	19,549	19,213	17,520
Sequence 9	10	30	57	44,781	22,014	21,209	18,998
Sequence 10	15	10	54	35,006	13,735	12,728	15,255
Sequence 11	15	15	58	43,811	15,366	13,751	16,542
Sequence 12	15	30	72	48,608	23,310	21,326	18,998
Sequence 13	20	15	73	44,618	16,503	15,448	16,542
Sequence 14	20	20	78	47,358	19,026	18,159	17,520
Sequence 15	20	40	96	51,959	25,812	23,526	-

Table C-6 Model parameters and design resilient modulus of the RCA-1 aggregate (upper limit) after conditioning with different LA abrasion cycles

Aggregate type	Gradation	LA abrasion cycles	K_1	K_2	Design resilient modulus (psi)
RCA-1	ODOT Type A (UL)	0	7,037.50	0.44	23,200
		100	4,628.90	0.34	11,620
		300	6,617.40	0.27	13,750
		500	6,567.10	0.29	14,400

Table C-7 Resilient modulus of the RCA-1 aggregate (lower limit) after conditioning with different LA abrasion cycle

Sequence No	Chamber confining pressure (psi)	Maximum axial stress (psi)	Bulk stress (psi)	Resilient modulus (psi)			
				RCA-1 (lower limit)			
				0 cycle	100 cycles	300 cycles	500 cycles
Sequence 1	3	3	12	12,029	12,030	13,592	12,042
Sequence 2	3	6	14	15,607	14,868	15,587	14,965
Sequence 3	3	9	17	18,541	18,254	17,676	16,994
Sequence 4	5	5	19	14,465	14,138	15,293	14,134
Sequence 5	5	10	24	19,495	19,352	18,555	17,564
Sequence 6	5	15	28	24,130	23,916	21,414	19,945
Sequence 7	10	10	39	19,163	19,988	18,387	17,564
Sequence 8	10	20	48	26,049	25,485	23,887	21,828
Sequence 9	10	30	57	30,683	-	26,826	24,787
Sequence 10	15	10	54	16,903	-	16,873	17,564
Sequence 11	15	15	58	20,820	-	19,367	19,945
Sequence 12	15	30	72	31,120	-	28,328	24,787
Sequence 13	20	15	73	20,960	-	20,174	19,945
Sequence 14	20	20	78	24,953	-	22,967	21,828
Sequence 15	20	40	96	32,262	-	30,948	27,126

Table C-8 Model parameters and design resilient modulus of the RCA-1 aggregate (lower limit) after conditioning with different LA abrasion cycles

Aggregate type	Gradation	LA abrasion cycles	K_1	K_2	Design resilient modulus (psi)
RCA-1	ODOT Type A (LL)	0	4,160.80	0.42	12,975
		100	4,507.60	0.44	14,800
		300	6,694.10	0.30	15,050
		500	5,560.20	0.35	14,300

Table C-9 Resilient modulus of The RCA-2 aggregate (upper limit) after conditioning with different LA abrasion cycles

Sequence No	Chamber confining pressure (psi)	Maximum axial stress (psi)	Bulk stress (psi)	Resilient modulus (psi)		
				RCA-2 (upper limit)		
				0 cycle	300 cycles	500 cycles
Sequence 1	3	3	12	12,081	12,768	13,319
Sequence 2	3	6	14	13,270	13,781	14,037
Sequence 3	3	9	17	14,225	14,585	14,500
Sequence 4	5	5	19	13,180	13,608	14,073
Sequence 5	5	10	24	14,849	15,046	14,966
Sequence 6	5	15	28	17,471	17,445	16,514
Sequence 7	10	10	39	15,191	15,068	15,136
Sequence 8	10	20	48	19,324	18,971	18,503
Sequence 9	10	30	57	23,606	22,246	20,827
Sequence 10	15	10	54	16,175	15,996	16,744
Sequence 11	15	15	58	17,596	17,213	17,096
Sequence 12	15	30	72	24,061	22,650	20,854
Sequence 13	20	15	73	18,017	17,405	17,317
Sequence 14	20	20	78	19,635	18,870	18,167
Sequence 15	20	40	96	27,963	25,767	23,263

Table C-10 Model parameters and design resilient modulus of the RCA-2 aggregate (upper limit) after conditioning with different LA abrasion cycles

Aggregate type	Gradation	LA abrasion cycles	K_1	K_2	Design resilient modulus (psi)
RCA-2	ODOT Type A (UL)	0	5108.5	0.34	12,800
		300	6343.9	0.27	13,100
		500	4445.7	0.35	11,450

Table C-11 Resilient modulus of the RCA-2 Aggregate (lower limit) after conditioning with different LA abrasion cycle

Sequence No	Chamber confining pressure (psi)	Maximum axial stress (psi)	Bulk stress (psi)	Resilient modulus (psi) RCA-2 (lower limit) 0 cycle
Sequence 1	3	3	12	9,486
Sequence 2	3	6	14	11,743
Sequence 3	3	9	17	13,537
Sequence 4	5	5	19	11,141
Sequence 5	5	10	24	14,349
Sequence 6	5	15	28	16,351
Sequence 7	10	10	39	14,349
Sequence 8	10	20	48	17,745
Sequence 9	10	30	57	21,501
Sequence 10	15	10	54	14,849
Sequence 11	15	15	58	16,351
Sequence 12	15	30	72	22,001
Sequence 13	20	15	73	17,351
Sequence 14	20	20	78	18,745
Sequence 15	20	40	96	25,932

Table C-12 Model parameters and design resilient modulus of the RCA-2 aggregate (lower limit) after conditioning with different LA abrasion cycles

Aggregate type	Gradation	LA abrasion cycles	K_1	K_2	Design resilient modulus (psi)
RCA-2	ODOT Type A (LL)	0	3,659.9	0.40	10,800

Table C-13 Resilient modulus of the RCA-3 aggregate (upper limit) after conditioning with different LA abrasion cycles

Sequence No	Chamber confining pressure (psi)	Maximum axial stress (psi)	Bulk stress (psi)	Resilient modulus (psi)			
				RCA-3 (upper limit)			
				0 cycle	100 cycles	300 cycles	500 cycles
Sequence 1	3	3	12	12,215	12,779	11,186	13,138
Sequence 2	3	6	14	15,883	16,491	14,424	16,499
Sequence 3	3	9	17	18,519	19,143	16,737	18,851
Sequence 4	5	5	19	14,823	15,421	13,491	15,540
Sequence 5	5	10	24	19,273	19,900	17,397	19,516
Sequence 6	5	15	28	22,471	23,101	20,186	22,298
Sequence 7	10	10	39	19,273	19,900	17,397	19,516
Sequence 8	10	20	48	25,058	25,679	22,433	24,509
Sequence 9	10	30	57	29,217	29,810	26,030	28,004
Sequence 10	15	10	54	19,273	19,900	17,397	19,516
Sequence 11	15	15	58	22,471	23,101	20,186	22,298
Sequence 12	15	30	72	29,217	29,810	26,030	28,004
Sequence 13	20	15	73	22,471	23,101	20,186	22,298
Sequence 14	20	20	78	25,058	25,679	22,433	24,509
Sequence 15	20	40	96	32,580	33,138	28,927	30,781

Table C-14 Model parameters and design resilient modulus of the RCA-3 aggregate (upper limit) after conditioning with different LA abrasion cycles

Aggregate type	Gradation	LA abrasion cycles	K_1	K_2	Design resilient modulus (psi)
RCA-3	ODOT Type A (UL)	0	8,385.73	0.38	23,386
		100	8,868.01	0.37	22,708
		300	7,770.70	0.37	23,945
		500	9,478.33	0.33	18,925

Table C-15 Resilient modulus of the RCA-3 aggregate (lower limit) after conditioning with different LA abrasion cycle

Sequence No	Chamber confining pressure (psi)	Maximum axial stress (psi)	Bulk stress (psi)	Resilient modulus (psi)			
				RCA-3 (lower limit)			
				0 cycle	100 cycles	300 cycles	500 cycles
Sequence 1	3	3	12	10,343	10,091	10,156	14,325
Sequence 2	3	6	14	14,145	13,450	13,160	19,488
Sequence 3	3	9	17	16,987	15,912	15,314	23,332
Sequence 4	5	5	19	13,027	12,471	12,293	17,972
Sequence 5	5	10	24	17,815	16,622	15,929	24,449
Sequence 6	5	15	28	21,394	19,664	18,537	29,272
Sequence 7	10	10	39	17,815	16,622	15,929	24,449
Sequence 8	10	20	48	24,363	22,155	20,642	33,260
Sequence 9	10	30	57	29,258	26,210	24,020	39,821
Sequence 10	15	10	54	17,815	16,622	15,929	24,449
Sequence 11	15	15	58	21,394	19,664	18,537	29,272
Sequence 12	15	30	72	29,258	26,210	24,020	39,821
Sequence 13	20	15	73	21,394	19,664	18,537	29,272
Sequence 14	20	20	78	24,363	22,155	20,642	33,260
Sequence 15	20	40	96	33,317	29,529	26,748	45,247

Table C-16 Model parameters and design resilient modulus of the RCA-3 aggregate (lower limit) after conditioning with different LA abrasion cycles

Aggregate type	Gradation	LA abrasion cycles	K_1	K_2	Design resilient modulus (psi)
RCA-3	ODOT Type A (LL)	0	6,604.70	0.45	22,437
		100	6,685.41	0.41	20,294
		300	7,005.51	0.37	18,401
		500	9,216.60	0.44	23,315

APPENDIX D: CHANGES IN SHAPE PARAMETERS

Table D-1 Average texture of RCA-1, RCA-2, RCA-3, and VLA-1 for the UL

Aggregate conditioning	Average texture (UL)							
	Retaining on 3/8" sieve				Retaining on #4 sieve			
	VLA-1	RCA-1	RCA-2	RCA-3	VLA-1	RCA-1	RCA-2	RCA-3
0 cycle	242.5	197.2	209.8	255.1	184.4	160.0	175.7	205.4
100 cycles	295.3	173.7	196.0	237.0	238.0	139.9	152.7	215.1
300 cycles	281.8	163.5	196.2	223.9	219.4	151.9	152.2	193.0
500 cycles	298.9	163.4	208.3	220.3	228.0	156.5	158.1	181.3

* 0 <Polished < 165 < Smooth < 275 < Low Roughness < 350

Table D-2 Average texture of RCA-1, RCA-2, RCA-3, and VLA-1 for the LL

Aggregate conditioning	Average texture (LL)								
	Retaining on 3/4" sieve			Retaining on 3/8" sieve			Retaining on #4 sieve		
	VLA-1	RCA-1	RCA-3	VLA-1	RCA-1	RCA-3	VLA-1	RCA-1	RCA-3
0 cycle	367.7	220.5	316.5	247.5	197.2	255.1	191.9	160.0	205.4
100 cycles	371.9	221.5	311.7	280.9	166.6	245.9	208.6	143.8	272.6
300 cycles	377.4	191.4	299.7	308.8	170.4	237.7	232.8	141.6	234.2
500 cycles	360.8	193.0	284.2	298.9	164.4	229.5	245.8	158.3	234.3

* 0 <Polished < 165 < Smooth < 275 < Low Roughness < 350

Table D-3 Angularity of RCA-1, RCA-2, RCA-3, and VLA-1 for the UL

Aggregate conditioning	Average gradient angularity (UL)							
	Retaining on 3/8" sieve				Retaining on #4 sieve			
	VLA-1	RCA-1	RCA-2	RCA-3	VLA-1	RCA-1	RCA-2	RCA-3
0 cycle	2,937.5	3,117.1	2,823.3	2,847.4	3,386.2	3,330.3	3,154.0	2,945.8
100 cycles	2,521.0	2,757.4	2,561.0	2,593.3	2,706.1	2,811.9	3,100.2	2,812.2
300 cycles	2,118.4	2,476.1	2,576.0	2,371.1	2,392.6	2,748.8	2,528.4	2,779.8
500 cycles	1,963.5	2,436.1	2,161.4	2,339.6	2,371.6	2,439.5	2,568.6	2,618.7

* 0 <Rounded < 2100; 2100 < Sub-rounded < 4000

Table D-4 Angularity of RCA-1, RCA-2, RCA-3, and VLA-1 for the LL

Aggregate conditioning	Average gradient angularity (LL)								
	Retaining on 3/4" sieve			Retaining on 3/8" sieve			Retaining on #4 sieve		
	VLA-1	RCA-1	RCA-3	VLA-1	RCA-1	RCA-3	VLA-1	RCA-1	RCA-3
0 cycle	2,920.5	2,701.5	2,532.2	2,864.4	3,117.1	2,847.4	3,386.2	3,330.3	2,945.8
100 cycles	2,134.0	2,252.8	2,375.2	2,587.6	2,605.5	2,632.7	3,055.9	3,044.4	2,643.5
300 cycles	2,057.6	2,037.4	2,174.2	2,149.1	2,444.5	2,584.2	2,610.6	2,852.2	2,910.5
500 cycles	1,990.1	1,877.0	1,966.8	1,963.5	2,157.9	2,417.7	1,963.5	2,662.2	2,569.1

* 0 <Rounded < 2100; 2100 < Sub-rounded < 4000

APPENDIX E: XRD SPECTRA FOR DIFFERENT AGGREGATES

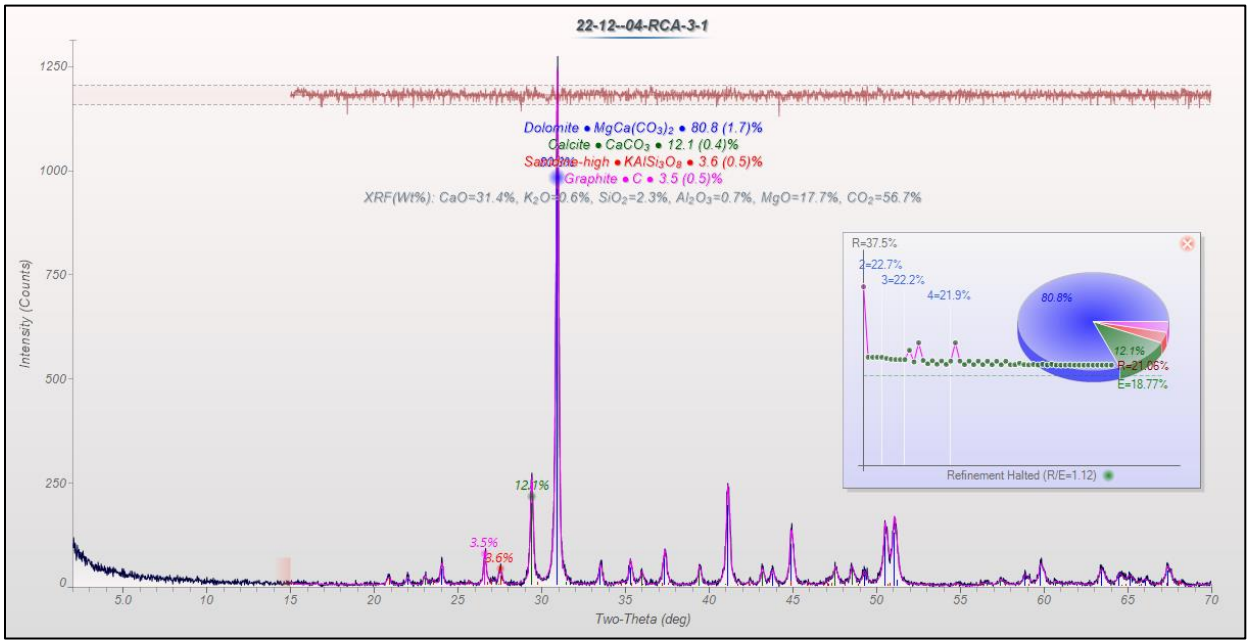

Figure E-1 XRD spectra for RCA-3 aggregate

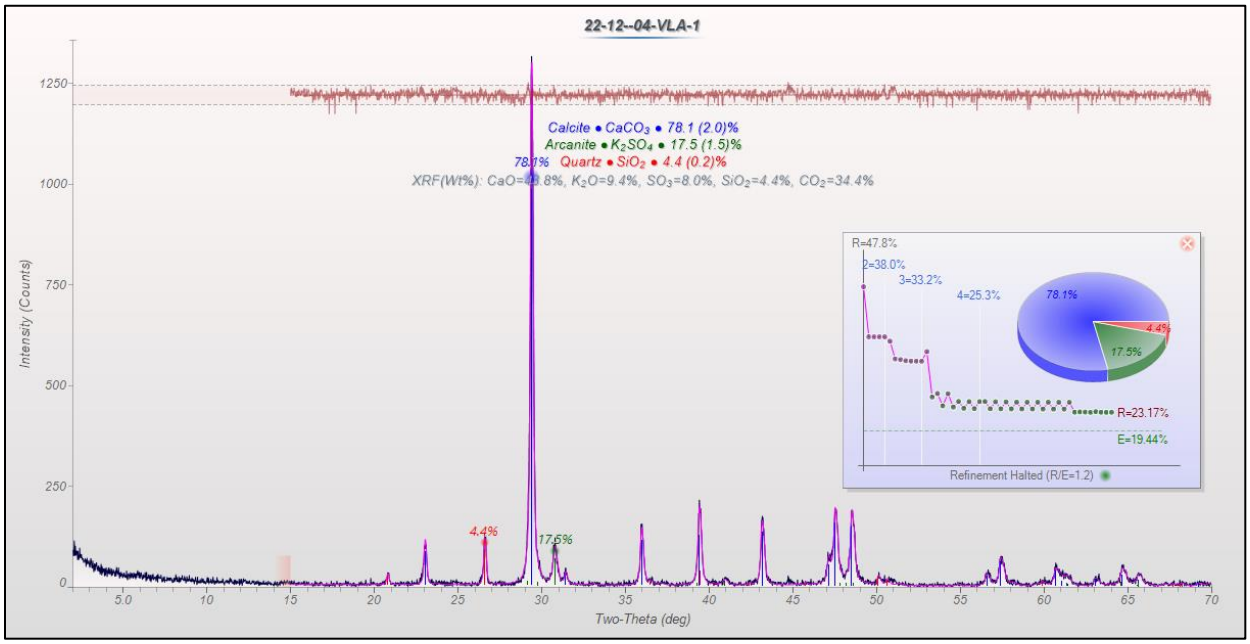

Figure E-2 XRD spectra for VLA-1 aggregate

APPENDIX F: PERMEABILITY GRAPHS (WITHOUT TEMPERATURE CORRECTIONS)

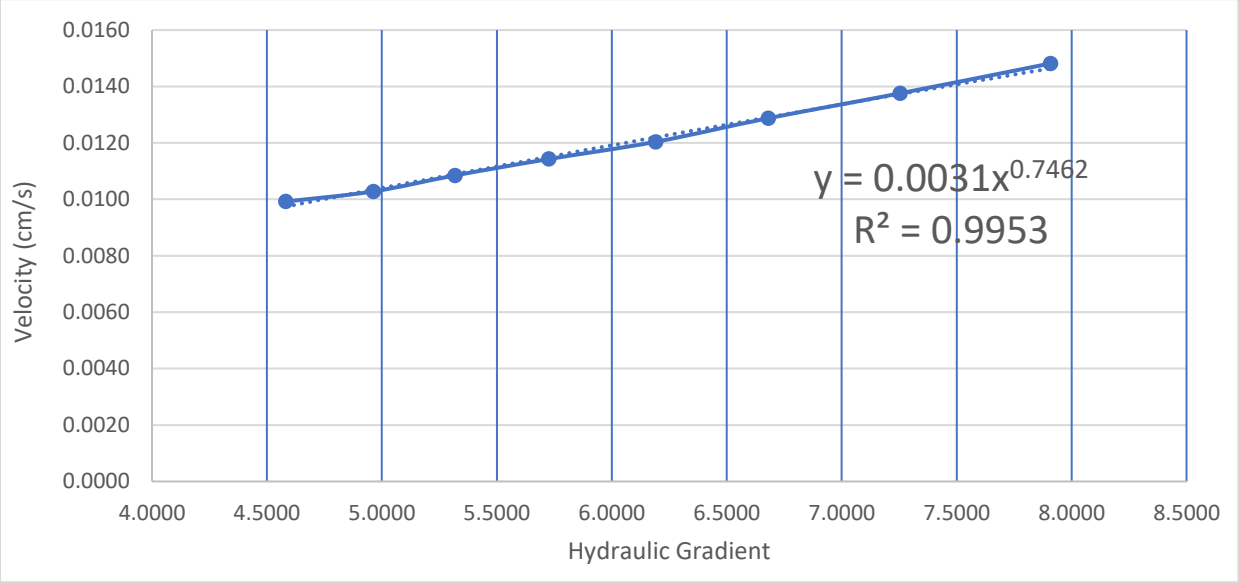

Figure F-1 Permeability of RCA-3-LA0 upper limit

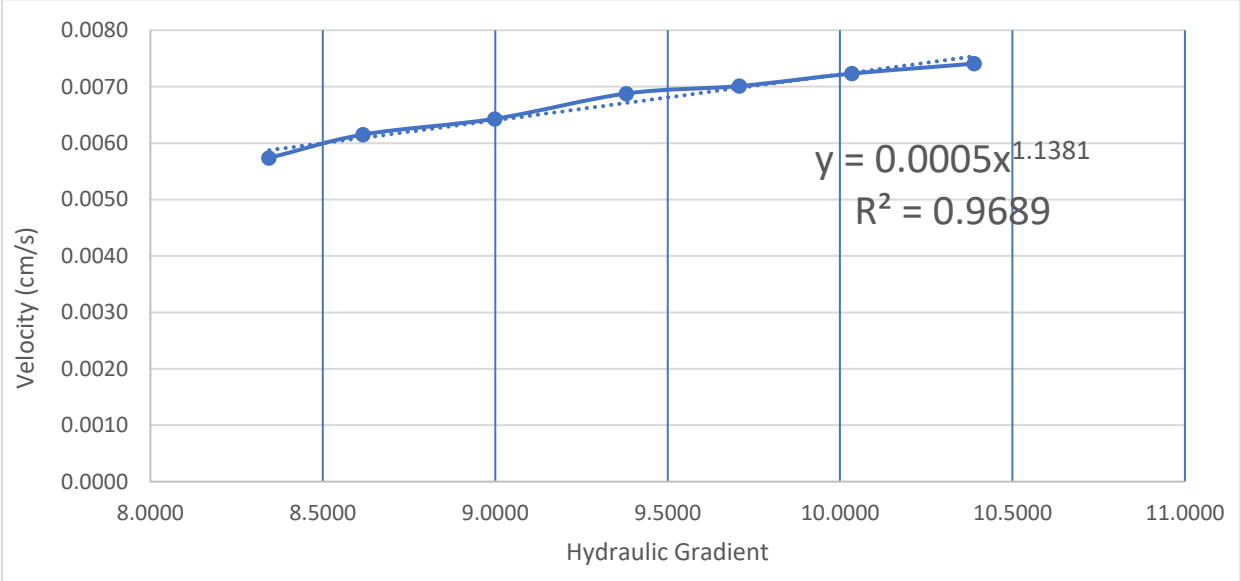

Figure F-2 Permeability of RCA-3-LA100 upper limit

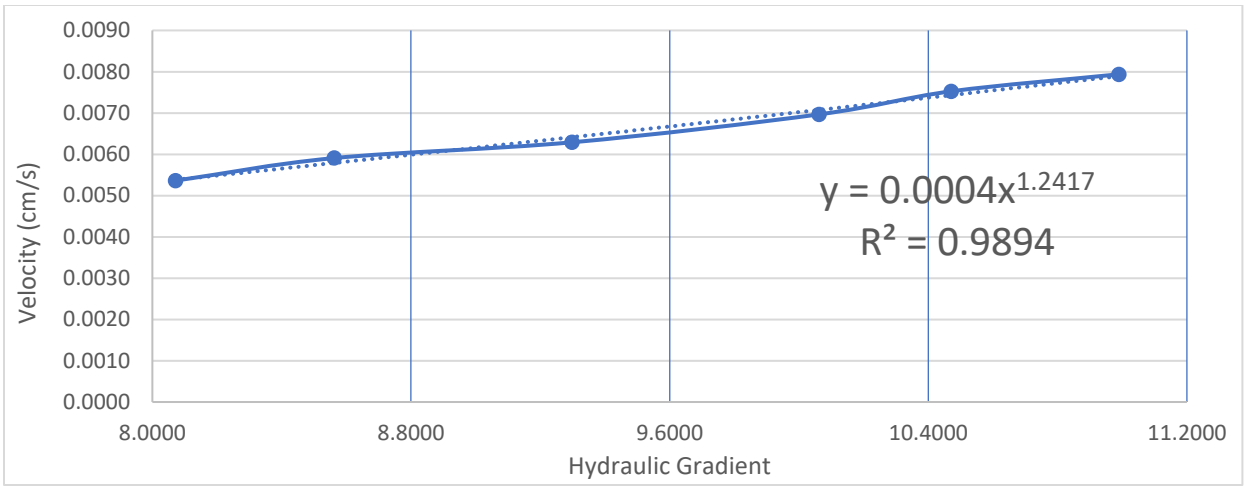

Figure F-3 Permeability of RCA-3-LA300 upper limit

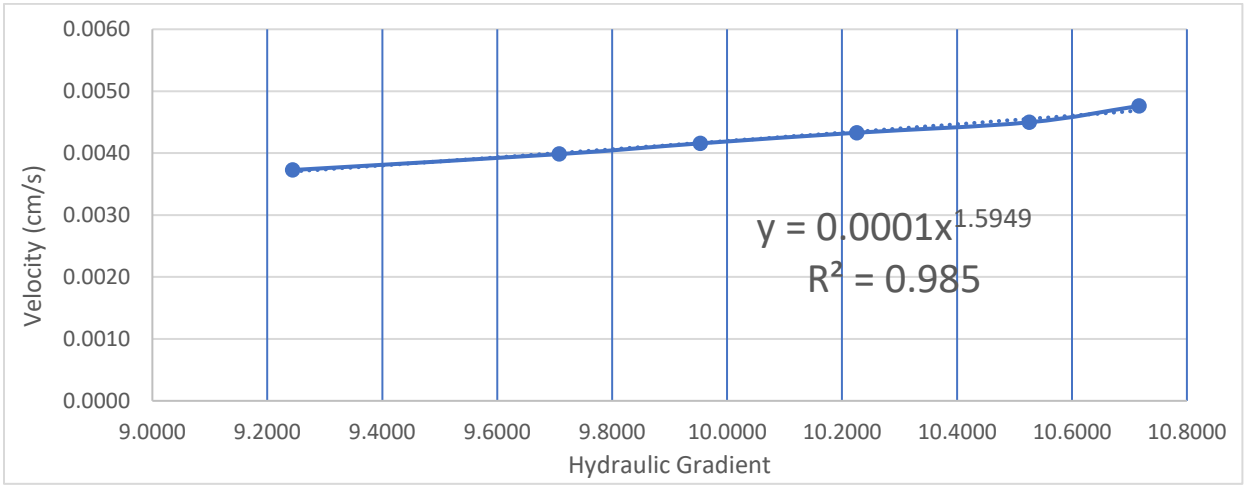

Figure F-4 Permeability of RCA-3-LA500 upper limit

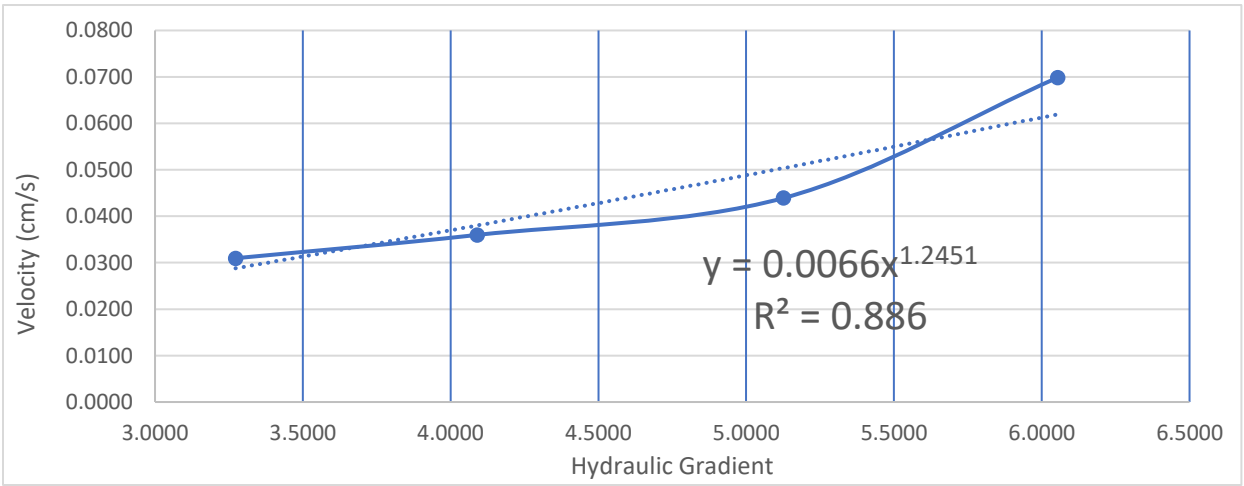

Figure F-5 Permeability of RCA-3-LA0 lower limit

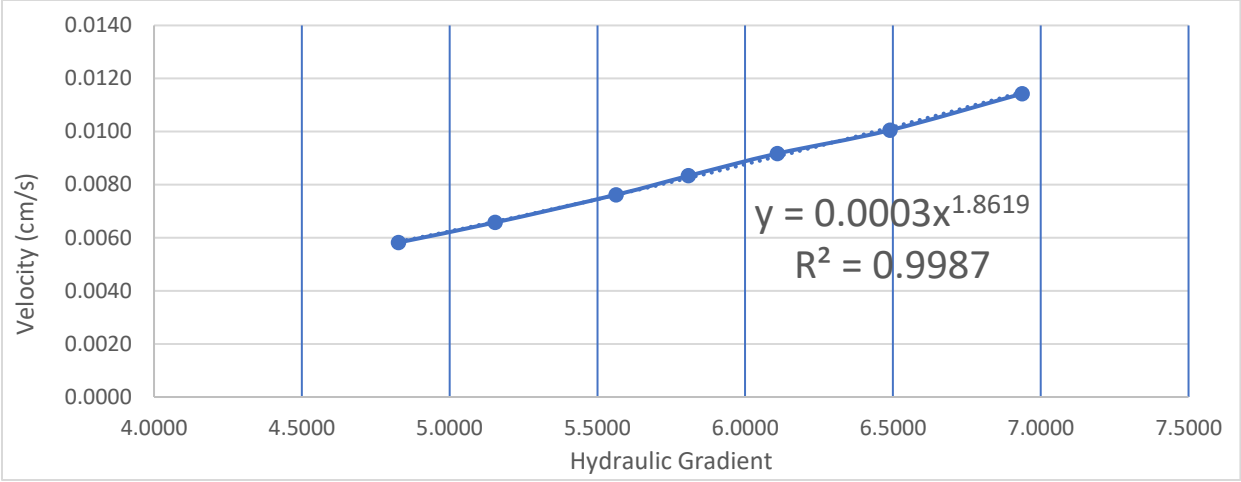

Figure F-6 Permeability of RCA-3-LA100 lower limit

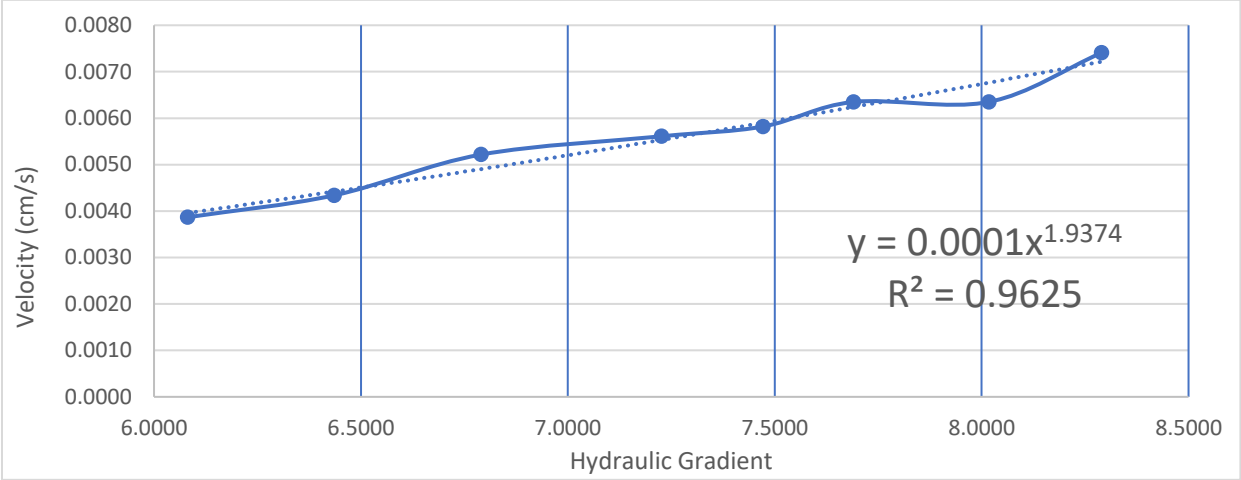

Figure F-7 Permeability of RCA-3-LA300 lower limit

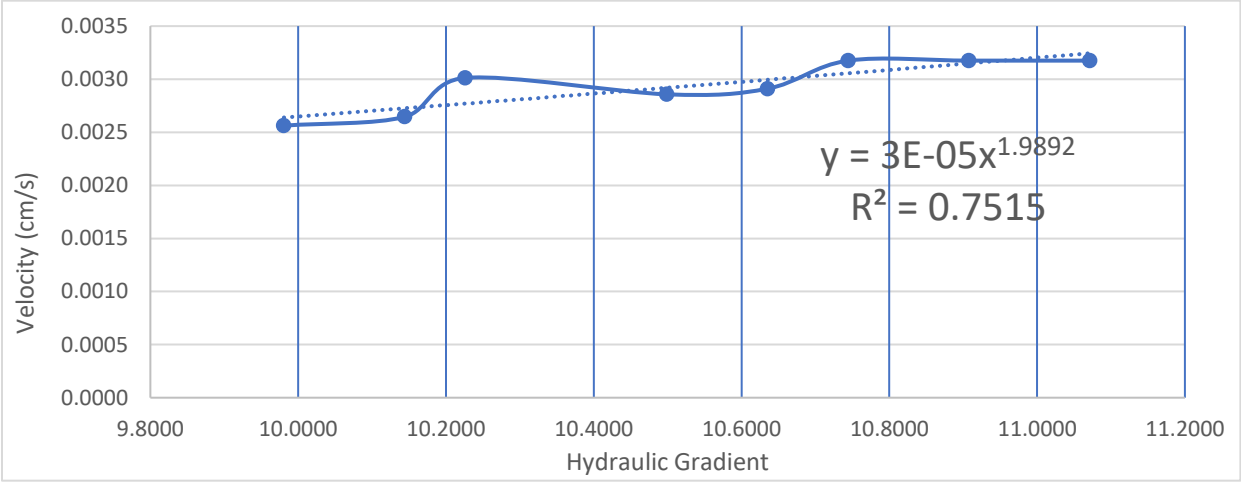

Figure F-8 Permeability of RCA-3-LA500 lower limit

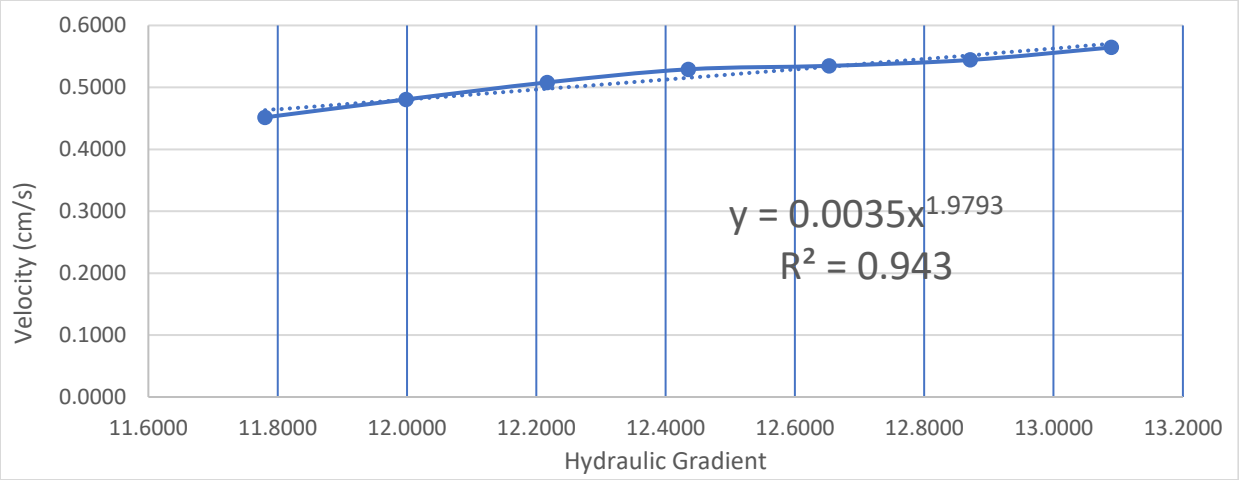

Figure F-9 Permeability of VLA-1-LA0 upper limit

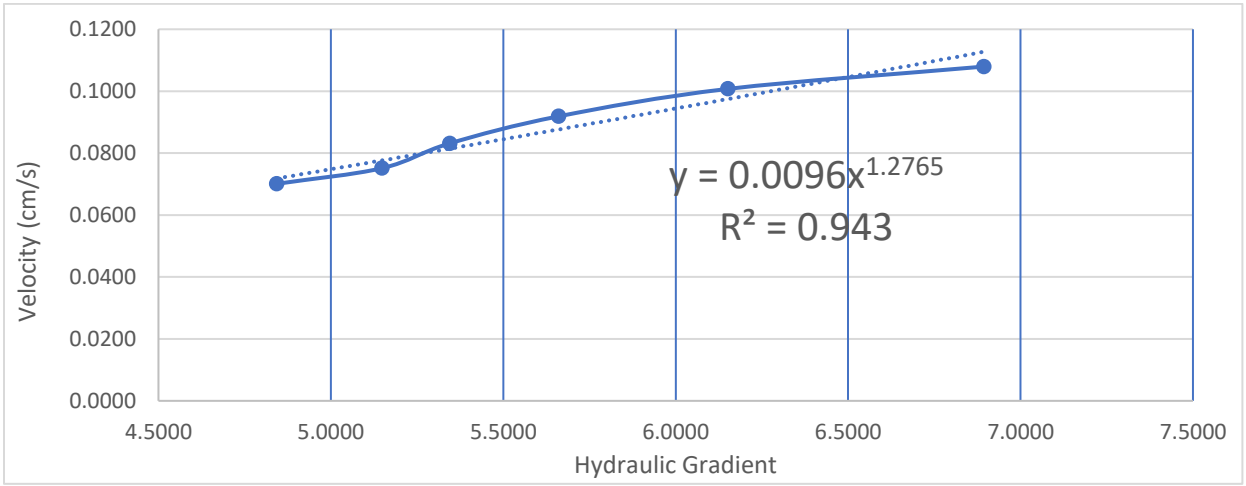

Figure F-10 Permeability of VLA-1-LA0 lower limit

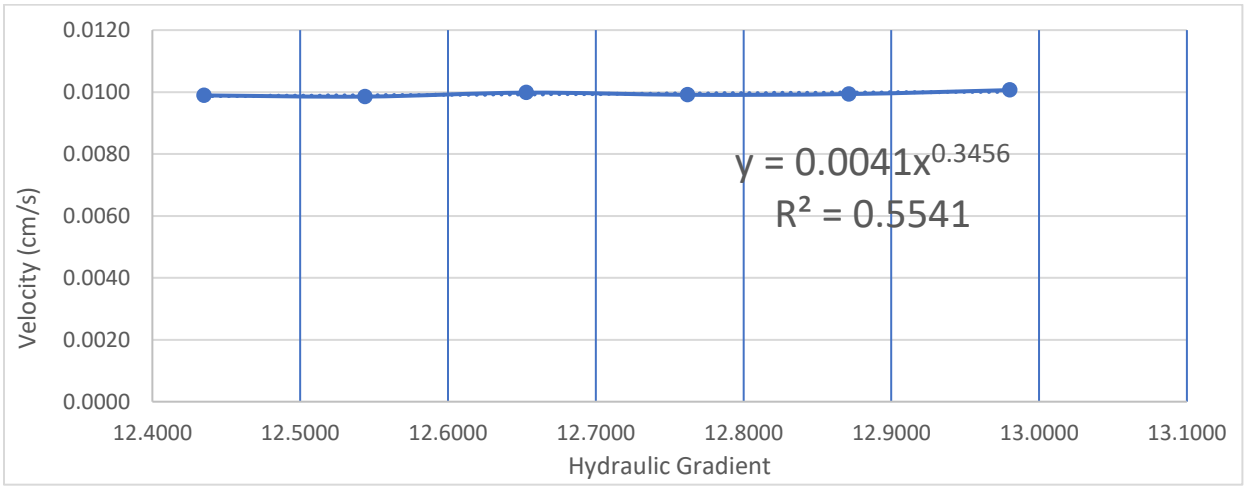

Figure F-11 Permeability of RCA-2-LA0 upper limit

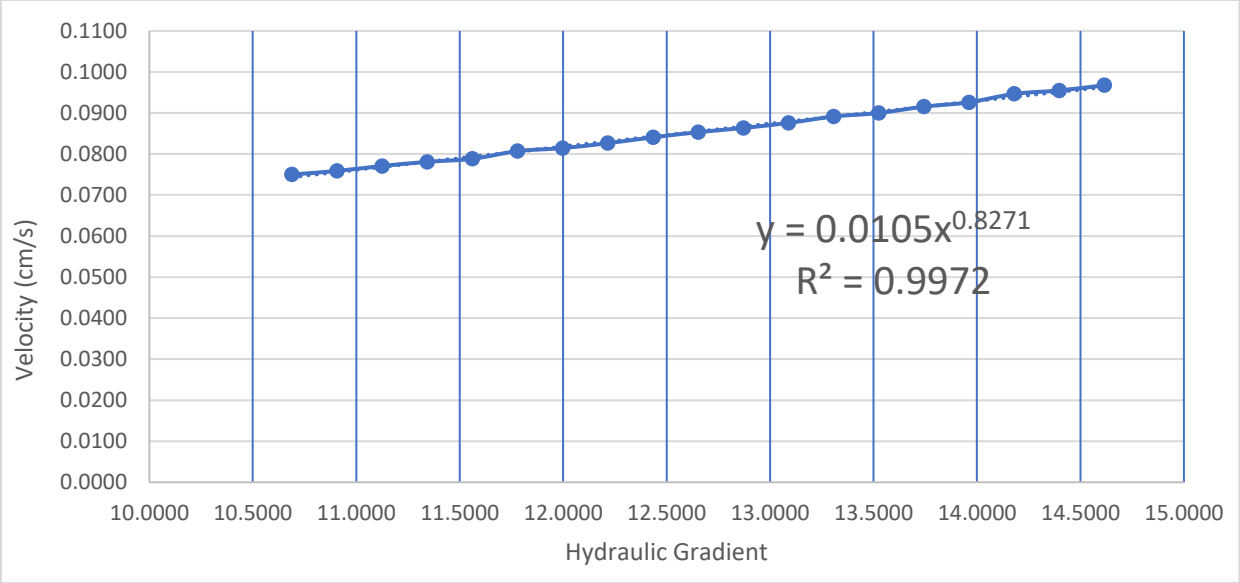

Figure F-12 Permeability of RCA-1-LA0 lower limit

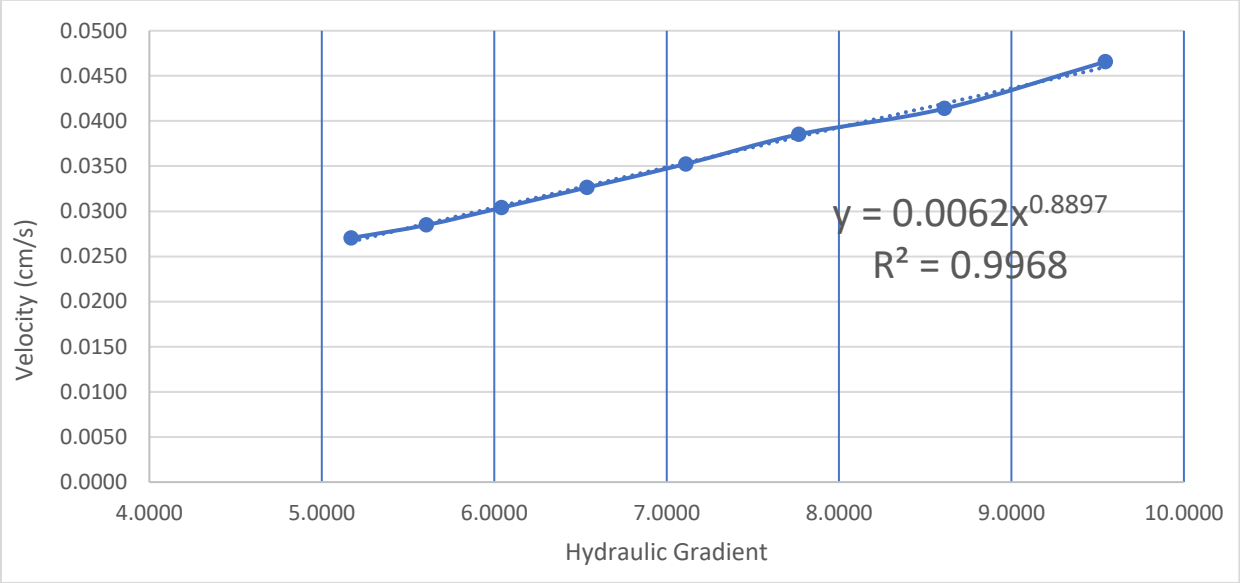

Figure F-13 Permeability of CRCA-3-LA0 lower limit

APPENDIX G: LCCA CALCULATIONS

Table G-1 Initial cost for pavement with VLA-1-UL (0 cycle) aggregate base thickness of 8 in.

Category	Description	Depth (in)	Width (ft)	Quantity per mile	Unit	Unit Price	Cost per mile
Under Pavement	EXCAVATION - SUBGRADE	12	12	2346.7	CY	$8.34	$19,571.50
Under Pavement	SUBGRADE, METHOD B (SY)		12	7040	SY	$2.45	$17,248.00
Under Pavement	STABILIZED SUBGRADE (SY)		12	7040	SY	$6.13	$43,155.20
Under Pavement	VLA-1-UL (0 cycle)	8	12	1564.4	CY	$35.70	$55,849.08
HMA	SUPERPAVE, TYPE S3(PG 64-22 OK)	4	12	1591	TON	$78.60	$125,052.60
HMA	SUPERPAVE, TYPE S3(PG 64-22 OK)	3	12	1193.3	TON	$78.60	$93,793.40
HMA	SUPERPAVE, TYPE S4(PG 64-22 OK)	2	12	795.5	TON	$91.60	$72,867.80
						Cost/Mile	$427,537.58
						Length (miles)	1
						Segment cost	$427,537.58

Table G-2 Initial cost for pavement with RCA (0 cycle) aggregate base thickness of 8 in., representative of RCAs

Category	Description	Depth (in)	Width (ft)	Quantity per mile	Unit	Unit Price	Cost per mile
Under Pavement	EXCAVATION - SUBGRADE	12	12	2346.7	CY	$8.34	$19,571.50
Under Pavement	SUBGRADE, METHOD B (SY)		12	7040	SY	$2.45	$17,248.00
Under Pavement	STABILIZED SUBGRADE (SY)		12	7040	SY	$6.13	$43,155.20
Under Pavement	RCA-UL (0 cycle)	8	12	1564.4	CY	$20.00	$31,288.00
HMA	SUPERPAVE, TYPE S3(PG 64-22 OK)	4	12	1591	TON	$78.60	$125,052.60
HMA	SUPERPAVE, TYPE S3(PG 64-22 OK)	3	12	1193.3	TON	$78.60	$93,793.40
HMA	SUPERPAVE, TYPE S4(PG 64-22 OK)	2	12	795.5	TON	$91.60	$72,867.80
						Cost/Mile	$402,976.50
						Length (miles)	1
						Segment cost	$402,976.50

Table G-3 Initial cost for pavement with RCA (0 cycle) aggregate base thickness of 10 in., representative of RCAs

Category	Description	Depth (in)	Width (ft)	Quantity per mile	Unit	Unit Price	Cost per mile
Under Pavement	EXCAVATION - SUBGRADE	12	12	2346.7	CY	$8.34	$19,571.50
Under Pavement	SUBGRADE, METHOD B (SY)		12	7040	SY	$2.45	$17,248.00
Under Pavement	STABILIZED SUBGRADE (SY)		12	7040	SY	$6.13	$43,155.20
Under Pavement	RCA-UL (0 cycle)	10	12	1955.5	CY	$20.00	$39,110.00
HMA	SUPERPAVE, TYPE S3(PG 64-22 OK)	4	12	1591	TON	$78.60	$125,052.60
HMA	SUPERPAVE, TYPE S3(PG 64-22 OK)	3	12	1193.3	TON	$78.60	$93,793.40
HMA	SUPERPAVE, TYPE S4(PG 64-22 OK)	2	12	795.5	TON	$91.60	$72,867.80
						Cost/Mile	$410,798.50
						Length (miles)	1
						Segment cost	$410,798.50

Table G-4 Initial cost for pavement with RCA (0 cycle) aggregate base thickness of 12 in., representative of RCAs

Category	Description	Depth (in)	Width (ft)	Quantity per mile	Unit	Unit Price	Cost per mile
Under Pavement	EXCAVATION - SUBGRADE	12	12	2346.7	CY	$8.34	$19,571.50
Under Pavement	SUBGRADE, METHOD B (SY)		12	7040	SY	$2.45	$17,248.00
Under Pavement	STABILIZED SUBGRADE (SY)		12	7040	SY	$6.13	$43,155.20
Under Pavement	RCA-UL (0 cycle)	12	12	2346.6	CY	$20.00	$46,932.00
HMA	SUPERPAVE, TYPE S3(PG 64-22 OK)	4	12	1591	TON	$78.60	$125,052.60
HMA	SUPERPAVE, TYPE S3(PG 64-22 OK)	3	12	1193.3	TON	$78.60	$93,793.40
HMA	SUPERPAVE, TYPE S4(PG 64-22 OK)	2	12	795.5	TON	$91.60	$72,867.80
						Cost/Mile	$418,620.50
						Length (miles)	1
						Segment cost	$418,620.50

Table G-5 Initial Cost for Pavement with RCA (0 cycle) Aggregate Base Thickness of 14 in., Representative of RCAs

Category	Description	Depth (in)	Width (ft)	Quantity per mile	Unit	Unit Price	Cost per mile
Under Pavement	EXCAVATION - SUBGRADE	12	12	2346.7	CY	$8.34	$19,571.50
Under Pavement	SUBGRADE, METHOD B (SY)		12	7040	SY	$2.45	$17,248.00
Under Pavement	STABILIZED SUBGRADE (SY)		12	7040	SY	$6.13	$43,155.20
Under Pavement	RCA-UL (0 cycle)	14	12	2737.7	CY	$20.00	$54,754.00
HMA	SUPERPAVE, TYPE S3(PG 64-22 OK)	4	12	1591	TON	$78.60	$125,052.60
HMA	SUPERPAVE, TYPE S3(PG 64-22 OK)	3	12	1193.3	TON	$78.60	$93,793.40
HMA	SUPERPAVE, TYPE S4(PG 64-22 OK)	2	12	795.5	TON	$91.60	$72,867.80
						Cost/Mile	$426,442.50
						Length (miles)	1
						Segment cost	$426,442.50

Table G-6 Maintenance plan for pavement with VLA-1-UL (0 cycle)

Year	Activity	Cost	Present cost
0	Construction	$427,537.58	$427,537.58
1		$ -	$ -
2		$ -	$ -
3		$ -	$ -
4		$ -	$ -
5	Crack treatment	$ 750.00	$ 646.96
6		$ -	$ -
7		$ -	$ -
8		$ -	$ -
9		$ -	$ -
10	Crack treatment	$ 787.50	$ 585.97
11		$ -	$ -
12		$ -	$ -
13		$ -	$ -
14		$ -	$ -
15	Mill/Overlay	$ 95,000.00	$ 60,976.89
16		$ -	$ -
17		$ -	$ -
18		$ -	$ -
19		$ -	$ -
20	Remaining life	$ 40,000.00	$ 22,147.03
		Total	$467,600.37

Table G-7 maintenance plan for pavement with RCA-1-UL (0 cycle)

Year	Activity	Cost	Present cost
0	Construction	$402,976.50	$402,976.50
1		$ -	$ -
2		$ -	$ -
3		$ -	$ -
4		$ -	$ -
5	Crack treatment	$ 750.00	$ 646.96
6		$ -	$ -
7		$ -	$ -
8		$ -	$ -
9		$ -	$ -
10	Crack treatment	$ 787.50	$ 585.97
11		$ -	$ -
12		$ -	$ -
13		$ -	$ -
14		$ -	$ -
15	Mill/overlay	$ 95,000.00	$ 60,976.89
16		$ -	$ -
17		$ -	$ -
18		$ -	$ -
19		$ -	$ -
20	Remaining life	$ 40,000.00	$ 22,147.03
		Total	$443,039.29

Table G-8 Maintenance plan for pavement with RCA-2-UL (0 cycle) 8 in.

Year	Activity	Cost	Present cost
0	Construction	$402,976.50	$402,976.50
1		$ -	$ -
2		$ -	$ -
3		$ -	$ -
4		$ -	$ -
5	Crack treatment	$ 750.00	$ 646.96
6		$ -	$ -
7		$ -	$ -
8		$ -	$ -
9		$ -	$ -
10	Mill/overlay	$ 92,500.00	$ 68,828.68
11		$ -	$ -
12		$ -	$ -
13		$ -	$ -
14		$ -	$ -
15	Crack treatment	$ 825.00	$ 529.54
16		$ -	$ -
17		$ -	$ -
18		$ -	$ -
19		$ -	$ -
20	Remaining life	$ 5,000.00	$ 2,768.38
		Total	$470,213.30

Table G-9 Maintenance plan for pavement with RCA-2-UL (0 cycle) 10 in.

Year	Activity	Cost	Present cost
0	Construction	$410,798.50	$410,798.50
1		$ -	$ -
2		$ -	$ -
3		$ -	$ -
4		$ -	$ -
5	Crack treatment	$ 750.00	$ 646.96
6		$ -	$ -
7		$ -	$ -
8		$ -	$ -
9		$ -	$ -
10	Crack treatment	$ 787.50	$ 585.97
11		$ -	$ -
12	Mill/overlay	$ 93,500.00	$ 65,579.02
13		$ -	$ -
14		$ -	$ -
15		$ -	$ -
16		$ -	$ -
17		$ -	$ -
18	Crack treatment	$ 850.00	$ 499.29
19		$ -	$ -
20	Remaining life	$ 15,000.00	$ 8,305.13
		Total	$469,804.61

Table G-10 Maintenance plan for pavement with RCA-2-UL (0 cycle) 12 in.

Year	Activity	Cost	Present cost
0	Construction	$418,620.50	$418,620.50
1		$ -	$ -
2		$ -	$ -
3		$ -	$ -
4		$ -	$ -
5	Crack treatment	$ 750.00	$ 646.96
6		$ -	$ -
7		$ -	$ -
8		$ -	$ -
9		$ -	$ -
10	Crack treatment	$ 787.50	$ 585.97
11		$ -	$ -
12	Mill/overlay	$ 93,500.00	$ 65,579.02
13		$ -	$ -
14		$ -	$ -
15		$ -	$ -
16		$ -	$ -
17		$ -	$ -
18	Crack treatment	$ 850.00	$ 499.29
19		$ -	$ -
20	Remaining life	$ 15,000.00	$ 8,305.13
		Total	$477,626.61

Table G-11 Maintenance plan for pavement with RCA-2-UL (0 cycle) 14 in.

Year	Activity	Cost	Present Cost
0	Construction	$426,442.50	$426,442.50
1		$ -	$ -
2		$ -	$ -
3		$ -	$ -
4		$ -	$ -
5	Crack treatment	$ 750.00	$ 646.96
6		$ -	$ -
7		$ -	$ -
8		$ -	$ -
9		$ -	$ -
10	Crack treatment	$ 787.50	$ 585.97
11		$ -	$ -
12		$ -	$ -
13		$ -	$ -
14		$ -	$ -
15	Mill/overlay	$ 95,000.00	$ 60,976.89
16		$ -	$ -
17		$ -	$ -
18		$ -	$ -
19		$ -	$ -
20	Remaining life	$ 40,000.00	$ 22,147.03
		Total	$466,505.29

Table G-12 Maintenance plan for pavement with RCA-3-UL (0 cycle) 8 in.

Year	Activity	Cost	Present cost
0	Construction	$402,976.50	$402,976.50
1		$ -	$ -
2		$ -	$ -
3		$ -	$ -
4		$ -	$ -
5	Crack treatment	$ 750.00	$ 646.96
6		$ -	$ -
7		$ -	$ -
8		$ -	$ -
9		$ -	$ -
10	Crack treatment	$ 787.50	$ 585.97
11		$ -	$ -
12		$ -	$ -
13		$ -	$ -
14		$ -	$ -
15	Mill/overlay	$ 95,000.00	$ 60,976.89
16		$ -	$ -
17		$ -	$ -
18		$ -	$ -
19		$ -	$ -
20	Remaining life	$ 40,000.00	$ 22,147.03
		Total	$443,039.29

8. REFERENCES

Alexandria, V. (2013). The aggregates handbook. National Stone Association, Alexandria.

Andrei, D., Witczak, M. W., Schwartz, C. W., and Uzan, J. (2004). "Harmonized resilient modulus test method for unbound pavement materials." Transportation Research Record, 1874(1), 29-37.

Apotheker, S. (1990). Construction and demolition debris-The invisible waste stream. Resource Recycling, 9(12), 66-74.

Arshad, M. (2019). Development of a Correlation between the Resilient Modulus and CBR Value for Granular Blends Containing Natural Aggregates and RAP/RCA Materials. Advances in Materials Science and Engineering, 2019, 1-16.

Arshad, M., & Ahmed, M. F. (2017). Potential use of reclaimed asphalt pavement and recycled concrete aggregate in base/subbase layers of flexible pavements. Construction and Building Materials, 151, 83-97.

Arulrajah, A., Disfani, M. M., Horpibulsuk, S., Suksiripattanapong, C., & Prongmanee, N. (2014). Physical properties and shear strength responses of recycled construction and demolition materials in unbound pavement base/subbase applications. Construction and Building Materials, 58, 245-257.

Arulrajah, A., Piratheepan, J., Ali, M. M. Y., & Bo, M. W. (2012). Geotechnical properties of recycled concrete aggregate in pavement sub-base applications. Geotechnical Testing Journal, 35(5), 743-751.

Bennert, T., Papp Jr. W., Maher, A. and Gucunski, N. (2000). Utilization of Construction and Demolition Debris Under Traffic-Type Loading in Base and Subbase Applications. Transportation Research Record, No. 1714, Washington, D.C., pp. 33-39.

Bozyurt, O., Tinjum, J. M., Son, Y. H., Edil, T. B., & Benson, C. H. (2012). Resilient modulus of recycled asphalt pavement and recycled concrete aggregate. In GeoCongress 2012: State of the Art and Practice in Geotechnical Engineering (pp. 3901-3910).

Bunaciu, A. A., UdriŞTioiu, E. G., & Aboul-Enein, H. Y. (2015). X-ray diffraction: instrumentation and applications. Critical reviews in analytical chemistry, 45(4), 289-299.

Cackler, T. (2018). Recycled Concrete Aggregate Usage in the US.

Cavalline, T. L., Snyder, M. B., & Taylor, P. (2022). Use of Recycled Concrete Aggregate (RCA) in Concrete Paving Mixtures [tech brief] (No. FHWA-HIF-22-020). United States. Federal Highway Administration

Cedergren, H. R. (1974). Methodology and effectiveness of drainage systems for airfield pavements. Construction Engineering Research Lab (Army) Champaign United States.

Cedergren, H. R. (1994) America's Pavements: World"s Longest Bathtubs, Civil Engineering, Vol. 64, Sep 1994, pp 56-58.

Cho, Y., Yun, T., Kim, I., & Choi, N. (2011). The application of Recycled Concrete Aggregate (RCA) for Hot Mix Asphalt (HMA) base layer aggregate. KSCE Journal of Civil Engineering, 15(3), 473-478.

Coban, H. S., Cetin, B., Ceylan, H., Edil, T. B., & Nazarian, S. (2020, February). Evaluation of Field and Laboratory Stiffness of Recycled Materials Used in Pavement Base Layers. In Geo-Congress 2020: Geotechnical Earthquake Engineering and Special Topics (pp. 582-590). Reston, VA: American Society of Civil Engineers.

da Conceição Leite, F., dos Santos Motta, R., Vasconcelos, K. L., & Bernucci, L. (2011). Laboratory evaluation of recycled construction and demolition waste for pavements. Construction and building materials, 25(6), 2972-2979.

Das, B. M. (2002). Soil mechanics laboratory manual. Engineering Press.

Das, B. M., & Sivakugan, N. (2018). Principles of foundation engineering. Cengage learning.

Edil, T. B., Tinjum, J. M., & Benson, C. H. (2012). Recycled unbound materials (No. MN/RC 2012-35).

Environmental Protection Agency. (2020). Advancing Sustainable Materials Management: 2018 Fact Sheet. EPA. Retrieved February 2022, from https://www.epa.gov/facts-and-figures-about-materials-waste-and-recycling/advancing-sustainable-materials-management

Etipola, S., Kosgolla, J., & Mallawarachchi, R. (2021). Evaluating the material properties of recycled aggregates as a pavement base or sub-base construction material in Sri Lanka. In AIP Conference Proceedings (Vol. 2409, No. 1, p. 020026). AIP Publishing LLC.

FHWA (2004). Transportation applications of recycled concrete aggregate, Federal Highway Administration, Washington, DC.

Fwa, T. F., Tan, S. A., and Chuai, C. T. (1998) Permeability Measurement of Base Materials using Falling-Head Test Apparatus, Transportation Research Record, No. 1615, 1998, pp 94-99.

Gabr, A. R., & Cameron, D. A. (2012). Properties of recycled concrete aggregate for unbound pavement construction. Journal of Materials in Civil Engineering, 24(6), 754-764.

Gabr, A. R., Mills, K. G., & Cameron, D. A. (2013). Repeated load triaxial testing of recycled concrete aggregate for pavement base construction. Geotechnical and Geological Engineering, 31(1), 119-132.

Gavilan, R. M., & Bernold, L. E. (1994). Source evaluation of solid waste in building construction. Journal of construction engineering and management, 120(3), 536-552.

Ghabchi, R., Zaman, M., Khoury, N., Kazmee, H., & Solanki, P. (2013). Effect of gradation and source properties on stability and drainability of aggregate bases: a laboratory and field study. International Journal of Pavement Engineering, 14(3), 274-290.

Guthrie, W. S., Cooley, D., & Eggett, D. L. (2007). Effects of reclaimed asphalt pavement on mechanical properties of base materials. Transportation Research Record, 2005(1), 44-52.

Hoff, I. (2004). Evaluation of different laboratory compaction methods for preparation of cyclic triaxial samples. SINTEF Civil and Environmental Engineering–Roads and Transport, Norway.

Hoyos, L. R., Puppala, A. J., & Ordonez, C. A. (2011). Characterization of cement-fiber-treated reclaimed asphalt pavement aggregates: preliminary investigation. Journal of Materials in Civil Engineering, 23(7), 977-989.

Huang, Y. H. (2004) Pavement Analysis and Design, Prentice-Hall, Inc., New Jersey,2004.

Hveem, F. N., & Smith, T. W. (1964). A durability test for aggregates. Highway Research Record, 62.

Khoury, N. N., Zaman, M., Ghabchi, R., & Kazmee, H. (2010). Stability and permeability of proposed aggregate bases in Oklahoma (No. FHWA-OK-09-05).

Kim, S. H., Ashtiani, R., Vaughan, D., Des Islets, J., & Beadles, S. (2013). Use of recycled concrete materials as aggregate base layer. In Airfield and Highway Pavement 2013: Sustainable and Efficient Pavements (pp. 1264-1277).

Kim, S., Ceylan, H., Gopalakrishnan, K., White, D. J., Jahren, C. T., & Phan, T. H. (2011). Comparative performance of concrete pavements with recycled concrete aggregate (RCA) and virgin aggregate subbases. In Transportation and Development Institute Congress 2011: Integrated Transportation and Development for a Better Tomorrow (pp. 710-719).

Liang, R. Y., Al-Akhras, K., Rabab'ah, S., Ashteyat, A., & Varri, A. (2006). Evaluation of drainable base materials under asphalt pavement. In Pavement Mechanics and Performance (pp. 142-149).

M. Arisha, A., Gabr, A. R., El-Badawy, S. M., & Shwally, S. A. (2018). Performance evaluation of construction and demolition waste materials for pavement construction in Egypt. Journal of Materials in Civil Engineering, 30(2), 04017270.

Masad, E., & Fletcher, T. (2005). Aggregate imaging system (AIMS): Basics and applications (No. FHAWA/TX-05/5-1707-01-1). Texas Transportation Institute, Texas A & M University System. Transportation. Report 5-1707-01-1

Mukhopadhyay, A. K., Shi, X., & Zollinger, D. G. (2018). Recycling and Reuse of Materials in Transportation Projects-Current Status and Potential Opportunities Including Evaluation of RCA Concrete Pavements Along an Oklahoma Interstate Highway (No. FHWA-OK-18-04). Oklahoma. Department of Transportation.

Nataatmadja, A., & Tan, Y. L. (2001). Resilient response of recycled concrete road aggregates. Journal of Transportation Engineering, 127(5), 450-453.

Olorunsogo, F. T., & Padayachee, N. (2002). Performance of recycled aggregate concrete monitored by durability indexes. Cement and concrete research, 32(2), 179-185.

Papagiannakis, A. T., & Masad, E. A. (2008). Pavement design and materials. John Wiley & Sons.

Poon, C. S., & Chan, D. (2006). Feasible use of recycled concrete aggregates and crushed clay brick as unbound road sub-base. Construction and building materials, 20(8), 578-585.

Poon, C. S., Qiao, X. C., & Chan, D. (2006). The cause and influence of self-cementing properties of fine recycled concrete aggregates on the properties of unbound sub-base. Waste management, 26(10), 1166-1172.

Ram, P., Van Dam, T., Meijer, J., & Smith, K. (2011). Sustainable recycled materials for concrete pavements (No. RC-1550).

Ramirez, J. D. (2018). Evaluation and Influence of Recycled Concrete Aggregate Base Layers on Hma Pavement Performance.

Randolph, B. W., Heydinger, A., and Gupta, J.D. (2000) Permeability and Stability of Base and Subbase Materials, FHWA-OH-2000-017 Final Report, Federal Highway Administration, Trenton, NJ, Aug 2000.

Reza, F., Wilde, W. J., & Izevbekhai, B. I. (2020). Performance of recycled concrete aggregate pavements based on historical condition data. International Journal of Pavement Engineering, 21(6), 677-685.

Tian, P., Zaman, M. M., & Laguros, J. G. (1998). Variation of resilient modulus of aggregate base and its influence on pavement performance. Journal of Testing and Evaluation, 26(4), 329-335.

Titi, H. H., Elias, M. B., & Helwany, S. (2006). Determination of typical resilient modulus values for selected soils in Wisconsin (No. WHRP 06-06).

Toka, E. B., & Olgun, M. (2021). Performance of granular road base and sub-base layers containing recycled concrete aggregate in different ratios. International Journal of Pavement Engineering, 1-14.

Wu, Y., Parker, F., & Kandhal, P. S. (1998). Aggregate toughness/abrasion resistance and durability/soundness tests related to asphalt concrete performance in pavements. Transportation Research Record, 1638(1), 85-93.

Zaman, M., Chen, D-H., and Laguros, J. (1994) Resilient Moduli of Granular Materials, Journal of Transportation Engineering, Vol. 120, No. 6, 1994, pp 967-988.

Zhang, Yang, Bora Cetin, and Tuncer B. Edil. (2021). Seasonal Performance Evaluation of Pavement Base Using Recycled Materials, Sustainability 13, no. 22: 12714.

Testing Standards

AASHTO (2014). Standard method for specific gravity and absorption of course aggregate. American Association of State and Highway Transportation Officials, Washington, DC

AASHTO T-180 (2019). Standard method of test for moisture-density relations of soils using a 4.54-kg (10-lb) rammer and a 457-mm (18-in.) drop. American Association of State and Highway Transportation Officials, Washington, DC

AASHTO T-210 (2010). Standard method for aggregate durability index. American Association of State and Highway Transportation Officials, Washington, DC

AASHTO T-307 (2021). Standard Method of Test for Determining the Resilient Modulus of Soils and Aggregate Materials. American Association of State and Highway Transportation Officials, Washington, DC.

AASHTOT T-176 (2012). Standard method for aggregate durability index. American Association of State and Highway Transportation Officials, Washington, DC

American Association of State Highway and Transportation Officials (AASHTO). (2020). Mechanistic-Empirical Pavement Design Guide - A Manual of Practice (3rd Edition). American Association of State Highway and Transportation Officials (AASHTO)

ASTM C131 (2014). Standard test method for resistance to degradation of small-size coarse aggregate by abrasion and impact in the Los Angeles machine. American Society of Testing and Materials (ASTM), West Conshohocken, PA.

ASTM D5084 (2016). Standard Test Methods for Measurement of Hydraulic Conductivity of Saturated Porous Materials Using a Flexible Wall Permeameter (ASTM), West Conshohocken, PA.

ASTM T-27 (2012). Standard Specifications for Transportation Materials and Methods of Sampling and Testing (32nd Edition) and AASHTO Provisional Standards, 2012 Edition. American Association of State Highway and Transportation Officials (AASHTO).

Caltrans Transportation (2018). Standard Specifications for Road and Bridge, California Department of Transportation.

CDOT Transportation (2021). Standard Specifications for Road and Bridge, Colorado Department of Transportation.

La DOTD Transportation (2026). Standard Specifications for Roads and Bridges, Louisiana Department of Transportation and Development.

MassDOT Transportation (2020). Standard Specifications for Highways and Bridges, Massachusetts Department of Transportation.

MoDOT Transportation (2021). Standard Specifications for Highway Construction, Missouri Highways and Transportation Division.

ODOT (2019). Standard Specifications for Highway Construction, Oklahoma Department of Transportation, Section 700: Materials, 2009.

TxDOT (2014). Standard Specifications for Construction and Maintenance of Highways, Streets, and Bridges, Texas Department of Transportation.